Freie Universität Berlin

Master's Seminar

The Role of Memory in Decision Making

Aug 28-29, 2012

A teaching event within the

Bernstein Focus Neuronal Basis of Learning (BFNL): Insect Inspired Robots

Funded by the German Federal Ministry of Education and Research (BMBF)

Responsible

Dorothea Eisenhardt and Martin Nawrot

bfnl
Insect Inspired Robots

Seminar/Module 23903 | SS 2012 | FU Berlin

Final Program

The Role of Memory in Decision Making

Venue Seminar Room 36.07, Takustraße 3

Date Aug 28-29 (Tue - Thu)

Faculty

Prof. Dorothea Eisenhardt
Systemic Neurobiology
Institute of Biology
Freie Universität Berlin

Prof. Martin Nawrot
Neuroinformatik
Institute of Biology
Freie Universität Berlin

Organization

Benjamin Auffarth, Kathrin Brackwehr, Martin Nawrot

Contact

Kathrin Brackwehr, AG Neuroinformatik, Königin-Luise-Str. 1-3, 14195 Berlin
fon: 838 57920 mail: k.brackwehr@fu-berlin.de

Tutors

Benjamin Auffarth (benjamin.auffarth@fu-berlin.de)
Tara Dezhdar (t.dezhdar@fu-berlin.de)
Farzad Farkhooi (farzad.farkhooi@gmail.com)
Joachim Hänicke (joachim.haenicke@fu-berlin.de)
Chris Häusler (chausler@gmail.com)
Lovisa Helgadottir (Tel. 838 57291)
Gundula Meckenhäuser (gundula@zedat.fu-berlin.de)
Evren Pamir (evren.pa@googlemail.com)
Thomas Rost (thomasrost@gmail.com)
Michael Schmuker (m.schmuker@fu-berlin.de)
Jan Sölter (j.soelter@fu-berlin.de)
Johannes Felsenberg (johannes.felsenberg@fu-berlin.de)
Christina Buckemüller (Christina.Buckemueller@rub.de)
Kathrin Marter (k.marter@fu-berlin.de)
Katrin Gehring (katrin.gehring@fu-berlin.de)

Topics

A Working Memory

[1 **Larissa Seek**] [Tutor: J. Felsenberg]

Zhang S, Bock F, Si A, Tautz J, Srinivasan MV (2005) Visual working memory in decision making by honey bees. Proc Natl Acad Sci USA 102(14):5250-5 (*behavior*)

[2 **Dennis Schmoldt**] [Tutor: F. Farkhooi]

Qi, X.-L., Katsuki, F., Meyer, T., Rawley, J. B., Zhou, X., Douglas, K. L., & Constantinidis, C. (2010). Comparison of neural activity related to working memory in primate dorsolateral prefrontal and posterior parietal cortex. Frontiers in systems neuroscience, 4(May), 12. doi:10.3389/fnsys.2010.00012 *(neurophysiology)* [extracellular recording, spike sorting]

[3 **Anja Wegner**] [Tutor: M. Nawrot]

Harvey, C. D., Coen, P., & Tank, D. W. (2012). Choice-specific sequences in parietal cortex during a virtual-navigation decision task. Nature, 484(7392), 62-68. Nature Publishing Group. doi:10.1038/nature10918 *(neurophysiology)*

Background reading

Curtis CE, Lee D. (2010) Beyond working memory: the role of persistent activity in decision making. Trends Cogn Sci. 14(5):216-22

B Reward encoding and reward prediction

[4 **Achim Meyer**] [Tutor: J. Haenicke]

Strube-Bloss, Nawrot MP, Menzel R (2011) Mushroom Body Output Neurons Encode Odor-Reward Associations. Journal of Neuroscience 31(8):3129-3140 *(neurophysiology)*

Reward prediction at the mushroom body output after classical conditioning

[5 **Anna Nowak**] [Tutor: J. Felsenberg]

Hammer, M. (1993) An identified neuron mediates the unconditioned stimulus in associative olfactory learning in honeybees. Nature 366:59-63 (*neurophysiology*) [intracellular recording]

Background reading

Glimcher PW (2011) Understanding dopamine and reinforcement learning: The dopamine reward prediction error hypothesis. Proceedings of the National Academy of Sciences 108: 15647-15645

C Perceptual decision making in animals

[6 **Masin Abo-Rady**] [Tutor: AG Nawrot]

Uchida N, Mainen ZF (2003) Speed and accuracy of olfactory discrimination in the rat. Nat Neurosci 6(11):1224-9 (*behavior*)

Wesson, D. W.; Carey, R. M.; Verhagen, J. V. & Wachowiak, M. (2008) Rapid encoding and perception of novel odors in the rat. PLoS Biol 6(4), e82 (*behavior*)

Uchida et al. describe fast behavioral discrimination of odorants in rats. Wesson et al. describe an even faster detection of an unknown odor. Combine both papers for presentation with a focus on Uchida et al.2003

For background reading and a more general definition of perceptual decision making see:

N. Uchida, A. Kepecs and Z.F. Mainen (2006) Seeing at a glance, smelling in a whiff: rapid forms of perceptual decision making. *Nature Reviews in Neuroscience* 7(6):485-491 (*review article*)

Kristan WB.(2008) Neuronal decision-making circuits. Curr Biol. 2008 Oct 14;18(19):R928-32 (review article)

Heekeren HR, Marrett S, Ungerleider LG (2008) The neural systems that mediate human perceptual decision making. Nat Rev Neurosci 9(6):467-79 (*review article*)

Kable, JW, Glimcher, PW (2009) The neurobiology of decision: Consensus and controversy, Neuron, 63: 733-745 (*review article*)

Kristan WB.(2008) Neuronal decision-making circuits. Curr Biol. 2008 Oct 14;18(19):R928-32 (*review article*)

D Perceptual decision making in humans

[7 **Florian Bilz**] [Tutor: C. Buckemüller]

Heekeren HR, Marrett S, Bandettini PA, Ungerleider LG (2004) A general mechanism for perceptual decision-making in the human brain. Nature 431(7010):859-62 [functional Magnetic Resonance Imaging, fMRI] (*human neurophysiology*)

Heekeren HR, Marrett S, Ungerleider LG (2008) The neural systems that mediate human perceptual decision making. Nat Rev Neurosci 9(6):467-79 (*review article*)

[8 **Isabell Groß**] [Tutor: K. Gehring]

Kahnt, T., Grueschow, M., Speck, O., & Haynes, J.-D. (2011). Perceptual learning and decision-making in human medial frontal cortex. Neuron, 70(3), 549-59. Elsevier Inc. doi:10.1016/j.neuron.2011.02.054 (*human neurophysiology*)

[9 **Gustav Schneider**] [Tutor: K. Gehring]

Rolls, E. T., Grabenhorst, F., & Parris, B. a. (2010). Neural systems underlying decisions about affective odors. Journal of cognitive neuroscience, 22(5), 1069-82. doi:10.1162/jocn.2009.21231 (*human neurophysiology*)

Background reading (see also C above)

Newcombe, V. F. J., Outtrim, J. G., Chatfield, D. a, Manktelow, A., Hutchinson, P. J., Coles, J. P., Williams, G. B., et al. (2011). Parcellating the neuroanatomical basis of impaired decision-making in traumatic brain injury. Brain : a journal of neurology, 134(Pt 3), 759-68. doi:10.1093/brain/awq388

Gleichgerrcht, E., Ibáñez, A., Roca, M., Torralva, T., & Manes, F. (2010). Decision-making cognition in neurodegenerative diseases. Nature reviews. Neurology, 6(11), 611-23. Nature Publishing Group. doi:10.1038/nrneurol.2010.148

E Value-based decision making / Neuroeconomics

[10 **Sulav Duwal**] [Tutor: D. Eisenhardt]

Peters J, Büchel C. (2009) Overlapping and distinct neural systems code for subjective value during intertemporal and risky decision making. J Neurosci. 29(50):15727-34. (*human physiology*)

For an introduction to value-based decision making see:

Rangle, A., Camerer, C., Montague, P.R. (2008) A framework for studying the neurobiology of value-based decision-making. Nature Reviews: 9, 545-556 (*review article*)

F Social decision making

[11 **Eva Carmarillo**] [Tutor: E. Pamir]

Wu, Y., Leliveld, M. C., & Zhou, X. (2011). Social distance modulates recipient's fairness consideration in the dictator game: an ERP study. Biological psychology, 88(2-3), 253-62. Elsevier B.V. doi:10.1016/j.biopsycho.2011.08.009 [EEG]

[12 **Sophie Kolbe**] [Tutor: G. Meckenhäuser]

King-Casas B, Tomlin D, Anen C, Camerer CF, Quartz SR, Montague PR (2005) Getting to know you: reputation and trust in a two-person economic exchange. Science. 308(5718):78-83. (*human physiology*)

[13 **Katharina Mangold**] [Tutor: K. Marter]

Ward, A. J. W., Krause, J., & Sumpter, D. J. T. (2012). Quorum decision-making in foraging fish shoals. PloS one, 7(3), e32411. doi:10.1371/journal.pone.0032411 (*behavior*)

For an introduction to game theory and social influences on decisions:

Katsikopoulos, K. V., & King, A. J. (2010). Swarm intelligence in animal groups: when can a collective out-perform an expert? PloS one, 5(11), e15505. doi:10.1371/journal.pone.0015505

Lee D (2008) Game theory and neural basis of social decision making. Nature Neuroscience 11, 404 - 409

Rilling JK, King-Casas B, Sanfey AG.(2008) The neurobiology of social decision-making. Curr Opin Neurobiol. 2008 Apr;18(2):159-65. Epub 2008 Aug 7 (*review article*)

G Computational models of decision making and decision making in artificial agents

[14 **Jörg Meier**] [Tutor: J. Sölter]

Deco G, Rolls ET (2006) Decision-making and Weber's law: a neurophysiological model.

Eur J Neurosci. 24(3):901-16. (*computational model*)

For overview start with: Wang et al. 2008 above; see other review articles cited above

This topic is closely related the previous topic on neural correlates of decision making in the macaque. Please also read Romo et al. 2003 above.

[15 **Philipp Norton**] [Tutor: J. Sölter]

Deco G, Rolls ET, Romo R. (2010) Synaptic dynamics and decision making. Proc Natl Acad Sci USA. 107(16):7545-9. (*computational model*)

This publication improves previous model above. Please also read Romo et al. 2003 cited for [16].

[16 **Michael Rauer**] [Tutor: C. Häusler]

Lo C-C, Wang X-J (2006) Cortico–basal ganglia circuit mechanism for a decision threshold in reaction time tasks. Nature Neuroscience 9, 956 - 963 (*computational model*)

[17 **Martin Seeger**] [Tutor: B. Auffarth]

van Maanen, L., Grasman, R. P. P. P., Forstmann, B. U., & Wagenmakers, E.-J. (2012). Piéron's Law and Optimal Behavior in Perceptual Decision-Making. Frontiers in neuroscience, 5(January), 143. doi:10.3389/fnins.2011.00143 (*experiment + model*)

For background reading, see

Deco, G., Rolls, E. T., Albantakis, L., & Romo, R. (2012). Brain mechanisms for perceptual and reward-related decision-making. Progress in neurobiology, 1-20. Elsevier Ltd. doi:10.1016/j.pneurobio.2012.01.010

Wang XJ (2008) Decision making in recurrent neuronal circuits. Neuron 60(2):215-34 (*review article*)

Lee, D., and Wang, X.-J. (2008). Mechanisms for stochastic decision making in the primate frontal cortex: Single-neuron recording and circuit modeling. In *Neuroeconomics: Decision Making and the Brain*, E.F.P.W. Glimcher, C.F. Camerer, and R.A. Poldrack, eds. (*book chapter 31, PDF version is included in the online seminar material*).

Chapters 5 'Probabilistic decision-making' + 6 'Confidence and Decision Making' in Rolls ET, Deco G (2010) The Noisy Brain. Stochastic Dynamics as a Principle of Brain Function. Oxford University Press, Oxford (available at the AG Nawrot, Neuroinformatik, Königin-Luisen Str. 1-3) (book chapter)

Gold J, Shadlen M (2007) The neural basis of decision making. Annu. Rev. Neurosci. 2007. 30:535–74 (*review article*)

Larissa Seek,

Visual working memory in decision making by honey bees - Summary

Background and experimental set-up

The honey bee is known to have a robust and flexible working memory. This cognitive capacity is defined as a memory system that holds information in temporary storage during the planning and execution of a certain task (Dudai Y. 2002). The aim of this study was to proof this mechanism by investigation of its function and role in the decision making process in honey bees. They realized this examination through a so called delayed match to sample (DMTS) paradigm where the bees learned to align a prior experienced sample to one of two samples (one is the same, one is novel) in a later choice situation (Blough, D. S. 1959). The simplest version of the here used task is a tunnel system in which the bee has to fly to a decision chamber (Fig. 1). The stimuli were realized through visual pattern. The bees had to learn matching a sample pattern in the tunnel with one of two comparison patterns in a decision chamber at the very end. Thus, the goal was choosing the same pattern in the decision chamber as presented in the tunnel. If the bee made a correct choice it received a sugar-reward in a subsequent cylinder. By making an incorrect choice, it arrived in a non rewarded cylinder. One important criteria for working memory is that performance accuracy decays as a function of time as distance increases (Zhang, S. *et al* 2005). Therefore the authors changed the time between the first sample and the choice in a decision chamber by varying the distance d2 between sample and choice (fig. 1 upper). The bees hade to retain the information about the identity of the pattern maintained in the working memory and to apply the learned rules to make a right choice (Roitblat, H. L 1987). Through this they measured the performance of working memory. The examination was realized by three different experimental setups of this apparatus and was conducted to the operation in accordance to three intrinsic considered questions (Zhang, S. *et al* 2005).

Procedure and results

The first of the 3 experiments (series I) asked the question, how long bees retain the sample in the working memory? By increasing the distance they increased the delay interval between the exposures to sample pattern and the choice situation. Thus, it is possible to estimate the retention time of the working memory. The results show that information could be held accurately in the working memory for at least 5 seconds before being used to make a decision. The significantly better performance than at random choice level decreases as the duration between the presentation of the sample stimulus and the presentation of comparison stimuli is increased. This could be approximated by an exponential decay function. The performance is reduced to a random choice levels at a distance of 475 cm and average delay time of 8 seconds.

Series II investigates the question whether bees can learn to perform a DMTS task correctly when an additional incorrect pattern is present in the tunnel? Bees were first trained with a single pattern placed at 120 cm distance to the decision chamber in a learning test. In one transfer test two sample patterns were placed at fixed distances to the decision chamber. The correct sample pattern was placed at 120 cm distance (= training distance) and an incorrect sample pattern at 170 or 50 cm distance. This means the incorrect sample was positioned either behind or in front of the correct sample pattern (Fig. 1 mean). The aim was to examine whether the trained bees would use

the sample at training distance to make a correct choice in the decision chamber or if they were interrupted by a second input of another sample pattern. They results show that the bees are able to learn using the relevant sample as “true” to perform the task. This is given if the relevant sample is always at a fixed position.
In another transfer test the sample pattern was placed at 50 cm and the incorrect one at 170 cm distance to the decision chamber. So in this experiment, neither a sample at the known training distance was present. Because of the revealed decline to random choice level of correct choices, they received that the bees “got confused”. This assumes the discrimination capability between correct and incorrect sample pattern of basis of position in the tunnel.
And finally series III, which had its focus on the question whether bees can learn which of two sequentially encountered patterns in the tunnel is the pattern to be matched in a decision cylinder? In the learning tests two sample patterns were placed with a displacement of 50 cm (Fig. 1 lower) to each other. Thus, they investigated whether the bees could learn to match the comparison stimuli by using just one of the two samples. They could show that if the relevant sample has always the same place in the sequence of presentation, the bees are able to learn using the relevant one as the right one to perform the task. Furthermore they could proof that bees are able to generalize the learned rule by including novel objects (e.g. sector and ring). In addition, in another transfer test they increased the distance between the two samples from 50 cm to 100 cm and could show that even at enlarged distance situation the bees performed well.
By performing well arranged control experiments the authors could exclude any bias by a side preference or olfactory hind in the used setups.

Conclusion

To summarize the results it can be concluded that this capability to learn relevant sample and to ignore irrelevant sample, even at enlarged distance and under novel situations illustrates the complexity of the honey bee’s working memory. Further studies should investigate whether bees can learn to perform similarly when more than two sample patterns are used. Additionally, the open question could be answered how the bees store the information about the position of the pattern either by using external landmarks or measuring the distance to some reference like the position to the tunnel entrance.

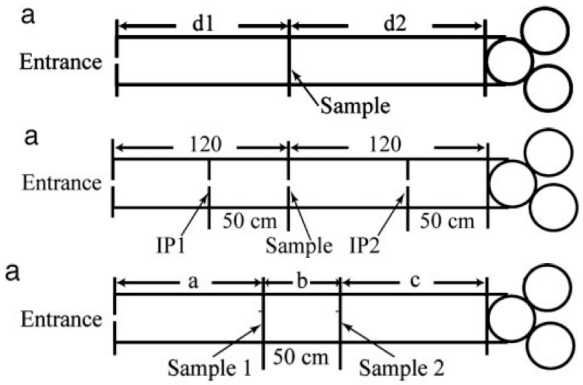

Figure 1. Schematic illustration of apparatus used in the experiments of series I to III consisting of a tunnel and a decision chamber. The length oft the tunnel is 4.8 m, the wide 22.5 cm and the height 21.5 cm. The three vertical cylinders representing the decision chambers have a height of 25 cm and a diameter 22.5 cm as well as three holes as entrance and exits. The top most apparatus was used in series I, the mean one in series II and the lower set-up in series III. IP1 and IP2 characterize the incorrect pattern placed in front or behind the sample pattern.

Literature:

Blough, D.S. (1959) J. Exper. Anal. Behav. **21**, 19-26.
Dudai, Y. (2002) Memory from A to Z, Keywords, concepts and beyond,
Oxford University Press. Oxford, New York.
Roitblat. H. L. (1987) in Introduction to Comparative Cognition (W.H. Freeman, New York), pp. 146-189.
Zhang S, Bock F, Tautz J, Srinivasan MV (2005) Visual working memory in decision

Larissa Seek,

making by honey bees. PNAS. **102**, 5250-55.

Term paper

Comparison of neural activity related to working memory in primate dorsolateral prefrontal and posterior parietal cortex

by

Xue-Lian Qi, Fumi Katsuki, Travis Meyer, Justin B. Rawley, Xin Zhou, Kristy L. Douglas and Christos Constantinidis

Dennis Schmoldt

Institut für Bioinformatik,

Freie Universität Berlin

Table of contents

1. Introduction

Working memory refers to the ability to maintain and manipulate information in memory over a time interval of seconds[1]. Neurophysiological recordings in animal models have provided a neural correlate of working memory in the form of neuronal discharges that are elicited by physical stimuli but which persist even after the stimuli are no longer present[2].

The study analyzed how patterns of activity relating to spatial working memory differ between cortical areas in the context of different tasks.

2. Materials and methods

2.1. Animals and Materials

In the experiment the authors used four male, rhesus monkeys.

The areas used for the neuronal recordings were area 46 and 8 of the dorsolateral prefrontal cortex and area 7a of the posterior parietal cortex. Furthermore the cauldal part of the Principal Sulcus, the region between the Principal and the Arcuate Sulcus and a part of superior convexity of the lateral prefrontal cortex were included to the prefrontal recordings.

In order to record the neuronal activity, two cylinders where implanted in the monkeys heads. Furthermore arrays of up to eight microelectrodes where used.

The depth of the cortex encountered by the electrodes provided a coarse map of anatomical locations. This allowed the authors to superimpose it onto an image, done by Magnetic resonance imaging.

The recorded action-potentials were sorted with the KlustaKwik-algorithm into separate units. Finally the focus was set on those neurons who responded on visual stimuli. Neurons with significantly different responses to the nine grid-stimulus locations were also observed. At the end patterns of the delay period activity of the neurons were observed, whether the firing rate increased in the delay period after a stimulus or not. If the firing rate increased the neurons were called anticipatory, but if it stayed the same or declined they were called sustained.

The monkeys sat in a primate chair, which was 60 or 68cm away from a computer monitor and their heads were fixed. In preparation for the experiment, the monkeys were trained to keep their gaze on a fixation target. To control this, their eye movement was tracked. If a monkey breaks the fixation the trail was terminated, otherwise if a monkey completes a trail successfully it gathers a liquid reward.

2.2. Behavioral Tasks

Two behavioral tasks had to be done by the monkeys. The first one was a Match/Nonmatch task, where two monkeys had to remember the spatial location of a stimulus that flashed on the screen and had to decide whether a second stimulus flashed on the same location or not. The trail started with a fixation period, followed by the first stimulus that had to be remembered. This stimulus could appear in one of nine positions in a 3*3 grid. The stimulus is succeed by a delay, a second stimulus in the grid and a second delay. At the end the monkey had to decide with his gaze between a blue and a green square. He should choose the green, if the stimuli matched and the blue if not. For each record they did ten repetitions and set the positions of the squares randomly (*Figure 1 A*).

However the other two monkeys did a delayed match-to-sample task. In this task the monkeys had to remember a first stimulus and release a lever if another stimulus occurs at same position of the first stimulus. In detail the monkey had to pull the lever and foveate a fixation point. Again a 3*3 grid was used for the stimuli. Each stimuli was followed by a delay and the

[1] Baddeley, 1992 [2]
[2] Fuster and Alexander, 1971; Funahashi et al., 1989 [3]

first stimulus was followed from up to two nonmatches. Also the monkeys were trained to release the lever in the delay after the match. Any other release of the lever caused the abortion of the trail *(Figure 1 B)*.

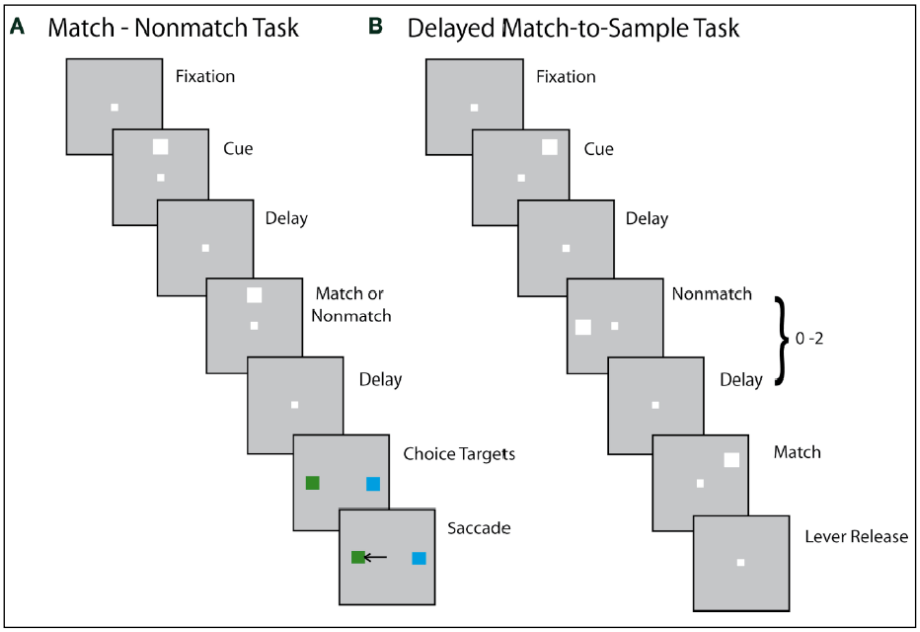

Figure 1 | Behavioral tasks. Successive frames indicate the series of stimulus presentations. (A) Stimulus presentations in the Match/Nonmatch task. (B) Stimuluspresentations in the Delayed Match-to-Sample task.[3]

3. Results

3.1. Database

As already mentioned the recorded areas had been 7a, 8 and 46. For each of the two tasks the focus was set on neurons that responded to visual stimuli, especially on spatial locations and in addition showed a special discharge in comparison to the baseline during the delay.

On the one hand for the Match/Nonmatch task the activity of 149 neurons was recorded from the dorsolateral prefrontal cortex. Furthermore 83 of those were used for further analysis because of their special behavior. On the other hand the authors recorded 60 neurons from the posterior parietal cortex and 38 were used for further analysis.

In the delayed match-to-sample task 48 out of 148 from the prefrontal and 36 out of 119 from the parietal cortex were analyzed.

3.2. Types of delay period activity

There were two types of delay period activity. Type one was the so called sustained activity which was described by a consistent or declining firing rate that extends a respond. 96 neurons of this type were recorded in the prefrontal and 36 in the parietal cortex. Type two showed an increasing firing rate and was called anticipatory. Here 35 and 38 neurons where recorded.

It was pointed out how activity during the delay period changed after a stimulus inside or outside of the receptive field.

[3] Xue-Lian Qi et al., 2010,S. 4 [1]

Within the Match/Nonmatch task the parietal neurons exhibited a sustained response if a stimulus was in the receptive field and stopped if it was out of the receptive field. Prefrontal neurons continued to discharge even after a transient decrease in activity caused by the nonmatch stimulus. Moreover a regression analysis showed that prefrontal neurons did not differ between a nonmatch out of the receptive field after a match on the one hand and a match within the receptive field after a match on the other hand. In contrast to this, the parietal neurons had a decreased firing rate in the nonmatch case. However both types continued to discharge if the first stimulus was outside and the second stimulus inside the receptive field. The anticipatory activity was not really significant in this task.

In the delayed match to sample task, the anticipatory activity was not significant, too. That is why the focus was set again on the sustained activity. So it was checked if a sustained activity from a stimulus within the field could be disturbed by a stimulus out of the field and vice versa. If the stimulus was out of the receptive field, there was no difference, both neurons where still active. The same holds true for a nonmatch within the receptive field (*Figure 2*). Of course the case of a match was not considered, because it terminates the trail.

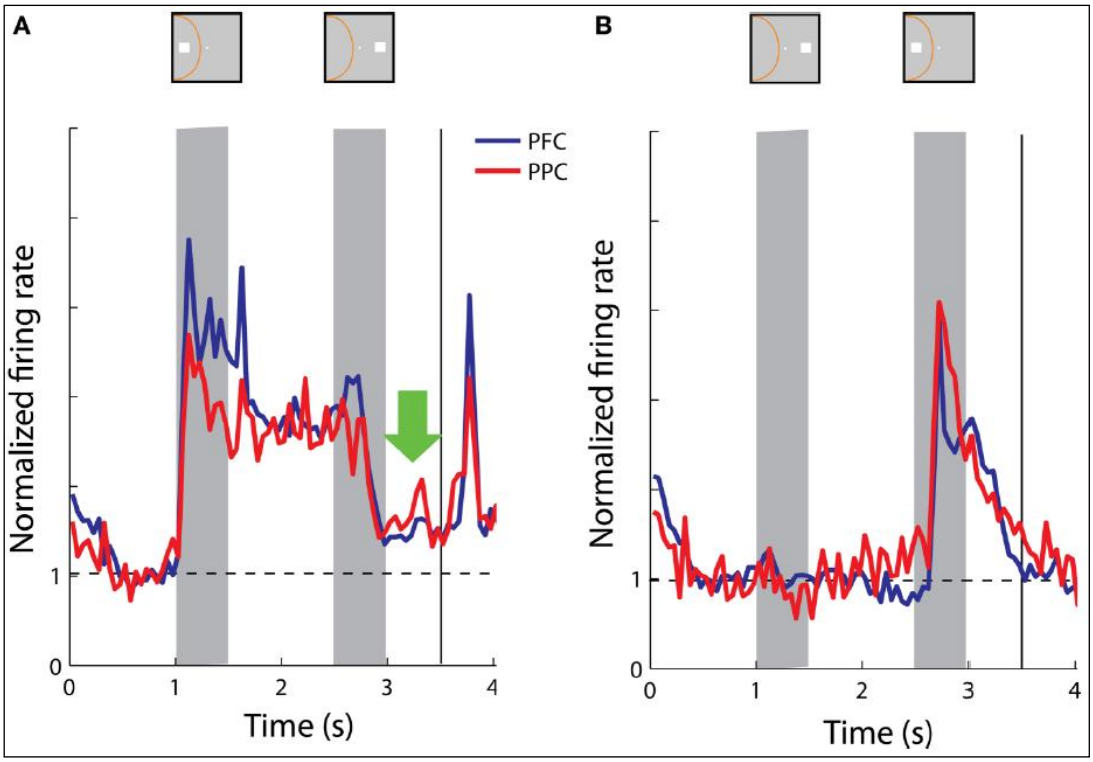

Figure 2 | Population responses from neurons with sustained activity recorded in the prefrontal (N = 38) and posterior parietal cortex (N = 17). Green arrow represents the delay period following a nonmatch stimulus out of the receptive field. Data are shown from the Delayed Match-to-Sample task. (A) Average, normalized responses to the cue presentation in the receptive field followed by a nonmatch stimulus out of the receptive field. (B) Average responses to the cue presentation out of the receptive field, followed by a nonmatch stimulus in the receptive field.[4]

[4] Xue-Lian Qi et al., 2010, S.9 [1]

4. Discussion

4.1. Overview over the findings

The study referred to the differences between the patterns of the delay activity from the prefrontal and parietal cortex. Distinct patterns of responses were observed in the populations of neurons with sustained responses which exhibited differences in the prefrontal versys the parietal cortex[5]. The main finding was that the dorsolateral prefrontal activity which represents the spatial location of a stimulus survives the presentation of a nonmatch stimulus out of the receptive field. Furthermore they found similarities between the two regions, for example that both regions continued to be active after a nonmatch in the Match/Nonmatch task as well as they continued to represent a nonmatch in the receptive field in the following delay even though it was not required.

4.2. Type of responses

The sustained activity was characterized by persistent discharges that extended beyond the initial response to a stimulus into the delay period and could encode the location of the preceding stimulus. This is the type of activity commonly thought to provide a neural correlate of working memory for the preceding stimulus[6].

The anticipatory activity seemed to appear after stimuli at any spatial location, most often outside of the neuron's receptive field and could be informative about the preceding stimulus.

4.3. Task-Effects

In the Match/Nonmatch task the animals had to compare an initial stimulus and with a second one, if they matched or not. Even it was not necessary one of the stimuli's still was represented in the prefrontal and parietal cortex. Within the delayed match-to-sample task no significant differences had been found.

4.4. Implications for functional specialization

The posterior parietal and dorsolateral prefrontal cortexes are strongly interconnected and share many functional properties[7]. The prefrontal cortex has the ability to preserve information. Although a number of candidates were identified, it is not clear yet, which gives the prefrontal cortex its unique ability. Candidates are dopamine, which stabilizes the working memory[8], the dendritic tree size and the composition of the interneurons. All in all it will be a mixture of these factors that gives the prefrontal cortex its unique ability.

[5] Xue-Lian Qi et al., 2010, S.9 [1]
[6] Goldman-Rakic, 1995 [4]
[7] Cavada and Goldman-Rakic, 1989 [5]
[8] Durstewitz et al., 2000 [6]

References

[1] Qi, X.-L., Katsuki, F., Meyer, T., Rawley, J. B., Zhou, X., Douglas, K. L., & Constantinidis, C. (2010). Comparison of neural activity related to working memory in primate dorsolateral prefrontal and posterior parietal cortex. Frontiers in systems neuroscience, 4(May), 12. doi:10.3389/fnsys.2010.00012 .

[2] Baddeley, A. (1992). Working memory *Science* 255, 556–559.

[3] Fuster, J. M., and Alexander, G. E. (1971). Neuron activity related to short-term memory. *Science* 173, 652–654.

[4] Goldman-Rakic, P. S. (1995). Cellular basis of working memory. *Neuron* 14, 477–485.

[5] Cavada, C., and Goldman-Rakic, P. S. (1989). Posterior parietal cortex in rhesus monkey: I. Parcellation of areas based on distinctive limbic and sensory corticocortical connections*. J. Comp. Neurol.* 287, 393–421.

[6] Durstewitz, D., Seamans, J. K., and Sejnowski, T. J. (2000). Dopaminemediated stabilization of delayperiod activity in a network model of prefrontal cortex. *J. Neurophysiol.* 83, 1733–1750.

ARTICLE

doi:10.1038/nature10918

Choice-specific sequences in parietal cortex during a virtual-navigation decision task

Christopher D. Harvey[1,3,4]†, Philip Coen[1,4] & David W. Tank[1,2,3,4]

| NATURE | VOL 484 | 5 APRIL 2012

„Am I right, or am I wrong?“

or

The parietal cortex,

a conductor of an orchestra where every musician just plays for a short time in a definied order to create a musical motif.

A term paper written by Anja Wegner.

Table of contents

1 Introduction

Our current knowledge about working memory can be traced back to the year 1936 where Jacobsen used a spatial delayed-response task performed by monkeys. They had to remember where the food or cue was located under two identical looking cups. After a delay, the cups were not visible during this time, the monkeys had to choose a cup. Large prefrontal cortex lesions in the monkeys impaired the performance of this task and it was concluded that this part of the brain is essential for cognitive processes. Later in 1973 Fuster conducted the same experiments but he simultaneously recorded the electrical activity of the neurons in the prefrontal cortex. Surprisingly he found neurons in the prefrontal cortex that had increased firing rates during the delayed period. This increased activity may be related to the retention of the food location needed to make the correct choice. With the advent of brain imaging methods, like Positron emission tomography (PET) and Functional magnetic resonance imaging (fMRI), it emerged that areas of activation during working memory tasks also include other brain areas in the cortex e.g. the posterior parietal cortex (PPC) [Smith et al.1999; Heekeren et al. 2008]. The PPC is interconnected with brain areas responsible for sensory and motor processing. In rats studies suggest that the PPC is important for the integration of spatial information, route planning and route progression during a memory-guided navigation task [Calton et al. 2009]. In previous experiments it was shown that different classes of cells exist because they had sustained firing rates in the cue-, delay or response period of the whole task [Curtis & Lee 2010]. On the other hand and to a much higher degree Harvey, Coen and Tank found that different neurons in each class were only shortly active at different times and formed sequences of activation.

2 Experimental setup

They used a virtual T-maze displayed on a toroidal screen, where head-restrained mice, via a titanium head plate affixed with dental cement to the skull, had to navigate through, while their limbs rested on an air-supported spherical treadmill (**Figure 1:**1a). They trained the mice to associate visual cues with a water reward and to memorize this information during a delay period (**Figure 1:** 2a). Once the mice were proficient at the task, they injected the AAV2/1-*synapsin*-1-GCaMP3 virus into the PPC to visualize calcium transients - an indicator for neuronal activity.

To image the Ca^{2+} transients in the layer 2/3 of the PPC they implanted a chronic imaging window and used two-photon microscopy. They imaged around 65 cells simultaneously in an area of about 300 µm by 150 µm.

The anatomical location of the PPC was identified by performing tracing experiments with retrogradely-transported red fluorescent beads to indentify potential inputs and to identify potential outputs, PPC neurons were labelled with GFP using viral methods.

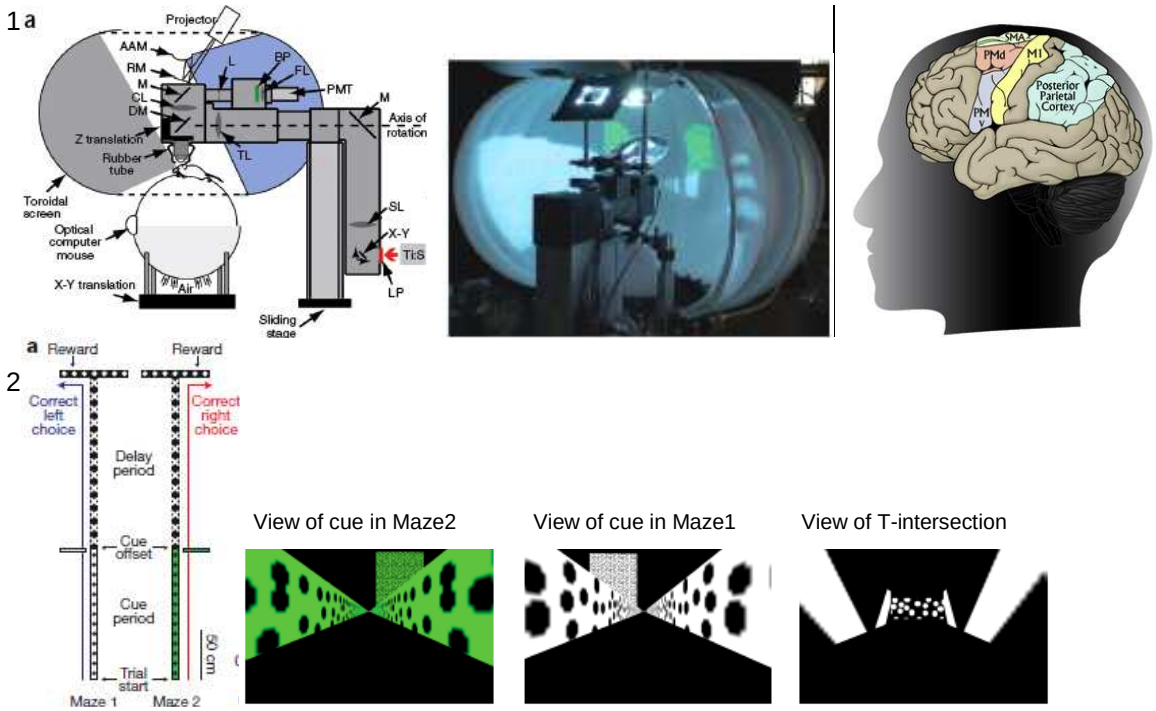

Figure 1: ***(1a left)*** “The experimental apparatus, consisting of a spherical treadmill, a virtual reality apparatus (projector, reflecting mirror (RM), angular amplification mirror (AAM), toroidal screen and optical computer mouse to record ball rotation) and a custom two-photon microscope (titanium:sapphire laser (Ti:S), long-pass filter (LP), galvanometers (X-Y), scan lens (SL), mirror (M), tube lens (TL), dichroic mirror (DM), collection lens (CL), biconcave lens (L), bandpass filter (BP), focusing lens (FL), photomultiplier tube (PMT), sliding stage (used to move microscope for treadmill access), X-Y translation (moves treadmill and mouse), Z-translation (objective focus control) and rubber tube (shown in cross-section, for light shielding)). ***(1a middle)*** Photograph of experimental setup.” (Dombeck et al., 2010) ***(1a right)*** “An illustration of the human brain showing the location of the posterior parietal cortex, the primary motor complex (M1), and the pre-motor areas (SMA, PMd and PMv)” © Barbara Martin / courtesy of Vanderbilt University ***(2a left)*** „Diagram of the two versions of the virtual T-maze that differed only in the cue period and the reward location. Patterns in the diagram reflect the patterns present on the virtual maze walls. ***(2a right)*** Screen captures of the virtual environment.“ (Harvey et al., 2012)

3 Results

The anatomical location of the mouse PPC using retrograde and anterograde tracing revealed the same position like in rats and primates (**Figure 1:** 1a right).

After the imaging they manually selected the interesting cell bodies (**Figure 2:** 3a left) to distinguish 53% of non-active cells with Ca^{2+} transients less than two per minute and 47% were active with more than two transients per minute. 73% of these cells were only highly active for a short and specific time in the task. These task-modulated cells had an increase in fluorescence variabilty ($\Delta F/F$) for more than 1,3 s of the task.

The majority, around 71%, of the task-modulated cells distinguished the trial type because the levels of activity were different during the correct right and left trials (**Figure 2:** 3a;3b).

The same pattern could be confirmed with extracellular electrophysiological recordings. In this group of the choice-specific cells, 25% were cue cells, 33% prefered the delay and 42% were active at the turn. Only a small fraction of neurons were active over the whole trial span or showed reward-related signals.

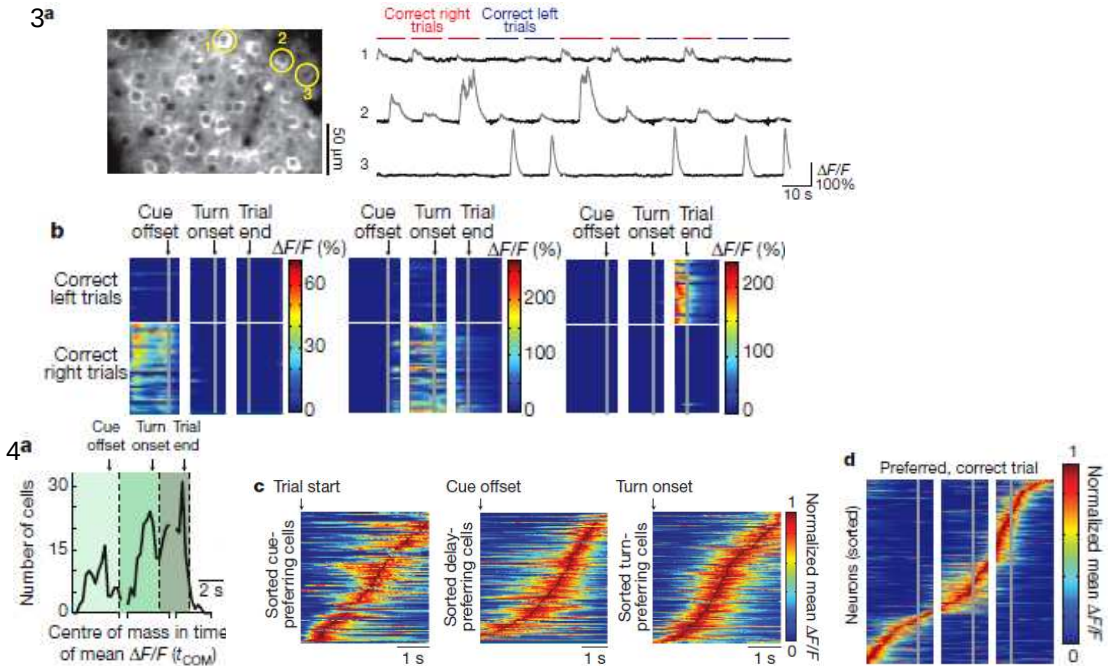

Figure 2: „ ***(3a left)*** Example image of GCaMP3-expressing neurons in layer 2/3. ***(3a right)*** Example fluorescence intensity traces (ΔF/F; grey portions indicate significant Ca^{2+} transients) for three example cells from the left panel on correct right (red) and left (blue) trials. ***(3b)*** Activity patterns during the task for cells 1–3 from 3a.Colour-coded ΔF/F traces for individual correct left and right choice trials.Each row is a single trial aligned to the cue offset, turn onset and trial end. ***(4a)*** Histogram of the times of the centre-of-mass of the mean ΔF/F trace (tCOM) for choice-specific, task-modulated cells.Cells were separated into three groups (cue-,delay- and turn-preferring cells; varying shades of green) based on peaks in the distribution. ***(4c)*** Sorted normalized mean DF/F traces for cuepreferring (n=101), delay-preferring (n=133) and turn-preferring (n=170) cells, aligned to the trial start, cue offset and turn onset, respectively, on the preferred trial-type. ***(4d)*** Normalized mean ΔF/F traces for all the choice-specific, task-modulated cells (one cell per row) imaged in all mice (n=404 cells from 6 mice) divided by left-preferring and right-preferring cells. Traces were normalized to the peak of each cell's mean ΔF/F trace on preferred trials and sorted by the peak time.“ (Harvey et al., 2012)

After they ordered the activity patterns according to the time it was obvious that the Ca^{2+} transients of the cells formed a sequence of neuronal activation over the whole trial length (**Figure 2:** 4d). Classes of cells with cue, delay or response activity could be seen when they checked the distribution of activity times of all cells in the population (calculated for each cell as the centre-of-mass (COM) in time of the mean ΔF/F, t_{COM}) (**Figure 2:** 4a). COM is a point, can be real or imaginary, where whole of the body's mass can be assumed to be located or concentrated. It is like balancing a ruler on your finger.

But still in each class different cells were active at different times and formed sequences (**Figure 2:** 4c). Nevertheless choice-specific sequential activation of neurons were not seen when the mice got the visual stimuli alone or just by the running patterns of the mouse.

As mentioned in the experimental setup 65 cells were simultaneously imaged and in each field-of-view (**Figure 2:** 3a) there are activity peaks from right and left preferring cells and the cell number of both types were approximately equal. No anatomical seperation of the task-modulated, choice-specific cells was present. Moreover different populations of cells were intermixed. This holds true in the same way for the cue-, delay or response cells.

4 Conclusions

In final consideration Harvey, Coen and Tank showed that movement planning through a virtual T-Maze, based on sensory information and on memory, relies on the parietal cortex. Furthermore the choice to make a left or right turn to get the reward, depending on the initial cue, was indicated by sequences of neuronal activity in different neuronal subpopulations (cue-, delay- and response cells), where a single neuron was only activated at a defined time point during the task. Following this further these neuronal dynamics are already present before the delay period, from the moment where the cue was presented. So it seems that the ordered progression of the neuronal activity patterns reflects the mouse future choice. Working memory including making a choice is reflected by a sequence of activation moving from one population of neuron to another in an ordered progression over time and the currently active cell contains all information about temporal and spatial progression. Contradictory to previous stereotypic models of PPC activity it can be that the PPC, during behavioural tasks including a spatial and temporal component, utilize different sequence dynamics to deal with the different demands of the task.
Some models for the cells with the same response pattern emphasized an anatomical patched clustering, but this new findings support a model in which subnetworks are intermingled in the PPC and where mouse brain microcircuits are composed of functional motifs of neuronal activation.

References

Baddeley A. "Working memory: looking back and looking forward". *Nature Reviews. Neuroscience* **4** (10): 829–39 (2003).

Bear Mark F, Connors Barry W., Paradiso Michael A.. Neuroscience: Exploring the Brain (3 ed.): Lippincott, Williams &Wilkins (2007)

Calton, J. L. & Taube, J. S. „Where am I and how will I get there from here? A role for posterior parietal cortex in the integration of spatial information and route planning.“ *Neurobiol. Learn. Mem.* **91**, 186–196 (2009).

Curtis CE, D'Esposito M . "Persistent activity in the prefrontal cortex during working memory". *Trends in Cognitive Sciences* **7** (9): 415–423 (2003).

Curtis CE, Lee D. "Beyond working memory: the role of persistent activity in decision making". *Trends in Cognitive Sciences* **14** (5): 216–222 (2010).

Dash Pramod K., Moore Anthony N., Kobori Nobuhide, Runyan Jason D.„Molecular activity underlying working memory“ *Cold Spring Harbor Laboratory Press Learning&Memory* **14**: 554-563 (2007).

Dias-Ferreira Eduardo, Coen Costa Rui M., „The symphony of choice“.*Nature Research News&Views* **484**, 42-43 (2012).

Dombeck D. A., Harvey Christopher D., Tian L., Looger L. L., Tank David W. „Functional imaging of hippocampal place cells at cellular resolution during virtual navigation“.*Nature Neuroscience* **13**, 1433–1440 (2010).

Fuster JM. "Unit activity in prefrontal cortex during delayed-response performance: neuronal correlates of transient memory". *Journal of Neurophysiology* **36** (1): 61–78 (1973).

Harvey Christopher D., Coen Philip, Tank David W. „Choice-specific sequences in parietal cortex during a virtual-navigation decision task“.*Nature* **484**, 62-68 (2012).

Heekeren H.R. et al. "The neural systems that mediate human perceptual decision making". *Nature Reviews. Neuroscience* **9**: 467–479 (2008).

Smith EE, Jonides J. "Storage and executive processes in the frontal lobes". *Science* **283** (5408): 1657–61 (1999).

Evidence for the Role of Mushroom Body Output Neurons in Memory Based Decision Making

Achim Meyer

August 21, 2012

Abstract

The role of single neuron activity in decision making is elusive. This term paper summarizes conditioning experiments, i.e. what could be understood as decision making, done by Strube-Bloss et al. [SBNM11]. In these experiments honey-bees learned correct responses while being conditioned. However, the pseudo single-neuron recordings from the bees mushroom-bodies output layer did not reflect quantifiable short-term plasticity in comparison between the pre- and post-phase of conditioning. Correspondingly it might be concluded that these putative neurons are not involved in learning and thus in the process of forming decisions.
In contrast results of the post-test indicate involvement of the mushroom-bodies output layer in memory formation. More exactly this memory formation seems to be the result of two putative kinds of plasticity in neuronal responses. On the one hand fast changes between responding and not responding to a stimulus was coined 'switching'. On the other hand the rather slow changing of response strength was called 'modulating'.
Moreover stimulus response could be encoded from the mushroom-body output layer 150ms after stimulus onset in the post-test. Thus, overall the mushroom-body is not only associated with memory formation, but also with memory based decision making.

1 Decision making in the bee

A crucial challenge in decision-neuroscience is to understand the neural basis of the process underlying decision making [Hue10]. This neural basis can be investigated at a single-neuron, population and whole brain level. Decoding single neuron activity is promising to understand decision processes as single neurons were shown to encode decision variables [SDM97]. Since measurements of single neuron activity are seldom available in humans they are frequently acquired in animal models.
Strube-Bloss et al.[SBNM11] investigated the decision making process in honey-bees at a single neuron level. They utilized an olfactory reward conditioning paradigm to explore the role of single neuron plasticity in the honey-bees mushroom-body. The resulting recordings provide evidence for how short and long-term plasticity give rise to memory formation with respect to a decision task.

2 Results

Single neuron recordings were acquired in more than 87 fixated honey-bees performing a conditioning experiment [SBNM11]. The experiment consisted of a control condition, a conditioning condition and a post-test.

2.1 Control

In the control condition all conditional olfactory stimuli (CS) were presented to the bees without the unconditioned stimulus (US; here a sucrose reward). Most (75%) of the recorded extrinsic neurons (EN) of the bees mushroom-body (MB) did significantly respond to at least one of the ten utilized odor stimuli. Majority of those responding ENs (70%; 52.5% overall) were sensitive to more than five of the presented scents.

2.2 Conditioning

During the conditioning condition - for every bee a different CS (CS+) was paired with the US. In this way the bees decision to reach out for feed by extending their proboscis was conditioned. They learned to exhibit the proboscis extension response (PER) within 500ms, when certain odors were presented. In the course of conditioning 50% of the ENs yielded, on average, a significant response to CS+. However, also around 50% of ENs responded to the other CS (CS-).

2.3 Post-test

2.3.1 Kinds of neuronal plasticity

Three hours after the conditioning condition the conditioning experiment was repeated in a post-test. During the post-test more than 80% of the EN yielded a significant response to CS+. I.e. the response to CS+ was stronger during post-test than during conditioning. In contrast, the response to CS- did not change significantly. In a comparison between baseline condition and post-test two types of plasticity in EN, namely 'switching' and 'modulating', were observed (figure 1). Switching neurons did either develop a response to the CS+ (they 'recruited') or they did seemingly drop response to unrewarded CS (they 'dropped'). Modulating neurons moderately changed response spectra by increasing (they 'increased') or decreasing (they 'decreased') response strength towards one or more CS. Notably switching and modulating plasticity were not present in a comparison between baseline condition and conditioning condition.

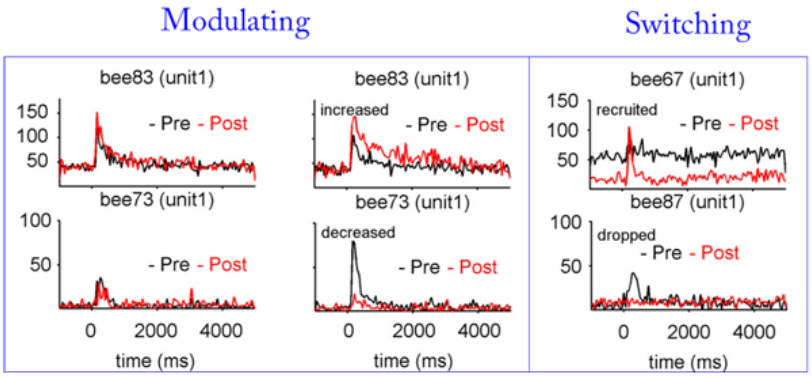

Figure 1: Data from four extrinsic mushroom body neurons [SBNM11]. The graphs show spike-rate histograms for the control condition (black line) and the post-test condition (red line). The histograms corresponding to neuron unit1 of bee83 is an example of an increasing/modulating EN. Unit1 of bee73 displays firing-rates of an decreasing/modulating EN. The plot from NE unit1 bee 67 illustrates recruitment. Finally the unit1 neuron of bee87 yields a dropped response.

2.3.2 Tuning of single neurons

Tuning characteristics of modulating and switching ENs are apparently different. While switching ENs feature higher life-time sparseness values than modulating ENs, modulating ENs generally present higher 'empiric' SNR (figure 2). This could be general reflection of the information processing trade-off between sensitivity and specificity. I.e. modulating ENs are more sensitive and hence less specific to certain stimuli. The contrary seems to be true for switching ENs.

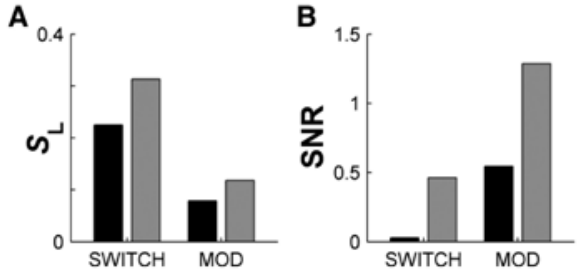

Figure 2: The two bar plots illustrate lifetime sparseness(S_L) of ENs in plot A and 'empiric' SNR in plot B [SBNM11]. The black bars represent results in the baseline condition, while the grey bars represent results of the post-test. Both kinds of ENs (switched and modulated ones) exhibit the same qualitative changes - sensitivity(SNR) and specificity(S_L) increase. However, modulating neurons in general yield higher sensitivity whilst switching neurons in general exhibit higher specificity.

2.3.3 Encoding the rewarding stimulus

Additionally activity of switching and modulating ENs can be grouped into corresponding population ensembles. Thus the difference in each of the two EN population with respect to CS+ and other odors can be computed. These contrasts between CS+ and other CS reach their significant maximum 150-200ms after stimulus presentation.

3 Methods

3.1 Conditioning paradigm

As a baseline/control condition naïve bees were fixated and they were presented ten different odors in a pseudo-random order. Each olfactory stimulus was presented ten times through a stream of air. The inter trial interval (ITI) was 1 minute. In the sequential reward conditioning condition five out of the ten

odors were presented again. In accordance to the first condition each odor was presented ten times in a pseudo-random order with a ITI of one minute. However one of the odors, the rewarding stimulus (CS+), was paired with a sucrose reward (US). In this way the proboscis extension response (PER), i.e. the bees decision to reach out for feed, was conditioned. Three hours later the conditioning condition was repeated as a post-test to research long-term effects of the conditioning.

3.2 Electrode placement

To quantize the decision, i.e. extending or not extending the proboscis, one electrode was attached to the muscle associated with the PER. In honeybees mushroom-body (MB) extrinsic neurons (EN) were shown to be involved in the PER [ORMM07]. Thus to record neural activity associated with the PER three electrodes were put near the alpha-lobe of the MB where ENs are located. In order to ensure correct placement of the electrodes an fluorescence agent was applied.

3.3 Data analysis

3.3.1 Unit identification

Respectively two out of the three EN electrodes were contrasted. This resulted into three 20kHz sampled signals. Those signals were bandpass filtered between 1Hz and 9kHz. In order to detect spikes the signals were again highpass filtered at 600Hz. Template-matching spike sorting served to identify action potentials potentially corresponding to single-neuron. PCA dimensionality reduction ensured that the same pseudo single-neuron were recorded in different conditions. To avoid double detection of single units in several channels an signal to noise (SNR) criterion was applied.

3.3.2 Response detection

If single neuron units were responding to a stimulus was determined by two methods: Firstly by testing for a significant difference in interspike intervals (ISI) before and after stimulus presentation. Secondly by pooling all measurements corresponding to a certain odor and testing for a significant difference between activity before and after stimulus onset. The first method is sensitive to rather slow responses (order of several 100ms) while the second method is sensitive to faster responses (order of several 10ms).

3.3.3 Tuning measurements

The firing-rate of a unit was estimated by a kernel method [NAR99]. The firing-rate was used to determine the tuning of units towards the presented odors.

Again two measurements were utilized. On the one hand lifetime-sparseness was computed [VG00]. On the other hand an 'empiric' SNR estimate was calculated [MRV$^+$03]. Additionally for every stimulus a vector of all responses pooled from all recorded neurons was created.

References

[Hue10] S.A. Huettel. Ten challenges for decision neuroscience. *Frontiers in neuroscience*, 4, 2010.

[MRV$^+$03] C. Mehring, J. Rickert, E. Vaadia, S.C. de Oliveira, A. Aertsen, and S. Rotter. Inference of hand movements from local field potentials in monkey motor cortex. *Nature neuroscience*, 6(12):1253–1254, 2003.

[NAR99] M. Nawrot, A. Aertsen, and S. Rotter. Single-trial estimation of neuronal firing rates: from single-neuron spike trains to population activity. *Journal of neuroscience methods*, 94(1):81–92, 1999.

[ORMM07] R. Okada, J. Rybak, G. Manz, and R. Menzel. Learning-related plasticity in pe1 and other mushroom body-extrinsic neurons in the honeybee brain. *The Journal of Neuroscience*, 27(43):11736–11747, 2007.

[SBNM11] M.F. Strube-Bloss, M.P. Nawrot, and R. Menzel. Mushroom body output neurons encode odor–reward associations. *The Journal of neuroscience*, 31(8):3129–3140, 2011.

[SDM97] W. Schultz, P. Dayan, and P.R. Montague. A neural substrate of prediction and reward. *Science*, 275(5306):1593–1599, 1997.

[VG00] W.E. Vinje and J.L. Gallant. Sparse coding and decorrelation in primary visual cortex during natural vision. *Science*, 287(5456):1273–1276, 2000.

Anna Nowak

Reward encoding and reward prediction

"An identified neuron mediates the unconditioned stimulus in associative olfactory learning in honeybees"

Hammer, M., *Nature*, Vol 366, 4 November 1993

For the first time, M. Hammer was able to identify a single neuron mediating the unconditioned stimulus in classical conditioning of the proboscis extension response in the honeybee.

Classical conditioning

In classical conditioning a neutral stimulus (conditioned stimulus = CS) can be trained to elicit a response that is originally evoked by another unconditioned stimulus (US). Pavlov first observed associative learning in 1927 when a neutral stimulus (CS = the ringing of a bell) elicited a conditioned response (CR = increased salivation) which is originally elicited (unconditioned response = UR) by an unconditioned stimulus (US = food; Pavlov I.P., 1927); with these findings he built the foundation for future theories of learning. Also honeybees can learn to associate two unrelated stimuli in this manner.

Proboscis extension in the honeybee

Proboscis extension is a reflex in honeybees that is part of its feeding behavior. The proboscis is a tubular mouthpart in bees that serves the sucking of liquids. Its extension is triggered by antennal sucrose stimulation. Sucrose stimulation of the antenna is the US that leads to proboscis extension (UR). Interestingly, a puff of odour as CS can also elicit proboscis extension (CR; Bitterman, M.E. et al., 1983).

Finding neurons that mediate the unconditioned stimulus

Neurons that are involved in mediating the US need to fulfill two criteria that allow it to function in associative learning. Firstly, they need to show a response to the US and secondly, they must converge with the pathway of the CS. To identify neurons that match the abovementioned criteria in honeybees, single impaled cells in the subesophageal ganglion were tested for their responsiveness to sucrose (US) and visualized by staining.

Intracellular recordings are used to study the activity of a specific neuron. During intracellular recordings, microelectrodes are inserted into a particular neuron to measure the membrane potential. The resting potential of a neuron is based on the ion concentration of sodium and potassium ions across the membrane and lies between -60mV and -80mV. During an action potential, changes in the ion concentration across the membrane lead to the depolarization of the neuron, the membrane potential reaches up to +40mV. This change in membrane potential during an action potential can be measured and quantified. The activity of the neuron can be described as the number of action potentials or the frequency of action potentials across time (Carter, M., Shieh, J., 2009).

VUMmx1 and its role in mediating the unconditioned stimulus

Hammer and colleagues measured the activity of different neurons in the subesophageal ganglion using *in vivo* intracellular recordings. They found a single neuron, the interneuron VUMmx1 (ventral unpaired median neuron maxillare 1), which responds to sucrose with a long burst of action potentials. Furthermore, it innervates neuropiles (synaptically dense networks of nerve fibers) in the brain that are involved in the processing of odour. VUMmx1 thus shows a response to the US (sucrose) and also converges with the pathway of the CS (odour). It consequently fulfills the aforementioned two criteria that suggest its involvement in associative learning.

Conditioning depends on temporal contiguity between the CS and US. Forward pairing describes a situation in which the onset of a CS precedes the onset of an US. In this case, the CS signals that the US will follow shortly after and results in the association between the two stimuli. In contrast, in backward pairing the sequence is reversed, the CS immediately follows the US. This does not lead to the association of the CS with the US and therefore acts as a control for non-associative effects.

To find out whether VUMmx1 mediates the US in honeybees the authors set up an experiment where they replaced the US delivery with the depolarization of VUMmx1. In a positive control, they used forward and backward training with a sucrose reward as US. They tested the change in response by comparing the pretest 5 minutes prior to the training with the test 10 minutes after the respective training. In another group of bees they did the same experiment but replaced the US with the depolarization of VUMmx1. Remarkably, they found that there is an increase in the response of M17 (the muscle responsible for the proboscis extension reflex) after forward pairing, but not after backward pairing, irrespectively of using sucrose as reward or the activation of VUMmx1. The increased motor response correlates

with a long-lasting increased action potential frequency (fig.1). To clarify the specificity of this effect the bees were differentially conditioned to two different odours (fig.2). This means that one odour was paired with the US (CS+); the other one remained unpaired (CS-). A prolonged excitation of VUMmx1 was recorded as response to the paired stimulus (CS+) but not to the unpaired stimulus (CS-). Thus, VUMmx1 responds similarly to a learned odour as it does to an US, which is in line with the idea for associative learning that the “meaning” of the US is transferred to CS.

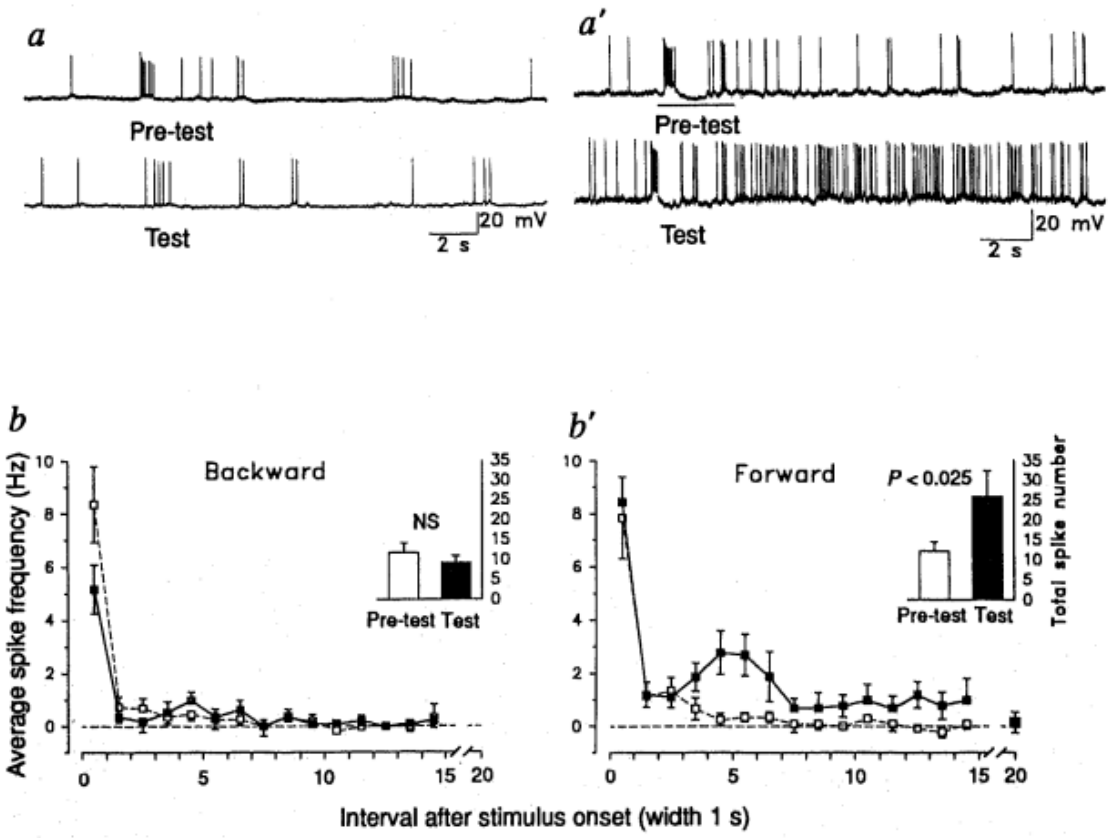

Fig.1: Plasticity of VUMmx1’s odour response in substitution experiments. *a* and *a’*: The rapid phasic odour response is reduced after backward paring compared to pre-test (*a*) but is increased after forward pairing (*a’*). *b* and *b’*: Post-stimulus interval histogram from 15 consecutive 1-s intervals after stimulus onset (Hammer, 1993).

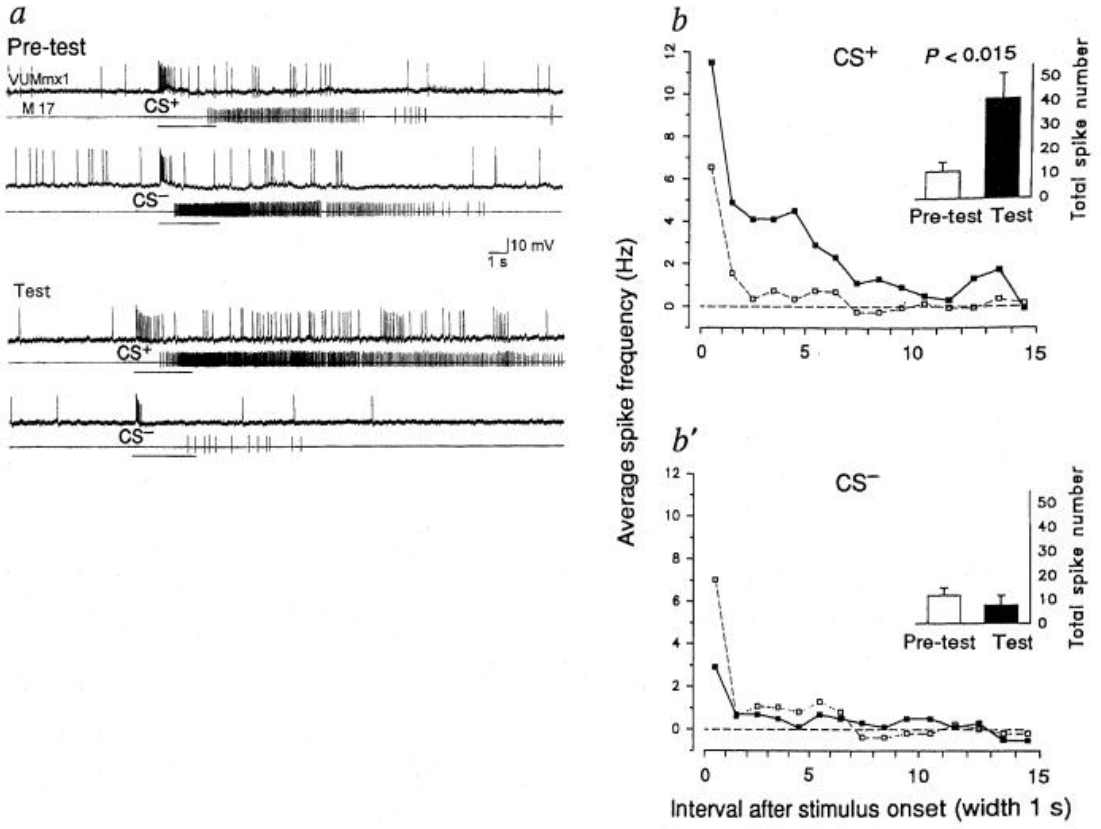

Fig.2: Response plasticity of VUMmx1 in differential conditioning experiments. Bees were differentially conditioned to two odours (carnation, orange-blossom). One odour was specifically paired with the US (CS+); the other (CS-) was delivered specifically unpaired inbetween. *a*: Responses recorded from VUMmx1 and M17 5 min before (pre-test) and 10 min after (test) differential conditioning. *b* and *b'*, post-stimulus interval histogram of CS+ (*b*) and CS- (*b'*) (Hammer, 1993).

Conclusion

In conclusion, it was possible to identify a specific neuron that appears to be the cellular basis of an unconditioned stimulus. The long-lasting discharge of VUMmx1 by odour allows the assumption that the responsiveness of the neuron to an odour could depend on the associative strength of the odour. This is also shown by the different responses to two differentially conditioned odours.

A follow up study showed that the molecular basis of associative learning mediated by VUMmx1 in honeybees is the neuromodulator octopamine (Hammer and Menzel 1998). They showed that replacing sucrose with octopamine injections into the mushroom bodies or antennal lobes and pairing those with odours also lead to associative learning.

References

Bitterman, M.E., Menzel, R., Fletz, A. Schäfer, S. (1983).: Classical Conditioning of Proboscis Extension in Honeybees (*Apis mellifera*). *J. comp. Physiol.,* Vol. 7, 107-119

Carter, M., Shieh, J. (2009): Guide to research techniques in neuroscience. Academic Press, Boston.

Hammer, M. (1993): An identified neuron mediates the unconditioned stimulus in associative olfactory learning on honeybees. *Nature*, Vol. 366, 59-63.

Hammer, M., Menzel, R. (1998): Multiple Sites of Associative Odour Learning as Revealed by Local Brain Microinjections of Octopamine in Honeybees. *LEARNING & MEMORY* 5:146–156.

Pavlov, I.P. (1927): Conditioned Reflexes: An Investigation of the Physiological Activity of the Cerebral Cortex (Dover, New York).

Summary: Speed and accuracy of olfactory discrimination in the rat; Uchida N, Mainen ZF (2003) and
Rapid encoding and perception of novel odors in the rat; Wesson DW, Carey RM, Verhagen JV, Wachowiak M (2008)

by Masin Abo-Rady

Perceptual decision making can be used at the discrimination of two odors to find out how neuronal and behavioral responses differ in reaction to those dissimilar odors. So it is interesting to study the limits of perception and corresponding behavioral translation.
The goal of this work is to show the temporal constrains on the accuracy of olfactory discrimination in rats. The following questions will be elaborated:
1. How fast is an odor discrimination performed?
2. Does it take more time to discriminate odors more accurately?
3. Are there differences in discrimination speed, if the odors are chemically similar?

Introduction
When an odor is perceived, the olfactory receptor neurons (ORNs) are stimulated and show odor specific spiking patterns. Subsequently the glomeruli in the olfactory bulb (OB) are activated and show a unique spatial pattern[1], which can be visualized and processed to spatial maps. It is known that odor discriminations show highly overlapping maps, which suggests that the information for discriminations can be provided by these fine differences in the spatial representation[2]. This summary will focus on Uchida et al. 2003.

Methods
Male rats were trained in a two-choice odorant discrimination test under water restriction as motivation. Each trial began with a nose poke into an odor sampling port, which started a computer controlled delivery of an odor A for 1 second. Subsequently the rat had to choose one out of two further ports, one with odor A and the other with odor B, to get water as a reward. The reward was only available for 2 seconds in the port presenting odor A. Different odors were used and the movement time and time for discrimination were measured. (This psychophysical test should underline the speed and accuracy of odor discrimination.)

Results
For dissimilar odor pairs the test showed that rats discriminated odors with an accuracy of 97,4% in a median odor sampling time of 223 ms. Almost the same results were received for odor pairs which show highly overlapping patterns of glomerular actions (229 ms at 95,6% accuracy). Completing this test, using four similar odor pairs (e.g. hexanol versus heptanol) and two not similar odor pairs (e.g. caproic acid versus hexanol), it was observed that the accuracy significantly correlated with the odor similarity (the higher the odor similarity the higher the accuracy of discrimination), but the odor sampling time did not.
To increase the difficulty of discrimination, eight mixtures of two odors in different proportions were presented to the rats (**Fig. 1a**). This performance revealed a sigmoidal function (**Fig. 1b**), in which the accuracy of discrimination dropped strongly for mixture ratios about 50/50 (**Fig. 1c**). On the contrary the speed of discrimination did not change significantly. Thus, rats seem to develop a rapid strategy for odor discrimination regardless of the task difficulty.

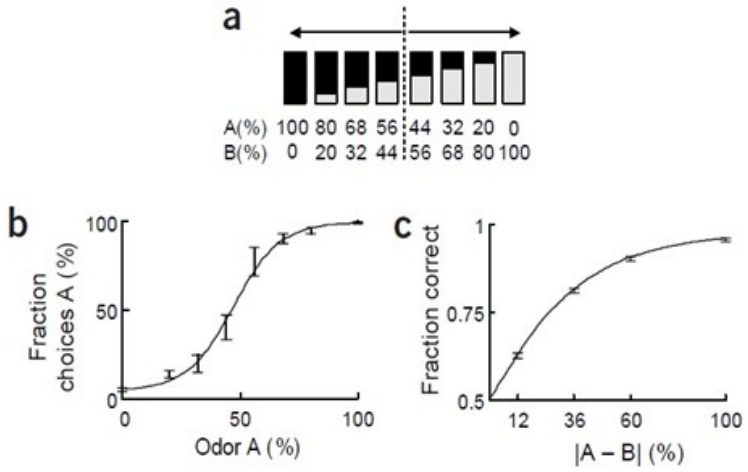

Figure 1: Binary odor mixture discrimination task with manipulated odor quality and discrimination difficulty
(**a**) Odor A and B were mixed in different ratios. The rat was rewarded when it chose the odor associated with the dominant odor in the mixture. (**b**) Performance of one rat in discriminating valeric acid and hexanol. Data from ten sessions (176-288 trials per session) were fitted using a logistic function. (**c**) Discrimination accuracy as a function of mixture ratio. On the abscissa the absolute value of the difference of the pairs is shown [3].

A further point was to see whether the accuracy is dependent on the sampling time irrespective of task manipulations. For each pair of odors and mixture ratio trials were divided according to the odor sampling time, in order to produce a conditional accuracy function [2]. It was observed that the accuracy of discrimination increased rapidly within the first 200 ms, and subsequently flattened (**Fig. 2a**). This happened regardless to mixture ratio (**Fig. 2b**). It was also shown that longer odor sampling times seemed to be associated with a lower accuracy instead of an enhanced one.
As it is known that rats only need short time to discriminate an odor accurately (about 200 ms), it is assumed that only one odor sample, detected with one sniff, is sufficient to show maximum performance in discrimination. To test the sniffing pattern, three rats were implanted with sensors measuring the temperature of nasal air flow. At odor onset the sniffing frequency was the highest followed by a slightly decline while odor sampling period. Despite the difficulty of odor mixtures the number of sniffs did not change (**Fig. 2c**). Every time one to two sniffs were enough to discriminate an odor properly.

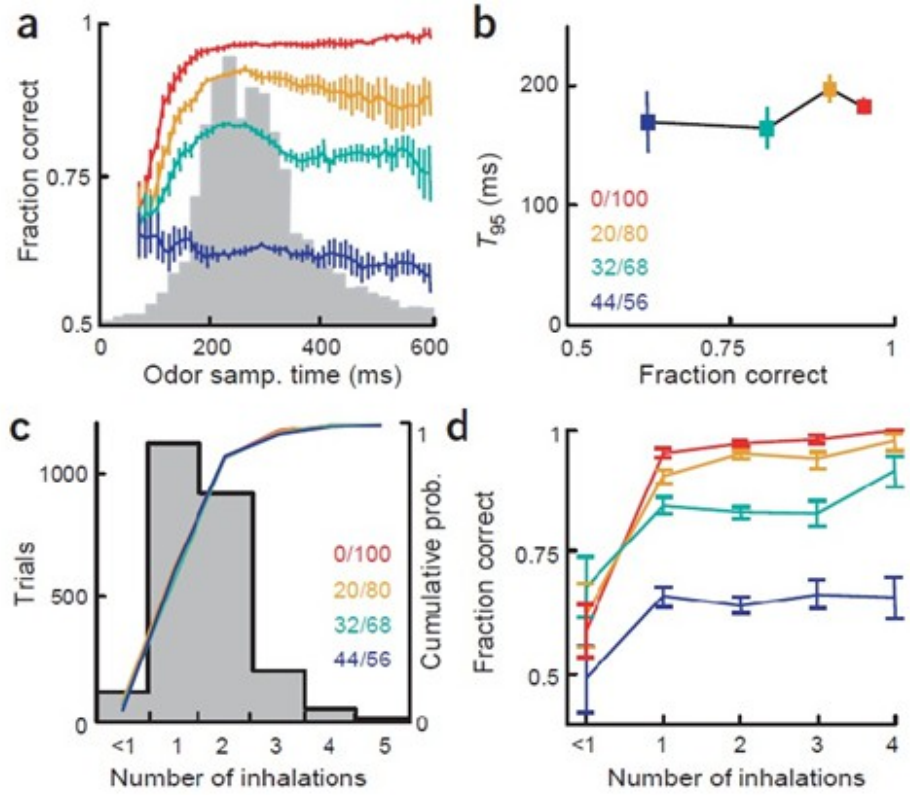

Figure 2 [4]: Odor discrimination accuracy shows asymptotic curve and requires one sniff, regardless of difficulty. (**a**) Accuracy as a function of odor sampling time. Colors correspond to mixture ratios as indicated in **b**. In the background the distribution of odor sampling times is shown (n= 4 rats, 6 odors) (**b**) Time to reach 95% of asymptotic accuracy (T_{95}) for all odor pairs. Colors indicate the mixture ratios. (**c**) Distribution of number of sniffs during the odor sampling period for a single rat pooled across all trials (grey shadings). Cumulative distribution functions for the number of sniffs are shown separated by mixture ratios. The category "<1" contains trials with no inhalation or in which odor occurred during an inhalation. (**d**) Choice accuracy as a function of number of sniffs. Line colors correspond to mixture ratios as indicated in **c**.

Discussion

The performed psychophysical tests which were performed showed some clear constraints of odor discrimination in rats. It was shown that discrimination is achieved in less than 300 ms or about two sniffs. The Analysis including natural variability in odor sampling period revealed that maximum accuracy was accomplished in less than 200 ms, which is equivalent to one sniff (**Fig. 2d**). The discrimination accuracy did not improve, even if more sniffs were taken. Further the test showed clear constraints of how fast perception and neural activity need to be processed to ensure proper odor discrimination. It was indicated that discrimination speed is independent of chemical similarity or the mixture difficulty of two odors. Apart from that the accuracy of odor discrimination evolves quickly, saturates after short odor sampling time and depends on the mixture difficulty.

The study of Uchida and Mainen (2003) focused on well-trained animals. To gain more insight in the mechanisms and the procedure of discrimination Wesson et al. performed some experiments with the focus on perception and encoding of novel odors in rats. Therefore optical imaging with calcium-sensitive dyes was used to demonstrate which receptor neurons, with input to the rat olfactory bulb, were activated. This method enabled the subtle outline of the timing of odor perception when a novel odor occurred. That novel odor evoked spontaneously expressed odor discrimination with high-frequency exploratory sniffing. Using this imaging allowed separate estimation of how long the transmission of sensory signals needed to the brain and the time needed for central events underlying odor discrimination and response initiation[1]. Interestingly, discrimination of a novel odor from a

learned one occurs in 150-200 ms, and is by so at least as fast as discrimination of learned odors. A probable explanation is that in the training of discriminating odor from another, the animal gets used to the repeatedly presented odor and thereby habituates to this stimulus, which is expressed in a slower and weaker reaction. Partitioning the whole process, 50 ms after sensory input arrived in the brain the behavioral response begins, which shows that the central processing of discrimination is extremely rapid. Moreover it is completed even before spatial maps of glomerular activity have fully developed. This indicates that activation of ORNs below maximum is sufficient so start a reaction, which means that the response amplitude of many glomeruli is reached after a behavioral response has already begun.
Further investigations showed that only the presence of an odor is not enough to trigger perception and discrimination. It is required that rats first inhale odors to activate the ORNs, which happens with the first sniff.

Conclusion

Uchida and Wesson showed that odor discrimination happens very quickly in about 200 ms. It was also displayed that discriminating a novel odor happens even a little bit faster than the determination between two learned odors. The different parts of odor discrimination were shown, and it became clear that discrimination is essential for estimating the significance of different odors and the ensuing actions and behavior of an animal.

References:

[1] Wesson DW, Carey RM, Verhagen JV, Wachowiak M (2008) Rapid encoding and perception of novel odors in the rat. PLoS Biol 6(4), e82
[2] Uchida N, Mainen ZF (2003) Speed and accuracy of olfactory discrimination in the rat.
Nat Neurosci 6(11):1224-9
[3] Text modified from Uchida et al. 2003 Figure 3
[4] Figure 2 a and b modified from Uchida et al. 2003 Figure 5 a and b, Figure 2 c and d modified from Uchida et al. 2003 Figure 6 c and d

The mechanism behind perceptual decision-making in humans

Florian Bilz (4544540, Master Biology, FU Berlin)

Original article: *A general mechanism for perceptual decision-making in the human brain* (Heekeren et al., 2004)

Introduction

Perceptual decision-making is the behavioural response to a perception in the environment.
An essential question is how and where these decisions are made in the human brain.
Former studies were performed using single-unit recordings in monkeys which had to perform discrimination tasks [1-5]. From the results it was proposed that environmental information coded by different pools of spike frequency specific neurons (selectively tuned to different perceptual conditions like the direction of motions) are integrated providing the base for the animals decision making [6]. Findings in other studies suggest that higher-level cortical regions (for instance the dorsolateral prefrontal cortex (DLPFC), [1, 6]) compute perceptual input by comparing the outputs of selectively tuned lower-level sensory neurons [7-9]. They also found that the neuronal activity in areas involved in decision-making gradually increased and then remains elevated until a response was given. The increase was slower during difficult trials than in easier ones [7, 8].
To investigate if these processes are also true for more complex cognitive operations in humans Heekeren et al. used functional magnetic resonance imaging (fMRI) while participants had to decide whether an image was a house or a face. From previous neuroimaging studies it is known that there are face and house selective regions in the human ventral temporal cortex [10-14]. Other studies found out that a change of the blood-oxygen-level-dependent (BOLD) signal in a specific region is a reliable indicator for changing neuronal activity in this region [15, 16].
In this study Heekeren and colleagues wanted to identify the regions for face and house recognition more precisely and wanted to know if there are higher-level cortical regions with outputs proportional to the differences of the activities of face and house responsive regions, respectively.

Methods

Two groups of 12 healthy volunteers without any neurological, visual or psychiatric disorders participated in the imaging and behavioural experiments, respectively.
Subjects were shown 38 pictures of faces and houses while using magnetic resonance imaging (MRI). To vary difficulty distracting noise was added to the presented pictures. Pictures were processed so that all resulting images had an identical frequency power spectrum [17] with graded amount of noise. The images had two different amounts of noise, lower noise (correctness above 95 % = suprathreshold) and higher noise (correctness down to 82 % = perithreshold).
Images were shown for 1 s on a back projection screen and after a forced delay (analogous to a compareable monkey study [7]) subjects had to decide (button press) whether the image showed a house or a face.
The whole brain data were collected by a 3T GE Signa scanner (GE Medical Systems). MRI data were pre-processed for analysis of brain image series and modelling. Trials, in which subjects gave no or incorrect responses, were pooled together and used as error trials. Thus,

only correct trials were used for modelling regressors for the four conditions (suprathreshold face and house and perithreshold face and house). For more details see *Methods*, Heekeren et al. (2004).

Results

Heekeren et al. identified for each subject voxels in the ventral temporal cortex responding more specific to faces than to houses and vice versa (Fig. 1a). These regions were selective for one category (faces or houses) and showed higher responses to suprathreshold than to perithreshold images. This indicates that activity in those regions represent the sensory evidence for the two respective categories (Fig. 2b).
The frontal eye field (FEF, Brodmann area (BA)6), the supplementary eye field (SEF) and the parietal regions (interparietal sulcus, IPS) gave larger responses to difficult trials indicating requiring more attentional resources for correct performances (Fig. 2a).

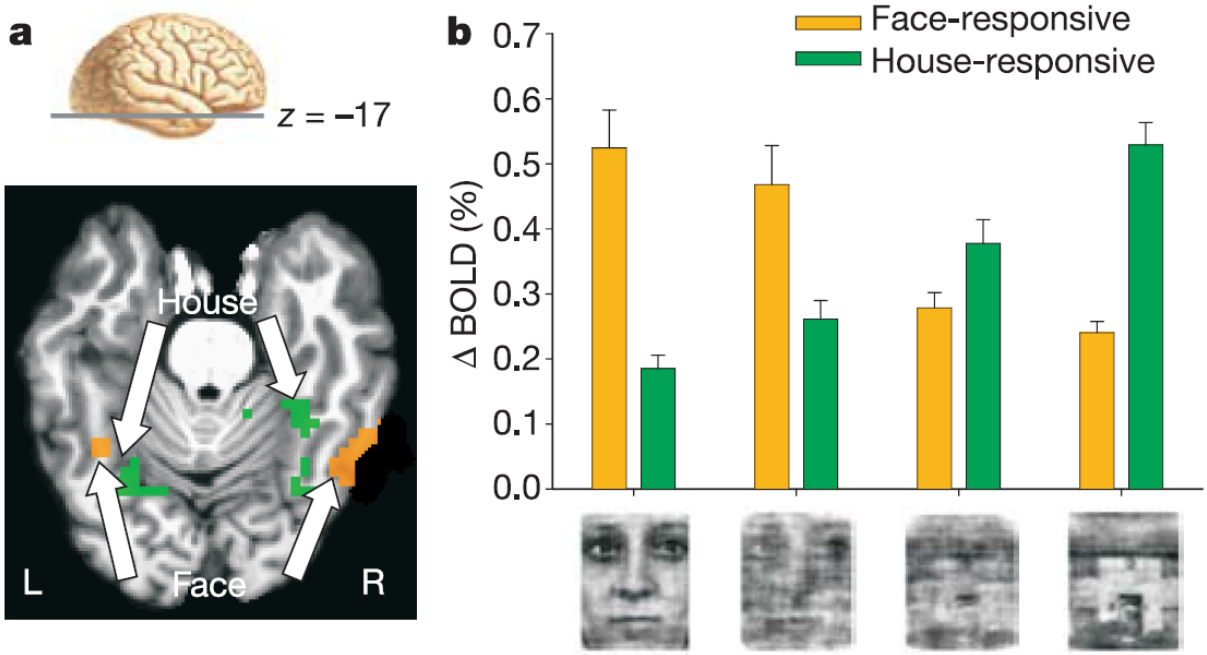

Figure 1: from Heekeren et al. (2004). FMRI data illustrating representation of sensory evidence in maximally face- and house-responsive voxels. **a**, Maximally face- (Face, orange) and house-responsive (House, green) voxels in one subject. **b**, BOLD change corresponds to perceptual evidence for respective classes of stimuli. Mean responses (n = 12, error bars represent standard error of the mean) in face- and house-selective voxels to the four different conditions (from left to right: suprathreshold face (~ 10% noise), perithreshold face (~ 45%), perithreshold house (~ 53%), suprathreshold house (~ 10%)). For the respective preferred category, both face- and house-selective regions responded more to suprathreshold than to perithreshold images (face-selective: $P < 0.041$, paired t-test one-tailed; houseselective: $P < 0.001$) while the opposite was true for the non-preferred category (faceselective: $P < 0.013$; house-selective: $P < 0.002$). For face-responsive: suprathreshold face > perithreshold face > perithreshold house > suprathreshold house (analysis of variance, linear contrast, $P < 0.001$); for house-responsive: opposite pattern ($P < 0.001$).

Furthermore in several higher-level decision-making brain regions, e.g. in the superior frontal sulcus (BA8/9), the posterior cingulate cortex (BA31) and the superior frontal gyrus (BA9), the response to suprathreshold images was greater than to perithreshold ones (Fig. 2a). Heekeren et al. also showed that a region in the depth of the superior frontal sulcus is the only region which showed a greater response to suprathreshold images and getting input from lower-level sensory regions (Fig. 2b). Furthermore, the task-related signal changes correlate positive with the task-performance (Fig. 2c).

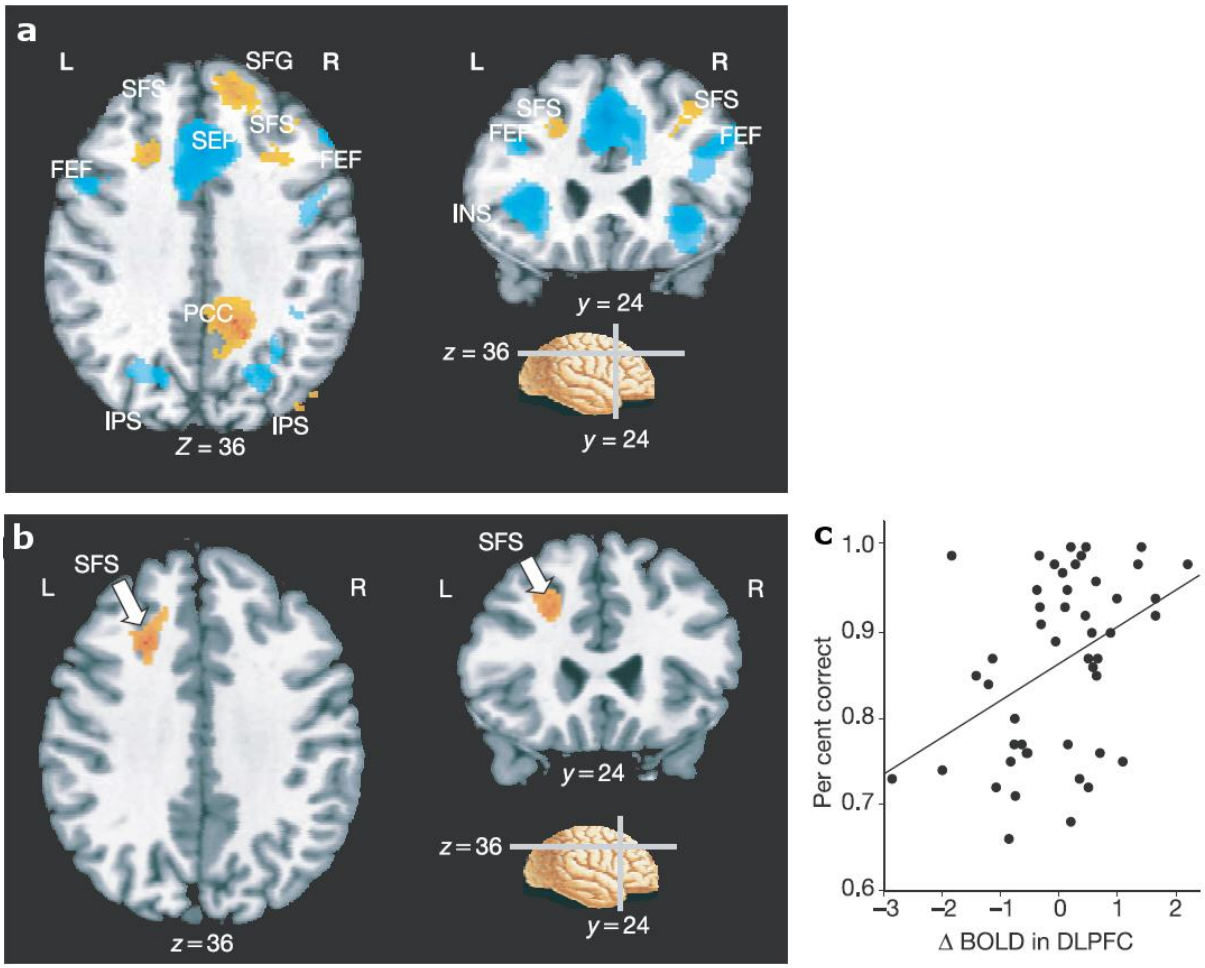

Figure 2: modified after Heekeren et al. (2004). **a**, Brain regions showing a main effect of task difficulty: orange: easier (low noise proportion) > harder (high noise proportion); blue: harder > easier. FEF, frontal eye field; INS, insula; IPS, intraparietal sulcus; PCC, posterior cingulate cortex; SEF, supplementary eye field; SFG, superior frontal gyrus; SFS, superior frontal sulcus. **b-c**: Perceptual decision-making in posterior DLPFC. **b**, Region in the depth of the left SFS, showing both a higher response to suprathreshold images of faces and houses relative to perithreshold images, and a correlation with |Face(t) - House(t)|, suggesting that this brain region integrates sensory evidence from sensory processing areas to make a perceptual decision (BA8/9, easier > harder: x = -24/y = 24/z = 36, z_{max} = 4.20; correlation with |Face(t) - House(t)|: x = -22/y = 26/z = 36, z_{max} = 3.66, coordinates in MNI system refer to local cluster maxima, and z_{max} to the corresponding z-value). **c**, Signal changes in the posterior portion of the DLPFC predicted task performance (r = 0.413, P = 0.004). Points represent average BOLD change and performance for each condition (suprathreshold face, perithreshold face, perithreshold house and suprathreshold house) and subject.

Conclusion

This study showed that pools of selectively tuned lower-level sensory neurons exist. In this case they are tuned to houses and faces and are lying in the ventral temporal cortex. As already shown in single-unit recordings in monkeys [8] the neural activity in lower-lever regions of humans increased proportionally to the strength of the signal. The output of these regions provides sensory information, both in humans and monkeys.

It was also shown that higher-level regions, namely the left posterior DLPFC, perform decision-making tasks by integrating and comparing the output of lower-level sensory neurons in a subtractive process. In Heekeren's study this region showed greater response to suprathreshold images and its activity was correlated to the difference between the signals of the face- and house-selective regions, indicating a putative site for signal convergence and a possible comparison act. These results are comparable to the Shadlen model of perceptual decision-making [7, 8]. Also, the measured signal changes predicted the task performance but were not in line with predicted model data derived from monkey studies. The comparisons process was also shown in electrical stimulations experiments [1]. In other

studies with experiments on perceptual decision-making [18-20] the left posterior DLPFC is activated, too, thus indicating that this prefrontal region has general decision-making function not only in comparing faces and houses.

In lower-level sensory neurons the rate of activity increased slower during more difficult trials (perithreshold images). Higher-level cortical regions responded more to decisions made about suprathreshold images whereas the opposite was true for brain regions associated with the attentional network. This indicates that these regions require attentional resources to form correct performances.

Because the studies in monkeys mostly parallel the studies in humans the basic neural process of perceptual decision-making seems to be some kind of conserved during brain evolution.

References

Reviewed article:

Heekeren,H. R., Marrett, S., Bandettini, P. A. & Ungerleider, L. G. A general mechanism for perceptual decision-making in the human brain. Nature 431, 895-862 (2004).

Further articles:

1. Ditterich, J., Mazurek, M. E. & Shadlen, M. N. Microstimulation of visual cortex affects the speed of perceptual decisions. Nature Neurosci. 6, 891–898 (2003).
2. Newsome,W. T., Britten, K. H. & Movshon, J. A. Neuronal correlates of a perceptual decision. Nature 341, 52–54 (1989).
3. Salzman, C. D., Britten, K. H. & Newsome, W. T. Cortical microstimulation influences perceptual judgements of motion direction. Nature 346, 174–177 (1990).
4. Schall, J. D. Neural basis of deciding, choosing and acting. Nature Rev. Neurosci. 2, 33–42 (2001).
5. Romo, R. & Salinas, E. Flutter discrimination: neural codes, perception, memory and decision making. Nature Rev. Neurosci. 4, 203–218 (2003).
6. Shadlen, M. N., Britten, K. H., Newsome, W. T. & Movshon, J. A. A computational analysis of the relationship between neuronal and behavioral responses to visual motion. J. Neurosci. 16, 1486–1510 (1996).
7. Shadlen, M. N. & Newsome, W. T. Neural basis of a perceptual decision in the parietal cortex (area LIP) of the rhesus monkey. J. Neurophysiol. 86, 1916–1936 (2001).
8. Kim, J. N. & Shadlen, M. N. Neural correlates of a decision in the dorsolateral prefrontal cortex of the macaque. Nature Neurosci. 2, 176–185 (1999).
9. Hernandez, A., Zainos, A. & Romo, R. Temporal evolution of a decision-making process in medial premotor cortex. Neuron 33, 959–972 (2002).
10. Haxby, J. V. et al. The functional organization of human extrastriate cortex: a PET-rCBF study of selective attention to faces and locations. J. Neurosci. 14, 6336–6353 (1994).
11. Kanwisher, N., McDermott, J. & Chun, M. M. The fusiform face area: a module in human extrastriate cortex specialized for face perception. J. Neurosci. 17, 4302–4311 (1997).
12. McCarthy, G., Puce, A., Gore, J. C. & Allison, T. Face-specific processing in the human fusiform gyrus. J. Cogn. Neurosci. 9, 605–610 (1997).
13. Epstein, R. & Kanwisher, N. A cortical representation of the local visual environment. Nature 392, 598–601 (1998).
14. Ishai, A., Ungerleider, L. G., Martin, A., Schouten, J. L. & Haxby, J. V. Distributed representation of objects in the human ventral visual pathway. Proc. Natl Acad. Sci. USA 96, 9379–9384 (1999).
15. Logothetis, N. K., Pauls, J., Augath, M., Trinath, T. & Oeltermann, A. Neurophysiological investigation of the basis of the fMRI signal. Nature 412, 150–157 (2001).
16. Logothetis, N. K. & Wandell, B. A. Interpreting the BOLD Signal. Annu. Rev. Physiol. 66, 735–769 (2004).
17. Rainer, G. & Miller, E. K. Effects of visual experience on the representation of objects in the prefrontal cortex. Neuron 27, 179–189 (2000).
18. Petrides, M., Alivisatos, B., Evans, A. C. & Meyer, E. Dissociation of human mid-dorsolateral from posterior dorsolateral frontal cortex in memory processing. Proc. Natl Acad. Sci. USA 90, 873–877 (1993).
19. Koechlin, E., Ody, C. & Kouneiher, F. The architecture of cognitive control in the human prefrontal cortex. Science 302, 1181–1185 (2003).
20. Heekeren, H. R., Marrett, S., Bandettini, P. A. & Ungerleider, L. G. Neural correlates of a decision in human dorsolateral prefrontal cortex. Soc. Neurosci. Abs Program No. 16.3 (2002); <http://sfn.scholarone.com/itin2002/main.html?new_page_id¼126&abstract_id=13054&p_num=16.3&is_tech=020.01.2004%2006:24:56>.

Summary: Perceptual Learning and Decision-Making in Human Medial Frontal Cortex (Kahnt et al.,2011)

By Isabel Groß, Matr.Nr. 4538164

Structure

1. Introduction

The article ‘Perceptual Learning and Decision-Making in Human Medial Frontal Cortex’ was written by Thorsten Kahnt, Marcus Grueschow, Oliver Speck and John-Dylan Haynes and was published in May 2011 in the journal Neuron. In it, the previous assumption that perceptual learning leads to changes in early visual areas (Sasaki et al., 2010; Seitz and Wannabe, 2005) is replaced by the theory of perceptual learning being part of the framework of reinforcement learning and with that it is based on changes in higher decision-making areas. Evidence for that is given by an orientation discrimination task with human subjects and associated functional magnetic resonance imaging (fMRI).

2. Improvements in Perceptual Decision-Making

The orientation discrimination task was executed with 20 human subjects and lasted 4 days. Subjects had to fixate a central cross while a low contrast Gabor was shown in the right upper visual field (Figure 1A). They had to decide whether the orientation of the Gabor has changed in clockwise or counterclockwise direction and the orientation deviated from 45° up to 4° in both directions. As a reward for a correct answer, the fixation cross turned green, whereas an incorrect answer resulted in a red fixation cross. FMRI data was recorded on the first and last day of the experiment during 6 training runs. The second and third day involved 15 training runs in a mock scanner (Figure 1B).

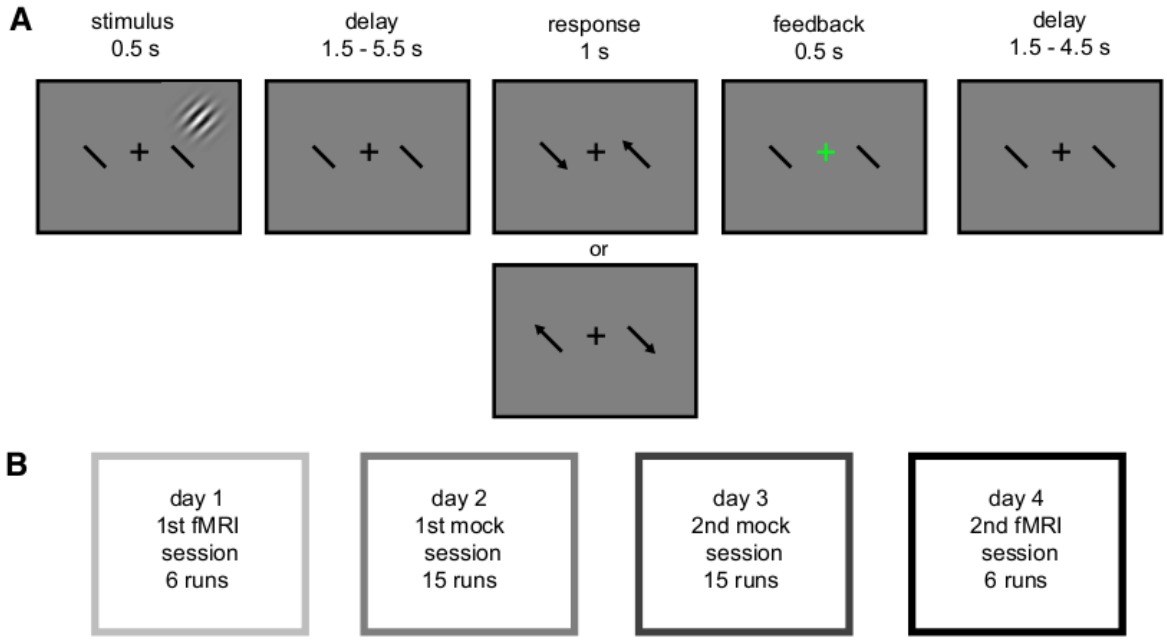

Figure 1. Experimental set-up and time course (Kahn et al. (2011), figure 1 A,B)

(A) Sketch of the orientation discrimination task
(B) Time course of the experiment with the events of each experimental day

The results of this task showed a distinct effect of perceptual learning in which performance of the subjects increased with training during the experiment. The number of correct answers increased with both, the number of training runs and the number of days during the experiment. It could also be shown that subjects became increasingly sensitive to small deviations from 45°.

3. A Reinforcement Learning Model for Perceptual Decision-Making

For better explanation of the results and the improvement of perceptual learning in general a reinforcement learning model was created and compared with the original data of the orientation discrimination task. In the model, the computed decision variable *DV* is the basis of the perceptual choice. *DV* is the product of a sensory stimulus *x* and a perceptual weight *w*. The sensory stimulus *x* is formed from the stimulus orientation minus 45°, whereas the perceptual weight *w* accounts for the ability to read out sensory information provided by the stimulus *x* and which changes over learning. For that it is updated by means of an error-driven reinforcement learning mechanism. A more positive *DV* results in a clockwise decision, whereas a negative *DV* indicate a counterclockwise decision. An expected value

EV is the probability that the current trial will be rewarded and is provided by the absolute value of *DV*. *EV* is then compared with the actual reward *r* of the trial and a reward prediction error δ can be computed, that updates the perceptual weight *w* in proportion to a learning rate α. The decision variables for each subject were calculated and compared with the original data of the task. It could be shown that the reinforcement learning model characterizes subjects' perceptual choices and improvements very well. A significant effect of training runs and of training days of the model data have been revealed and learning process was also accompanied by a steepening of the psychophysical function.

4. Neural Representations shown by fMRI

Once the authors knew that the model makes computations of perceptual learning possible, the neural representations of stimulus orientation and decision variable in the brain were investigated. Therefore functional magnetic resonance imaging (fMRI) was used, where brain activity is measured by detecting associated changes in blood flow. The orientation of the Gabor during the stimulus presentation was significantly encoded in the lower left early visual cortex (Figure 2A), the left lateral parietal cortex (Figure 2B), the precuneus and the medial frontal gyrus. The data also shows that predictions about the orientation of the Gabor can be made (Figure 2A and B, scatterplot on the right) and that activity in some specific subregions increases or decreases with larger angle changes of the Gabor. This suggests that information about the physical properties of the stimulus is encoded in the early visual cortex as well as in higher brain regions. Because the model says that the orientation is not directly responsible for the decision, but the decision variable *DV* plays an important role, the activity patterns of brain regions that are involved in decision making were identified and representations of *DV* were searched. These were found in the left putative lateral intraparietal area (LIP), the anterior cingulated cortex (ACC) and the precuneus but not in the early visual cortex.

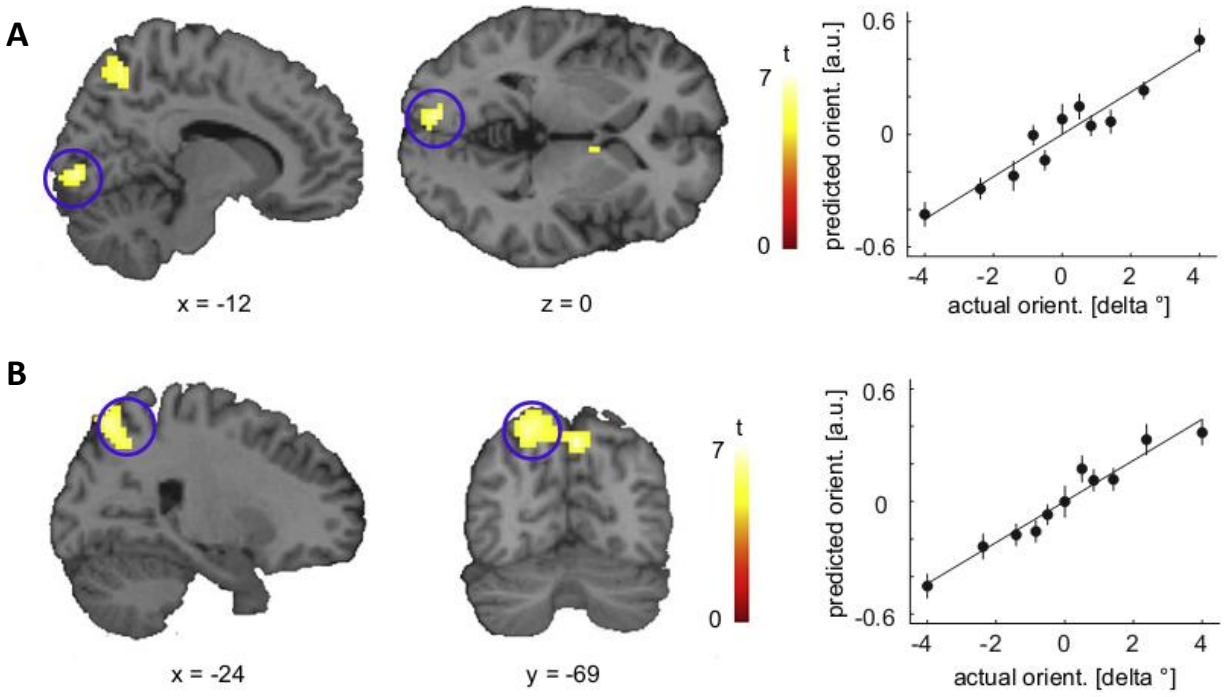

Figure 2. Encoding of stimulus orientation in the brain (Kahnt et al., 2011, figure 4 A,C)

(A) Information about stimulus orientation is encoded in the early visual cortex (blue circle). Scatterplot on the right visualizes the relationship between actual orientations and the predicted ones by the model.

(B) Same as in (A) but for information about stimulus orientation in the lateral parietal cortex (blue circle).

Because the physical stimulus orientation and *DV* of the model are correlated to each other it is difficult to separate the regions where sensory evidence is represented from the regions which are involved in perceptual learning and decision-making. A distinguishable point is that *DV* changes during the learning process, and responsible regions should follow the changes and have more information about *DV* than about the stable stimulus orientation. A t-test analysis of a voxel-wise comparison of the fMRI data between information maps of *DV* and stimulus orientation revealed only one significant cluster in the ACC. In this region there is more information about *DV* present than about the orientation of the Gabor, which leads to the assumption that the ACC plays a key role in perceptual learning.

Next, the possibility of changes in the early visual stimulus representations during the learning process was investigated, because a previous study has suggested this possibility

(Schoups et al.,2001). There were no significant differences if the information about stimulus orientation and the information about *DV* in the early visual cortex. Also, no significant evidence for a changing of the representation of stimulus orientation with training could be shown, because there was no difference in orientation encoding between the first and the second scanning session. All together these results suggest that the course of learning does not lead to changes in the representation of sensory evidence in early sensory areas.

Because alternative learning models could also predict a decision variable which increases over the learning process, more evidences for a real reinforcement learning mechanism were needed. As signed reward prediction error signals can be seen as evidence for reinforcement learning processes (Bayer and Glimcher, 2005; Schultz et al. 1997), these signals from the model were regressed against the feedback-locked BOLD signal of the fMRI analysis of each voxel. It could be shown that there are significant correlations between model-derived prediction errors and activity in reward related regions such as the ventral striatum, which indicates further evidence for reinforcement learning process in perceptual learning. Nevertheless, it had still to be proven that learning related changes in *DV* are related to an updating mechanism that is based on signed prediction errors as proposed by the computational model. For that a conjunction analysis was carried out which searched for voxels which fulfill two criteria. They should contain more information about *DV* than orientation and the fMRI BOLD signal should correlate with signed prediction errors derived from the model. A cluster of voxels in the ACC fulfilled both criteria and supports the assumption that there is an important role of reinforcement processes in perceptual learning and decision-making in the ACC.

5. Summary

To summarize the results, strong evidence for perceptual learning-related changes in higher order areas was provided, like e.g. in the ACC where behavioral improvements in a specific orientation discrimination task led to activity changes. A reinforcement learning model was created and it could have been shown that the model explains perceptual improvements during the learning course very well. It shows that learning leads to an enhanced readout of sensory information, which in turn leads to noise-robust representations of decision variables. The used updating mechanism is based on signed prediction errors, like in classical reward learning.

All together these results suggest that perceptual learning is based on reinforcement learning processes and that the same neural processes as in reward-based learning are also

activated during decision-making. These findings question the distinction between perceptual and reward-based learning and increases the understanding of the neurobiological bases of perceptual learning processes.

Refrences

Kahnt, T., Grueshow, M., Speck, O., Haynes, J.-D. (2011). Perceptual Learning and Decision-Making in Human Medial Frontal Cortex. Neuron *70*, *549-559*

Sasaki, Y., Nanez, J.E., Wantanabe, T. (2010). Advances in visual perceptual learning and plasticity. Nat. Rev. Neurosci. *11*, *53-60*

Seitz, A., Wannabe, T. (2005). A unified model for perceptual learning. Trends Cogn. Sci. (Regul. Ed.) *9*, *329-334*

Schoups, A., Vogels, R., Qian, N., Orban, G. (2001). Practising orientation identification improves orientation coding in V1 neurons. Nature *412*, *549-553*

Bayer, H.M., Glimcher, P.W. (2005). Midbrain dopamine neurons encode a quantitative reward prediction error signal. Neuron *47*, *129-141*

Schultz, W., Dayan, P., Montague, P.R. (1997). A neural substrate of prediction and reward. Science *275*, *1593-1599*

Report

Neuronal Systems Underlying Decisions about Affective Odors

Edmund T Rolls, Fabian Grabenhorst, and Benjamin A. Parris

by Gustav Schneider

Main Message

Representations of the affective (reward or punishment) value of many stimuli and events and their subjective correlate pleasantness versus unpleasantness are present in the mid orbitofrontal cortex (OFC) and the anterior cingulate cortex (ACC). These involve all different kinds of stimuli like olfactory[1;2;3;4], taste[5;6;7], somatosensory[8], temperature[9], visual[10], monetary[11;12], and social stimuli[13;14;15;16]. If a stimulus is presented a representation of the affective value on a continuous scale may be formed, and that may be followed by a binary decision process. This could involve separable brain systems.

One aim was to test whether different brain systems have activity that is differently related to taking a categorical decision versus rating on a continuous scale and if different brain systems are involved.

Methods

To investigate these problems they performed a fMRI study in which the same set of stimuli was used in different trials. Either only the affective value and intensity had to be rated on a continuous scale or binary decisions had to be made about whether a second stimulus was more or less pleasant or more or less intense. They used olfactory stimuli because many of them have affective value (e.g. pleasant or not) and they can be delivered with a short delay between them. The participants were twelve healthy volunteers (7 men and 5 women, mean age=27 years). The set of olfactory stimuli used were selected based on previous fMRI studies[3]. The unpleasant odors were hexanoic acid (10% v/v) and isovaleric acid (15%) and the pleasant odors 1M citral and 4 M vanillin. The stimuli were delivered with a purpose-built continuous airflow 10-channel computer-controlled olfactometer in a MRI scanner[3]. The system was free of any auditory, tactile, or thermal shifts and medical clean air was continuously delivered with a pressure regulator and a flow meter. Each trial started at t = 0 sec with the first odor delivered at t = 2 sec accompanied by a visual label stating “sniff first stimulus”. After a clean-air-delivering period of 6 sec the participants had to decide the pleasantness, intensity or rate the stimulus. The second odor was presented for 2 sec accompanied by a visual label stating either “sniff decide pleasantness”, “sniff decide intensity” or “rate stimulus”. Then there was a 6-sec period with clean air and at t = 16 sec the words “first stimulus” and “second stimulus” appeared on the screen for 2 sec and the participants had to make a decision **(Figure 1)**. On rating trials the subjective ratings were made at t = 16 sec. The first rating was for the pleasantness of the second odor (-2 – 2) and the second for the intensity (0 – 4).

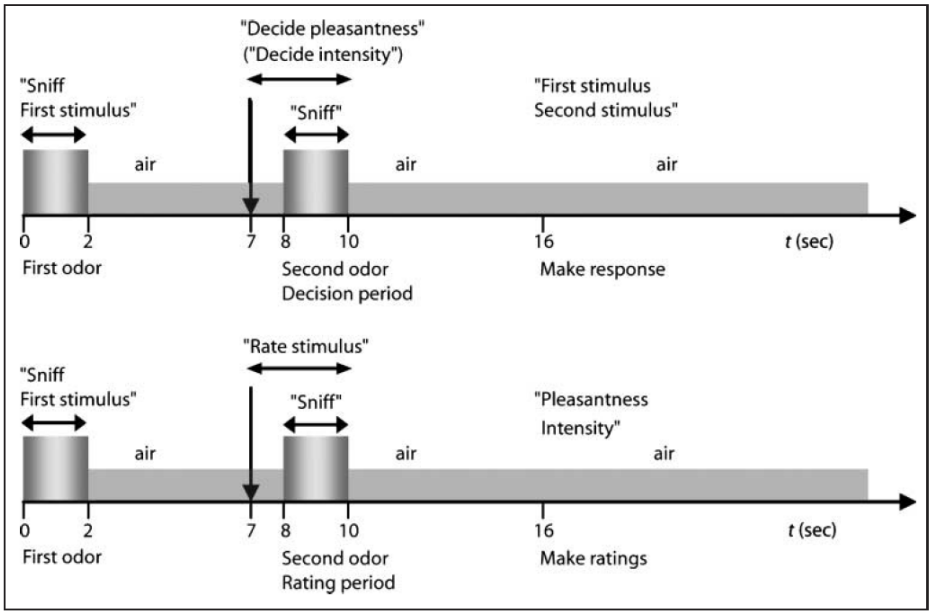

Figure 1. Task design for trials of the olfactory task. On decision trials (top), the task required a binary decision starting during the second odor about which of the two odors was more pleasant or (on different trials, as indicated by the instruction at $t = 7$ sec) more intense. On rating trials (bottom), identical stimuli were used, but no decision was required, and instead participants rated the second odor for pleasantness and intensity on continuous analog visual rating scales. The trial types were identical until $t = 7$ sec, when the instruction indicated whether the trial type was decide or rate. The second odor was delivered at $t = 8$ sec, the subjects were deciding or rating at that time, and the imaging was with respect to this period starting at $t = 8$ sec. No responses to indicate the decision made or the rating value could be made until $t = 16$ sec.

Results and Discussion

They found significantly larger BOLD signals in the medial prefrontal cortex area 10 when a decision had to be made compared with when the same affective olfactory stimuli had to be rated for affective value and intensity **(Figure 2A, pink circle)**. The term “BOLD-signal” is used to refer to the level of signal from the BOLD effects that are measured by fMRI. The implication is that this part of the medial area 10 contributes in some way beyond representing affective value to the decision-making process. At least the more dorsal part of medial area 10 had signals that were related to decisions about pleasantness. Furthermore, the signals in medial area 10 were not correlated with the pleasantness (or intensity) ratings supporting the hypothesis that activity in medial area 10 is more closely related to decision-making than to the representation of affective value. Additionally they found that that the medial area 10 BOLD signal related to decision-making versus rating extended down into a part of medial OFC (**Figure 2A, yellow circle)**. The activations there were not related to the pleasantness of the olfactory stimuli. So at least parts of the medial OFC may be involved in decision-making and not in representing the affective value of the stimuli or may receive feedback connections from brain regions such as medial area 10[17] implicated in the decision-making. The mid part of the OFC is not implicated in processing that is special to taking the decision, but it is implicated in the continuous affective representation of the stimuli. An anterior part of insula had activations related to decisions about intensity versus only rating whereas agranular insula had activations related to decisions about pleasantness versus only rating. This suggests that affective decision-making recruits the far anterior (agranular) insula, which is activated by taste-olfactory convergence that can contribute to making a flavor pleasant[18] and might be involved in autonomic effects resulting from the decision[19]. The dorsal part of the ACC was also implicated more in decision-making then representing affective value **(Figure 2A, white circle)** and in decision-making about both pleasantness and intensity. The dorsal ACC region showed more

activation on difficult than on easy trials, consistent with the possibility that difficult decisions require more attention or conflict, which engage this brain region[20].

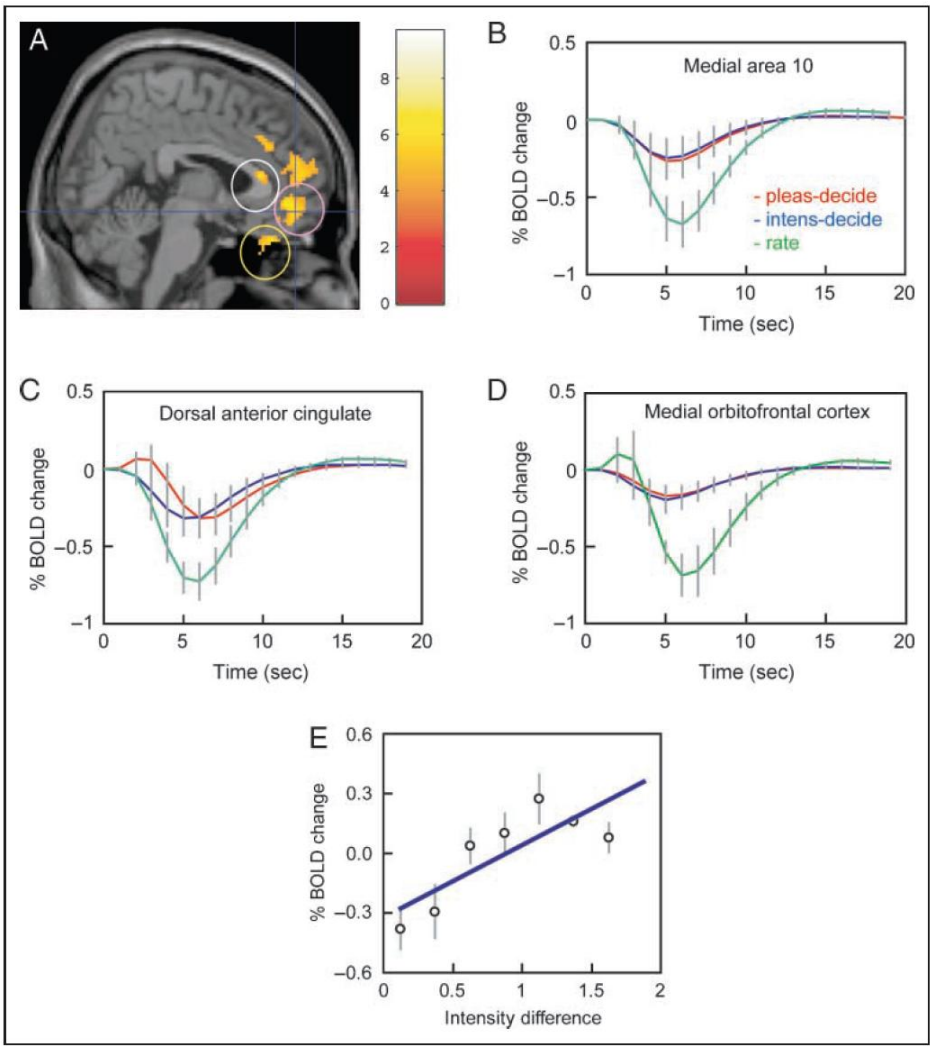

Figure 2. (A) A contrast of all trials on which decisions were made versus all trials on which ratings were made. An extensive region with more BOLD signal in this contrast was found in medial area 10 with peak at [2 50 −12], $z = 3.78$, $p < .001$ (pink circle, at cursor). (B) The time course of the BOLD signal in medial area 10 (mean across subjects ± *SEM*) for the different conditions, decide about whether the second odor is more pleasant (pleas-decide), decide about whether the second odor is more intense (intens-decide), and rate the pleasantness and the intensity without any choice (rate). Significant effects are also found in dorsal ACC, [6 28 12], $z = 4.09$, $p < .001$ (white circle), with time courses in panel C, and in the medial OFC, [8 36 −28], $z = 4.40$, $p < .001$ (yellow circle), with time courses in panel D. An exclusive mask with activations related to motor responses illustrated in Figure 7 was applied. The time courses start at the time at which the second odor was presented. (E) The percent BOLD signal in medial area 10 on the decision trials was correlated with the absolute value of the difference between the intensity ratings made to the same set of stimuli on the rating trials ($r = 0.81$, $df = 6$, $p < .03$). The relation shows that the activations were correlated with the easiness of the decision. (The percent BOLD values were calculated by obtaining the average ± *SEM* BOLD signal for intensity ratings binned at increments of 0.25 for each subject and then averaging across subjects.)

They suggest that decision-making parts of the medial prefrontal cortex are anterior to the region further posterior in the mid OFC where there is a correlation with the pleasantness ratings. Additionally they found that that the medial area 10 BOLD signal related to decision-making versus rating extended down into a part of medial OFC.

In medial prefrontal areas in which the BOLD signal was larger during choice decision-making it was the case that even during decision-making some deactivation was found, which may be past dependent. Although these regions were somewhat deactivated during decision-making **(Figure 2)** the signal was much lower when choice decisions were not being made and

continuous was being assessed. Moreover, the signal present in medial prefrontal cortex during decision-making does appear to be relevant to decision-making because lesions of these in humans impair decision-making. As future study it would be very interesting to examine exactly how neuronal activity in this region is related to decision-making.

The activity of human ventral premotor cortex was greater for decisions about the intensity than for decisions about the pleasantness of olfactory stimuli.

The activations in the medial prefrontal cortex area 10 region were correlated with the easiness of the decisions about intensity. No significant effects of this type of analysis of task easiness were found in the OFC regions described here, where there was a correlation of the BOLD signal with the continuous-valued pleasantness ratings. An interesting finding, however, is that areas such as DLPFC may be especially related to decision-making about the physical properties of stimuli such as their intensity. Other brain regions such as the more dorsal parts of medial prefrontal cortex area 10 **(Figure 2)** may be more closely involved in affective decision-making. Their engagement in decision-making tasks may be related to greater attentional or emotional processing on difficult trials.

References

[1] Grabenhorst, F., Rolls, E. T., Margot, C., da Silva, M. A. A. P., & Velazco, M. I. (2007). How pleasant and unpleasant stimuli combine in different brain regions: Odor mixtures. Journal of Neuroscience, 27, 13532–13540.

[2] Anderson, A. K., Christoff, K., Stappen, I., Panitz, D., Ghahremani, D. G., Glover, G., et al. (2003). Dissociated neural representations of intensity and valence in human olfaction. Nature Neuroscience, 6, 196–202

[3] Rolls, E. T., Kringelbach, M. L., & de Araujo, I. E. T. (2003). Different representations of pleasant and unpleasant odors in the human brain. European Journal of Neuroscience, 18, 695–703

[4] Rolls, E. T., Critchley, H. D., Mason, R., & Wakeman, E. A. (1996). Orbitofrontal cortex neurons: Role in olfactory and visual association learning. Journal of Neurophysiology, 75, 1970–1981

[5] Grabenhorst, F., Rolls, E. T., & Bilderbeck, A. (2008). How cognition modulates affective responses to taste and flavor: Top down influences on the orbitofrontal and pregenual cingulate cortices. Cerebral Cortex, 18, 1549–1559

[6] Small, D. M., Gregory, M. D., Mak, Y. E., Gitelman, D., Mesulam, M. M., & Parrish, T. (2003). Dissociation of neural representation of intensity and affective valuation
in human gustation. Neuron, 39, 701–711

[7] Rolls, E. T., Sienkiewicz, Z. J., & Yaxley, S. (1989). Hunger modulates the responses to gustatory stimuli of single neurons in the caudolateral orbitofrontal cortex of the macaque monkey. European Journal of Neuroscience, 1, 53–60

[8] Rolls, E. T., O'Doherty, J., Kringelbach, M. L., Francis, S., Bowtell, R., & McGlone, F. (2003). Representations of pleasant and painful touch in the human orbitofrontal and cingulate cortices. Cerebral Cortex, 13, 308–317

[9] Guest, S., Grabenhorst, F., Essick, G., Chen, Y., Young, M., McGlone, F., et al. (2007). Human cortical representation of oral temperature. Physiology and Behavior, 92, 975–984

[10] O'Doherty, J., Winston, J., Critchley, H., Perrett, D., Burt, D. M., v& Dolan, R. J. (2003). Beauty in a smile: The role of medial orbitofrontal cortex in facial attractiveness. Neuropsychologia, 41, 147–155

[11] Knutson, B., Rick, S., Wimmer, G. E., Prelec, D., & Loewenstein, G. (2007). Neural predictors of purchases. Neuron, 53, 147–156

[12] O'Doherty, J., Kringelbach, M. L., Rolls, E. T., Hornak, J., & Andrews, C. (2001). Abstract reward and punishment representations in the human orbitofrontal cortex. Nature Neuroscience, 4, 95–102

[13] Spitzer, M., Fischbacher, U., Herrnberger, B., Gron, G., & Fehr, E. (2007). The neural signature of social norm compliance. Neuron, 56, 185–196

[14] Moll, J., Krueger, F., Zahn, R., Pardini, M., de Oliveira-Souza, R., & Grafman, J. (2006). Human fronto-mesolimbic networks guide decisions about charitable donation.
Proceedings of the National Academy of Sciences, U.S.A., 103, 15623–15628

[15] Hornak, J., Bramham, J., Rolls, E. T., Morris, R. G., O'Doherty, J., Bullock, P. R., et al. (2003). Changes in emotion after circumscribed surgical lesions of the orbitofrontal and
cingulate cortices. Brain, 126, 1691–1712

[16] Kringelbach, M. L., & Rolls, E. T. (2003). Neural correlates of rapid reversal learning in a simple model of human social interaction. Neuroimage, 20, 1371–1383

[17] Petrides, M., & Pandya, D. N. (2007). Efferent association pathways from the rostral prefrontal cortex in the macaque monkey. Journal of Neuroscience, 27, 11573–11586

[18] de Araujo, I. E. T., Rolls, E. T., Kringelbach, M. L., McGlone, F., & Phillips, N. (2003). Taste-olfactory convergence, and the representation of the pleasantness of flavour, in the human brain. European Journal of Neuroscience, 18, 2374–2390

[19] Critchley, H. D., Wiens, S., Rotshtein, P., Ohman, A., & Dolan, R. J. (2004). Neural systems supporting interoceptive awareness. Nature Neuroscience, 7, 189–195

[20] Greene, J. D., Nystrom, L. E., Engell, A. D., Darley, J. M., & Cohen, J. D. (2004). The neural bases of cognitive conflict and control in moral judgment. Neuron, 44, 389–400.

Summary report on 'Overlapping and Distinct Neural Systems Code for Subjective Value during Intertemporal and Risky Decision Making, Peters et al 2009'

by

Sulav Duwal

August 19, 2012

Contents

Introduction

The neural mechanism for valuation of different types of reward may consist of regions or network specific to the reward type and a generic system where results from domain-specific regions are integrated. In the study, the authors considered two type of rewards, namely delayed reward and risky reward and attempted to delineate the underlying neural process. Delay discounting (DD) or intertemporal choice refers to the phenomenon that the current, subjective value of a reward decreases as the delay until its receipt increases, whereas, probabilistic discounting (PD) or risky choice refers to the phenomenon that the subjective value of a reward decreases as the odds against receiving it increases (See *Rangel et al. 2008* [7] for detailed introduction). Though subjective choice preferences have been well studied in domain of PD and DD, only few have investigated the underlying neural mechanism.

Material and Methods

Experiment 1

Peters et al. 2009 [6] conducted two types of experiments. The first type of experiment, which included 22 subjects, consisted of three sessions. Subjects showing stability of discounting across the first and the second sessions, which included behavioral tests without

fMRI (functional magnetic resonance imaging) scanning, were selected for the third session, which consisted of behavioral tests accompanied by fMRI scanning. A total of 13 subjects was selected for the third session and subjects' BOLD (BLOOD OXYGENATION LEVEL-DEPENDENT) changes were analyzed. Median time between the first and the second sessions and between the second and third session were 9 days and 4 days respectively.

The behavioral test comprised of two parts. In each part, subjects made repeated binary choices either between a fixed immediate reward and a greater reward delivered with delay or between a fixed immediate reward and a greater reward delivered with a given probability. The amount of the delayed and probabilistic reward was reduced in a stepwise fashion after two successive choices of the delayed and probabilistic reward and increased in a stepwise manner after two successive choices of the immediate reward. The purpose of adjusting the reward amount was to induce the reversal of preference (for e.g from immediate reward to delay reward) allowing to estimate indifference amounts at which subjects showed indifference between the immediate and the delayed/probabilistic options. For a number of delays and probabilities, their indifference amounts were estimated and the subjective discounted value (SV) were calculated. For delay discounting and probabilistic discounting, equation 1 and equation 2 were fitted to data respectively.

$$SV = \frac{1}{1+kD} \tag{1}$$

$$SV = \frac{1}{1+k\theta} \tag{2}$$

where D is delay in days and θ is odds for losing. The best-fitting discount rate k was estimated for each subject. k describes the propensity of subject to be patience in case of delay discounting and risk aversive in case of probabilistic discounting. In the third session, subjects performed the behavioural test as in previous session with delay and probabilistic options computed based on previous pretests in such a way that a subject chosed delayed or risky rewards roughly over immediate rewards in 50 % of trials. The brain-hemodynamic activity of subjects were scanned using fMRI during the test.

Experiment 2

The first type of experiment was designed based on the assumption that delayed and probabilistic rewards with same subjective value are valuated equally. The purpose of the second type of experiment was to test the validity of that assumption. In contrast to the previous behavioural test, the behavioural test in second type of experiment comprised of repeated binary choices between delayed and probabilistic options. Based on previous pretests (from the first and the second session), the delay and probabilistic rewards were computed in a such manner that in half of trails delay rewards have higher subjective value and in other half lower subjective value than probabilistic rewards. The assumption would be refuted, if delayed options (probabilistic options) are systematically preferred over probabilistic options (delayed options) of similar subjective value.

Result

Equal Valuation of Rewards with Same Subjective Value

In the second experiment, the proportion of trials in which subjects showed preference for delayed rewards over probabilistic rewards was plotted as a function of subjective discounted value difference between them. Logistic functions were fitted to individual subject data and the subjective values at which subjects were indifferent about choices were estimated. The mean indifference point over all subjects was determined to be close to and insignificantly different than zero, which showed the validity of assumption on which the first experiment was based.

Stability of Individual's Discount Rates

In 13 subjects out of 22, assessment of discount rates in first and second sessions which were on average 119 days apart showed good stability providing support for trait like stability of individual preferences over a long time period. Across all subjects, high correlation was observed between discount rates from a behavioural pretest shortly before the fMRI session and during fMRI session (median time interval between the second pretest and scanning was 4 days). The observation indicated that the participants' propensities to be patient or risk-averse are well preserved over long period of time.

Characterization of DD and PD by Hyperbolic Function

The choices for both DD and PD in the third session were also well characterized by hyperbolic function. Discount rates showed considerable inter-subject variation and there was a negative but non-significant correlation between the DD and PD discount rates for individuals.

Analysis of Reaction Time

In the third session with fMRI scanning, the reaction times (RT) were analyzed as a function of subjective value. Firstly, the trials were ordered according to subjective value of delay/probabilistic rewards and divided into three categories of roughly the same size. The categories consist of trials with delay/probabilistic rewards with subjective value

1. higher than fixed immediate reward.
2. similar to fixed immediate reward.
3. lower than fixed immediate reward.

The RTs were generally faster in the first category than in other two categories.

Analysis of Hemodynamic Activity

In the third session, brain regions in which the magnitude of hemodynamic response showed a positive correlation with subjective (discounted) value were searched.

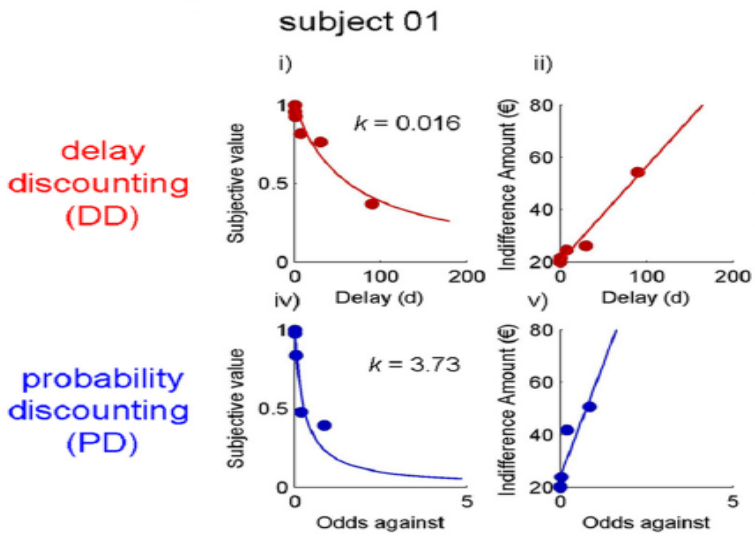

Figure 1: (Figure extracted from *Peters et al. 2009* [6]) Figures at the left side showing the fitting of equation 1 and equation 2 on data of subject 001 from the study [6]. The figures on the right side shows the increment of indifference value as a function of delay or risk.

A Distinct Network for Subjective Valuation During DD

Kable and Glimcher et al. 2007 [3] previously performed experiments which showed that certain brain regions correlate to the subjective value of delayed reward during intertemporal choice and identified them. The authors were able to replicate the previous finding by *Kable and Glimcher et al. 2007* [3]. During delay discounting, following regions showed strong correlation with subjective value.

1. Posterior Cingulate Cortex
2. Ventral Striatum
3. Medial Prefrontal Cortex

Furthermore, they identified regions which showed significantly higher correlation with SV for DD than with SV for PD.

A Distinct Network for Subjective Valuation During PD

The regions showing pronounced correlation with subjective value during PD are given below.

1. Right Superior/Inferior Parietal Lobule

2. Left Middle Occipital Gyrus

3. Ventral Striatum

They also identified brain regions showing significantly higher correlation to SV during PD than during DD.

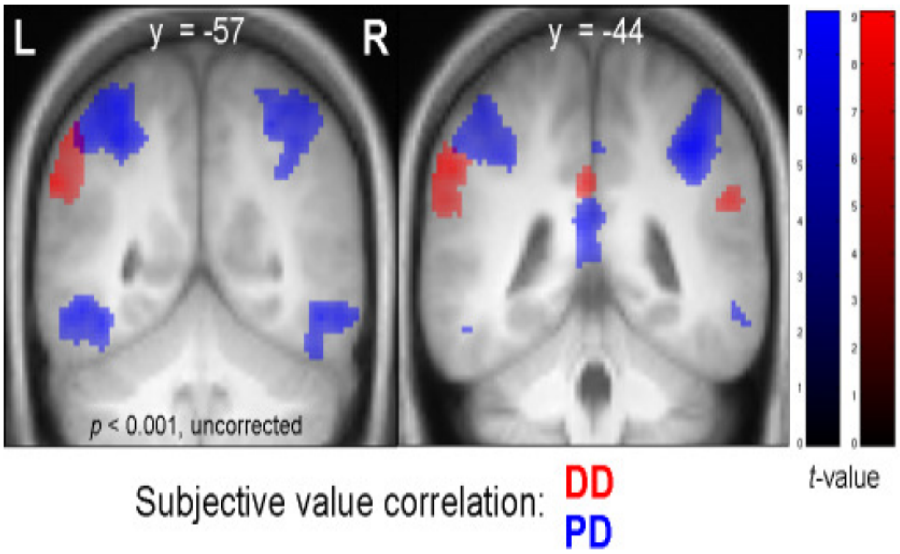

Figure 2: (Figure extracted from *Peters et al. 2009* [6]) Regions marked with blue (lateral parietal cortex) showed correlation with subjective value of DD, while regions marked with red (superior parietal regions) correlated with subjective value during PD. Minimal overlap of clusters can be observed.

A Common Core Network

Left ventral striatum and right central orbito frontral cortex (OFC) were found to code for subjective value in both cases strongly implicating these regions form or are part of domain-general reward valuation.

Discussion

Subjective discounted values were well modeled by hyperbolic function of delays or odd for losing. Furthermore, preservation of individual traits like risk aversion or impulsiveness was also observed for a long period of time. From fMRI scanning, brain regions involved in subjective valuation of rewards were identified. A distinct network of regions was identified which codes the subjective value for DD and PD. A common system coding for subjective value of both delayed and risky reward was also observed strongly implicating the network in providing neural basis of a common neural currency of stimulus value. In line with

previous observation where activities in OFC correlated with the value of decision options (*Padoa-Schioppa and Assad et al. 2006* [5]) as well as value difference between decision options (*FitzGerald et al. 2009* [1]), the authors also found OFC activities correlating with subjective value of rewards. The role of ventral striatum ,however, is not clear. Some studies (*Kable and Glimcher et al. 2007* and *Knutson et al. 2007* [4]) reported ventral striatum to code subjective value, whereas, other like *Hare et al. 2008* [2] argued that it codes a prediction error rather than a value signal. Nevertheless, OFC and ventral striatum are part of a system which integrates different and distinct valuation system, in a manner that is independent of the precise nature of the decision option.

In summary, the study delineates neural mechanism of reward valuation into domain-specific and domain-general networks. The ventral striatum and OFC are the part of the common system which integrates the result from domain-specific valuation in a manner such that the intrinsic value is independent of the precise nature of reward. The study further suggests that different decision options may compete for neurocognitive resources through the domain-general networks.

Bibliography

[1] T. H. B. FitzGerald, B. Seymour, and R. J. Dolan. The role of human orbitofrontal cortex in value comparison for incommensurable objects. *J Neurosci*, 29(26):8388–8395, Jul 2009.

[2] T. A. Hare, J. O'Doherty, C. F. Camerer, W. Schultz, and A. Rangel. Dissociating the role of the orbitofrontal cortex and the striatum in the computation of goal values and prediction errors. *J Neurosci*, 28(22):5623–5630, May 2008.

[3] J. W. Kable and P. W. Glimcher. The neural correlates of subjective value during intertemporal choice. *Nat Neurosci*, 10(12):1625–1633, Dec 2007.

[4] B. Knutson, S. Rick, G. E. Wimmer, D. Prelec, and G. Loewenstein. Neural predictors of purchases. *Neuron*, 53(1):147–156, Jan 2007.

[5] C. Padoa-Schioppa and J. A. Assad. Neurons in the orbitofrontal cortex encode economic value. *Nature*, 441(7090):223–226, May 2006.

[6] J. Peters and C. Büchel. Overlapping and distinct neural systems code for subjective value during intertemporal and risky decision making. *J Neurosci*, 29(50):15727–15734, Dec 2009.

[7] A. Rangel, C. Camerer, and P. R. Montague. A framework for studying the neurobiology of value-based decision making. *Nat Rev Neurosci*, 9(7):545–556, Jul 2008.

Social distance modulates recipient's fairness consideration in the dictator game: An ERP study.

Yin Wu[a], Marijke C. Leliveld[b], XiaolinZhou[c, d]

Social Distance (SD) is closely related to decision-making. SD is a relationship between two people; it is defined by physical and social features. People use different scripts when they meet friends to the ones they use when they contact strangers. (Fiske and Taylor, 1991); It appears moreover that friends are more concerned about the sense of various moral norms such as fairness (Shapiro 1975). Social distance can be manipulated to show how the fairness norm is activated and how it influences people's fairness consideration (Lind and Tyler, 1988; Mandel, 2006; Parks et al., 1996; Singer, 1998). In this study, participants play a dictator game (DG) in which they receive (un) fair offers from either friends or strangers while their brain potentials are recorded. Results show that after manipulating the social distance, the fairness consideration is active (Charness and Gneezy, 2008) but is not clear how the recipient reacts to fair or unfair offers from the allocator due to the lack of recipient participation. Event Related Potentials (ERP) technique makes it possible to know the implicit response from the recipient. It derives from Electroencephalogram (EEG) technique and measures changes in the mental states in response to one external event. Medial Frontal Negativity (MFN) and P300 components are two deflections in the signal wave of the ERP, negative and positive respectively. Each one has a specific window time. In addition, it is evoked by some specific processes, such as high-order cognitive operations (for P300) and outcome evaluation (for MFN) (Donchin and Coles, 1988). P300 also is sensible to the magnitude (Sato et al., 2005; Yeung and Sanfey, 2004) and valence reward (Hajcak et al., 2005, 2007; Wu and Zhou, 2009; Yeung et al., 2005). As a result, P300 reflect an increase in during attentional/affective process in friend's condition. However, in economic transactions recipient and allocator are in conflict because the amount of reward does not correspond with their expectative. As for the MFN, the results show that the magnitude of this component decreases in unfair offers from friends in contrast with P300 that is higher for fair offers than for unfair ones, irrespectively of friends or stranger consideration.

METHOD

The experiment was conducted as a 2X2 factorial design in which the first factor was the fairness level (fair vs unfair) and the second factor refers to the SD from the allocator to the recipient (friends and strangers). The participants were informed about the rules of the game and the considerations of the experiment. Furthermore, the recipients filled up some questionnaires for "True Scale" before the experiment and some other after it to assess the grade of satisfaction with the allocator offer.

The EEG was recorded from 64 electrodes sites but only some anterior-posterior and central posterior electrodes signal were statistically analyzed due to their relevance for the study (Gehring and Willoughby, 2002; Hajcak et al., 2005, 2007).

RESULTS

The "Setup Questionnaire" and the "True Scale" disclosed the faithfulness and trustworthiness of the friends, respectively. Furthermore the EEG analysis evidences the close relationships between friends. As far as satisfaction rating goes, the results prove that the recipient was particularly resentful to the unfairness coming from a friend (Fig 1A). ANOVAs statistical analysis from ERPs responses show that MFN component is more negative in unfair offers than in fair offers in friend-allocation condition (Fig 1B up and down) in both anterior-posterior and central posterior regions. Nevertheless the P300 component is more positive in fair offers than in unfair offers in central-posterior region (Fig 1C up 1D down)

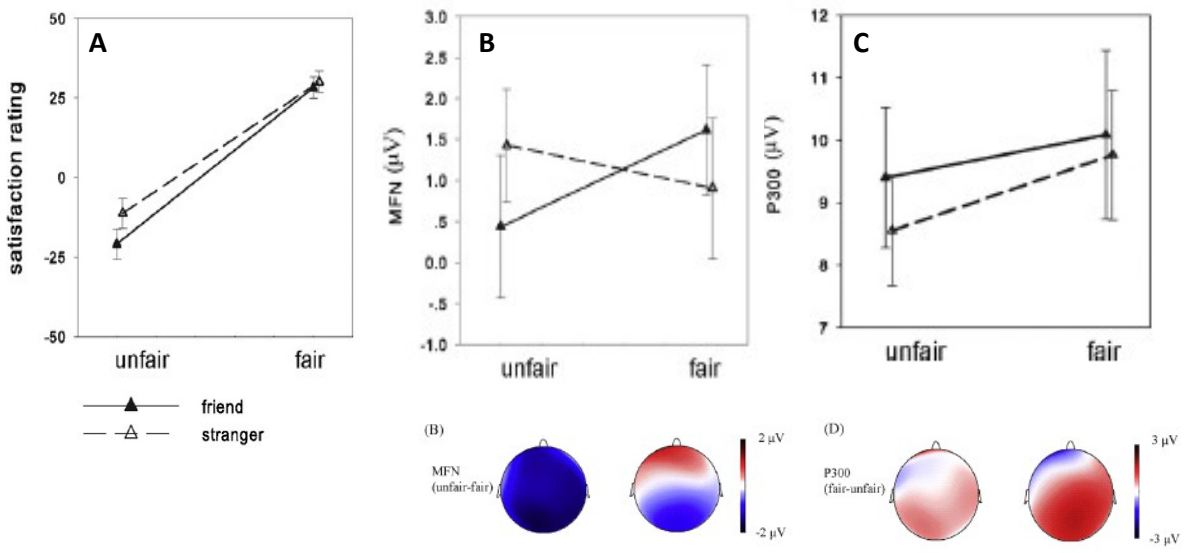

Fig. 1. Upper line shows behavioral and ERP results. (A) Satisfaction rating for fair and unfair offers; **(B)**mean amplitudes (MFN) in the 240–340 ms time window for fair and unfair offers at the anterior-frontal region; **(C)** peak amplitudes in the 250–600 ms time window for fair and unfair offers at the central-posterior region.
Bottom line shows topographic maps for (B) topographic map for MFN in the 240–340 ms time window; (D) topographic map for P300 in the 400–550 ms time window.

DISCUSSION

This study demonstrated that the recipient's consideration of fairness in the dictator game can be modulated by the social distance between the recipient and the allocator. The differential MFN responses to fair and unfair offers in the friend-allocation condition may

reflect the detection of social expectancy violation (Fehr and Gachter, 2002; Fehr and Fischbacher, 2004; Messick and Sentis, 1983) and this norm is strongly adhered to friend condition in social interaction (Mandel, 2006; Shapiro, 1975). During evolution, the human brain developed mechanisms to detect deviations from social norms (Montague and Lohrenz, 2007) and these mechanisms share the same neural ways that reinforcement learning (Harris and Fiske, 2010). Dopamine signals input in the cortex to generate MFN responses that encode error prediction for monetary reward as well as violations of expectancy towards social norms. The null effect in MFN response for fair and unfair offers in the stranger -allocation condition may be due to the introduction of the friend-allocation condition into the experimental setup. External studies suggest that MFN responses can be context-dependent (Holroyd et al., 2004; Yu and Zhou, 2006b, 2009) thus the participation of friends in the experiment may automatically activate people's social identity and influence recipient's fairness expectancies regarding friend's and stranger's offers (Bohnet and Frey, 1999; Halpern, 1994, 1997; Mandel, 2006; Shapiro, 1975).

The finding s of P300 component suggests that fair offers are intrinsically linked with larger rewards in magnitude and more positive responses (Sato et al., 2005; Yeung and Sanfey, 2004). This insights could reflect differential distribution of attentional resources (Leng and Zhou, 2010; Nieuwenhuis et al., 2005; Wu and Zhou, 2009; Yeung and Sanfey, 2004). Moreover, the lack of an interaction between fairness level and social distance might indicate that the neural system could evaluate the fairness of offers in a parallel way during the late stage of elaborated processing.

To conclude, the results suggest that violation of the social norms can be detected at an early stage of evaluative processing, as indexed by the MFN effect in brain potentials; and that this detection could be context-dependent and modulated by social distance.

REFERENCES

Wu, Y., Leliveld, M. C., & Zhou, X. (2011). Social distance modulates recipient's fairness consideration in the dictator game: an ERP study. Biological psychology, 88(2-3), 253-62. Elsevier B.V. doi:10.1016/j.biopsycho.2011.08.009 [EEG]

Katsikopoulos, K. V., & King, A. J. (2010). Swarm intelligence in animal groups: when can a collective out-perform an expert? PloS one, 5(11), e15505. doi:10.1371/journal.pone.0015505

Lee D (2008) Game theory and neural basis of social decision making. Nature Neuroscience

11, 404 – 409

Rilling JK, King-Casas B, Sanfey AG.(2008) The neurobiology of social decision-making. Curr Opin Neurobiol. 2008 Apr;18(2):159-65. Epub 2008 Aug 7 (review article)

Getting to Know You: Reputation and Trust in a Two-Person Economic Exchange

B. King-Casas, D. Tomlin, C. Anen, C. F. Camerer, S. R. Quartz, P. Read Montague
Science, 2005

Summary by Sophie Kolbe

Introduction

In our every day life we have to make several decisions and choices, some of them made in the context of social interactions. Many neurobiological studies used game theory to probe the neural basis of decision making and suggested that these features might be reflected in brain areas involved in reward evaluation and reinforcement learning [1, 2]. One important social signaling mechanism is the expression and repayment of trust. Although this human behaviour is very complex instances of it can be encoded into economic exchange games. The given study by King-Casas et al seeks to reveal the human brain areas involved with trust and reputation as well as their change over time and experience through a series of economical exchange games.

Two-Person Exchange Game and Measurement of its Neural Correlates

During the game, one person plays the investor and the other person the trustee. At the beginning of each round the investor gets 20$. Then he can invests any fraction of 20$ with the trustee, who obtains three times the investment and decides afterwards how much he wants to repay the investor. In this context, trust is defined as the amount of money which is send between the players. Ten consecutive rounds were played by 48 subject pairs. With the multiround format of the game trust becomes bidirectional and it is possible to study reputation building as the partners develop internal models of each other with proceeding rounds. In order to minimize influences on trust (e.g. context and communication) player identities were never revealed. Neural correlates were measured using event-related hyperscan-functional magnetic resonance imaging (h-fMRI), which enables to monitor homologous brain regions of two subjects simultaneously. Measured brain activity was converted into a blood oxygenation dependant (BOLD) signal.

Investor Reciprocity as Best Predictor of Changes in Partner Trust

Investements (I) and repayments (R) were scaled by the amount available to be sent. With linear regression analysis different predictors of change in trust by trustees (ΔR_j) and investors (ΔI_j) were examined: previous investment/repayment, change in investment/repayment and previous investor/trustee reciprocity. The term reprocitiy in this context depicts the fractional change of money sent across rounds in response to a fractional change in money sent by the partner.

King-Casas et al identified reciprocity by the investor as the best predictor for future trust expressed by the partner and therefor declared it as the focus of analysis. Investor reciprocity on round j was defined as $\Delta I_j - \Delta R_{j-1}$, where ΔI_j is the fractional change in investment from round $j-1$ to j and ΔR_{j-1} the last fractional change repayment.
The exchanges were divided into three groups corresponding to benevolent, malevolent and neutral reciprocity. For benevolent reciprocity, investors are sending more money in response to a decrease in repayment by the trustee. For malevolent reciprocity the investor decreases his investment although the trustee has increased his repayment in the preceding round.

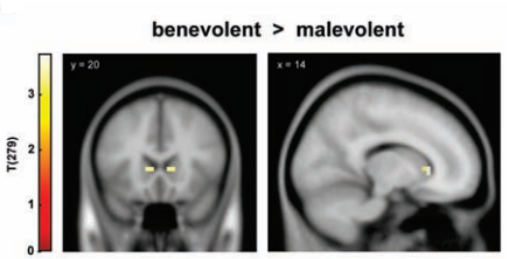

Figure 1: BOLD signal of head of caudate in trustee brain for different kinds of investor reciprocity.

With general linear model analysis four brain regions were identified, whose BOLD signal was greater for benevolent or malevolent investor reciprocity than for neutral reciprocity. These regions (inferior frontal sulcus, superior frontal sulcus, thalamus and inferior/superior colliculli) correspond to regions most activated for a surprise signal. In the head of caudate the BOLD signal was significantly greater for benevolent reciprocity, compared to malevolent reciprocity (two-tailed t test, $P < 0.005$) and neutral reciprocity (two-tailed t test, $P < 0.05$) (**Fig. 1**).

Intention to trust signals and Model building of partner

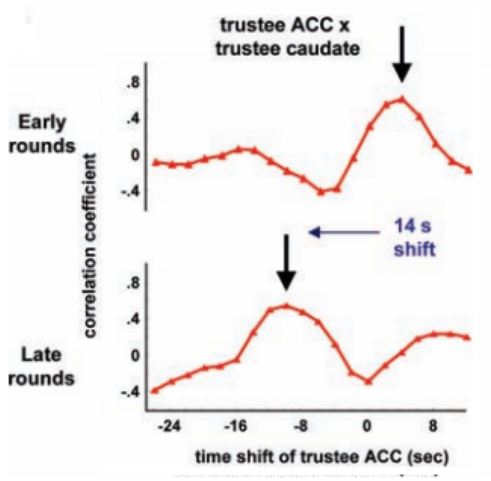

Figure 2: Timeshift of the "intention to trust" signal.

The head of caudate was subjected to a region-of-interest analysis and the signal was identified as the "intention to trust" signal. It was expected that this signal would show strong cross-brain correlations: benevolent/malevolent reciprocity by the investor is expected to generate the intention to increase/decrease repayment (trust) in the brain of the trustee. Some region of investors brain should anticipate the trustees next decision, reflecting changes in their own reciprocity. Indeed correlations could be found between the MCC (middle cingulate cortex) of investors, the ACC (anterior cingulate cortex) of trustees and the caudate of trustees. Interestingly the peak of the cross correlogram between investor MCC and the trustees "intention to trust" signal in the caudate, showed a 14-s shift from early to late rounds. This "Intention to trust" signal was then segregated according to the next decision of the trustee to increase or decrease repayment. **Fig. 2** shows the corresponding time series. In early rounds of the game the peak of the signal for intended increases in trust occurs after the investors decision is revealed. In late rounds this peak shifts 14-s and occurs just before the revelation of the investors decision (only in the case of benevolent reciprocity). These data suggest that the trustee is building a virtual model of the investor. In order to evaulate this assumption the game was played again with the modification that the trustee should guess the next investment. With proceeding rounds of this game the guesses got more accurate.

Discussion

The results suggest that different regions of the brain are involved in trust and reputation during social decision making. The head of the caudate seems to recieve and compute information about the fairness of a social partner's decision and the intention to repay that decision with trust. The observed time shift of this "intention to trust" signal in late rounds of the game is similar to shifts of reward prediction error signals from reinforcement learning, which involve dopaminergic neurons. The scheme of such classical conditioning experiments is simple: a neutral stimulus is combined with a delayed surprising reward. After repeated pairing a burst in dopaminergic activity occurs just after the neutral stimulus, but not after the reward like before. In the trustee brain the neutral stimulus is the cue for the partner to invest. The analog to the reward is the revelation of the increased investment. Left is the question why the "intention to trust" signal transferred to the time just before the revelation. Asides

Finally it should be mentioned that the complexity of social decision making modelled into a game alters the neural basis. In such games anonymous agents are interacting with each other. But in reality people pay attention to the characteristics of others and their interactions are dependent on their observations of others. Many factors are influencing the expression and repayment of trust. Possible influences include cultural or genetic differences, moral character, facial expression and gender [2, 3]. For example it could be shown that women participating the trust game show significantly more reciprocity than men [4].

References

1. JK. Rilling, B. King-Casas, AG. Sanfey (2008) *The neurobiology of social decision-making.* Curr Opin Neurobiol. 18(2):159-165.
2. D. Lee (2008) *Game theory and neural basis of social decision making.* Nature Neuroscience 11, 404 - 409.
3. CC. Eckel, RK. Wilson (2003) *Conditional trust: sex, race and facial expressions in a trust game.* Trust and Institutions, Harvard University, April 24, 245-74.
4. R. Croson, N. Buchan (1999) *Gender and culture: International experimental evidence from trust games.* The American Economic Review 89, 386-391.

Quorum Decision-Making in Foraging Fish Shoals

Ashley J.W. Ward, Jens Krause, David J.T. Sumpter

PLoS ONE, March 2012, Volume 7

A term paper written by Katharina Mangold

Table of contents

1. Introduction

Social group living animals receive both information from their own and information from their group members, whereas observing other group members provide the individuals with a large amount of information at low cost (Ward et al., 2012). The social information may often be helpful for an individual, e.g. information about food patches whereas 'blind copying' of defective social information from other may be unprofitable. Each individual seek to maximize their self-interests (Lee, 2008), so individuals may be in a decision conflict and must balance between their own experience and that of others. A model which explains the decision-making in group-living animals is the quorum response. Ward and colleagues investigated the role of quorum responses in the movement decisions of fish (Ward et al., 2008). They showed that individuals respond only when a threshold number of individuals perform a particular behavior. The quorum response explains how group-living animals can integrate and filter social information to produce accurate group decisions (Ward et al., 2012).

In this experiment Ward et al. examined the mechanisms used in the movement decisions of foraging fish shoals which first approach to a food patch and then leave it. To analyze whether the behavior of the test fish is group dependent, they compared their observations to a quorum response model.

2. Methods

Experimental setup

To investigate the decision-making behavior of three-spined sticklebacks which are group-living fish, an experimental arena was constructed that offered a two-choice decision to the fish. The Y-maze experimental area consisted of a starting point, from which two monofilament lines guide to two identical refuges. The refuges were marked as shading areas at the opposite end of the aquarium. On the monofilaments, replica sticklebacks could be mounted and pulled along by an electric motor at a speed of 4 cm/second. Direction was from the starting point to one of the refuge. The replica sticklebacks were introduced to stimulate the experimental fish producing a following response. Along the route of the replica fish, a simulated food patch containing bloodworms were placed to test both the approach to a food patch and the leaving from the food patch.

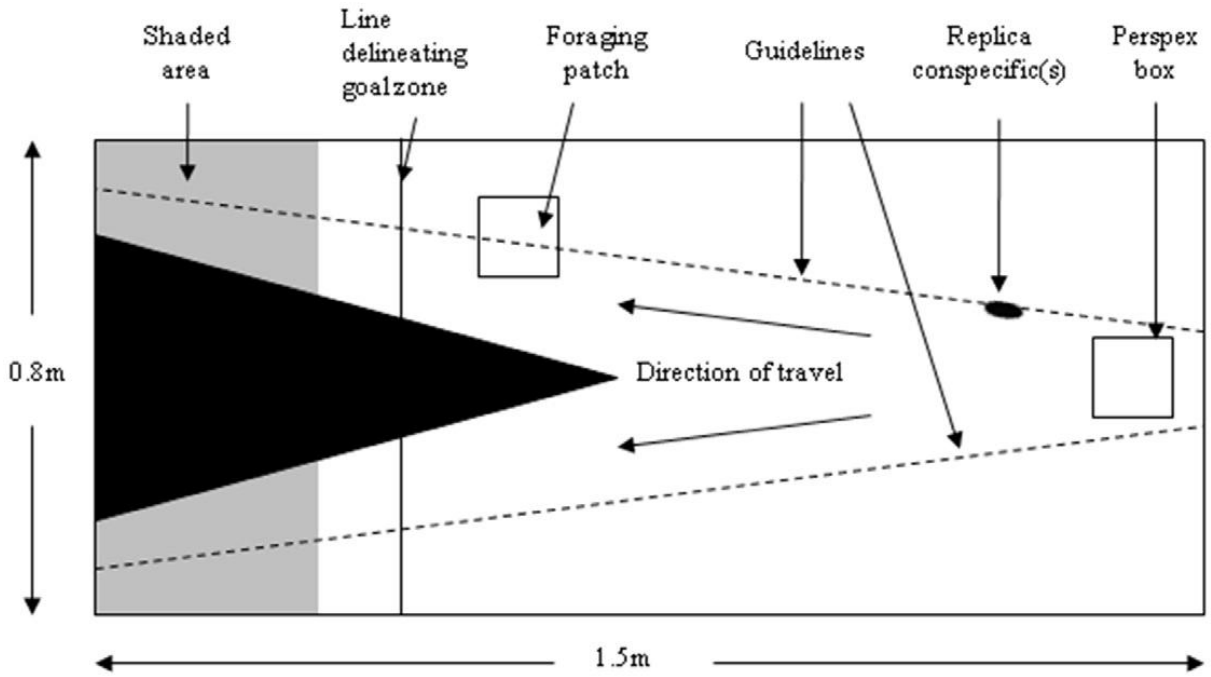

Figure 1: Experimental setup. The Y-maze experimental area consists of a starting point from which two guidelines guide to two identical separated refuges which are marked as shading areas. The test fish are introduced to the experimental area at the starting point. Replica fish are mounted on one of the guidelines and pulled along by an electric motor. Along the route of the replica fish a food patch were placed. (Ward et la., 2012)

Experimental protocol

The test fish were introduced to the experimental aquarium in a clear box at the starting point and were allowed to habituate for 5 minutes before tests started. Either 0,1 or 2 replica fish were positioned randomly at one of the two guidelines. When test fish were released from their box, replica fish were moved simultaneously by the onset of the electric motor in the

direction of one of the refuge. When replica fish reached the food patch, it paused for 30 seconds before moving off again to the refuge. The experiments finished when all fish had entered the shaded goal zones or 60 seconds after the replica fish had moved off from the food patch. The number of replica fish which were presented at each trial was 0, 1 or 2 respectively and the group size of test fish varied from 1, 2, 4 to 8.

Data

The experiment was divided in two stages: approach to the food patch and leaving from the food patch. The number of approaching and leaving were counted and then compared to the quorum response, which was investigated in further experiments (Ward et al., 2008).

3. Results

The number of test fish which approach to the food patch increased with the number of replica fish.

In the first part of the experiment the number of test fish which approach to the food patch were measured. Figure 2.1 shows the distribution of the number of fish that went to the food patch for each group size (1, 2, 4 and 8) for no replica fish (figure 2.1a), one replica fish (figure 2.1b) and two replica fish (figure 2.1c). When there is no replica fish presented, the test fish choose the left or right channel at random at a group size of 1 (figure 2.1a). This expectation can be referred to the null hypothesis. Furthermore, at a group size of 4 and 8 individuals the distribution of the number going to the food in the absence of a replica fish is U-shaped (figure 2.1a).

In the presence of one or two replica fish, the test fish moved more often to the food patch compared to trials where no replica fish was presented (figure 2.1b and 2.1c). This result is consistent in all group size treatments. Only at a group size of 8, two replica fish increased the approaching frequency compared to the presence of one replica.

The solid line compares the quorum model with the experimental data. Figure 2.1 shows that there is no significantly difference between the experimental data and the model prediction in any different replica fish size and group size combination.

The presence of replica fish increased the movement away from the food, whereas the leaving decreased with the initial group size.

The second stage of the experiment measured the movements away from food patch and the tendency of test fish to decide between following the replica fish and collecting food.

Figure 2.2 shows the proportion of fish at the food patch that left the food patch immediately following the departure of the replica fish.

When there was no replica fish presented the movement away from the food patch was independent from the initial group size (figure 2.2a). However in the trials where one or two replica fish were presented, the movements away from the food patch increased with the number of the replica fish (figure 2.2b and 2.2c) but decreased at the same time with the number of the group size.

2.1

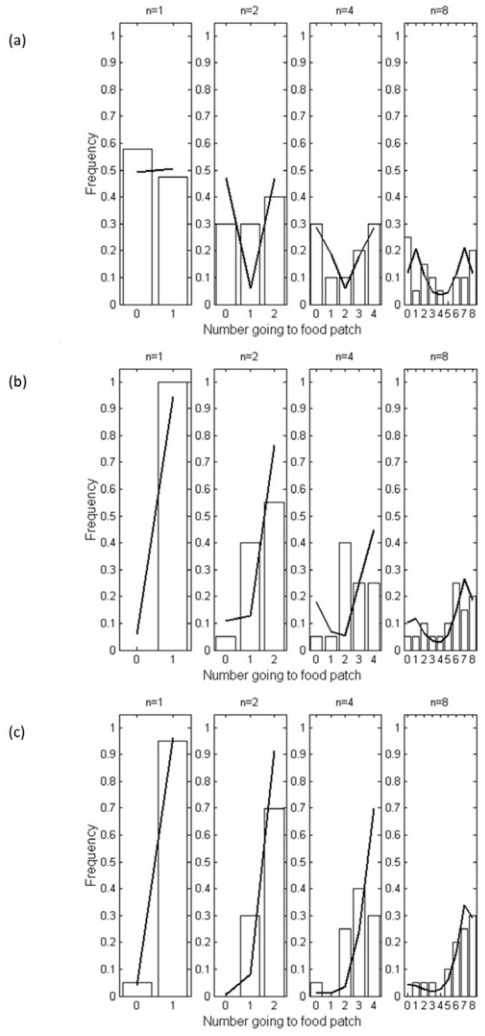

2.2

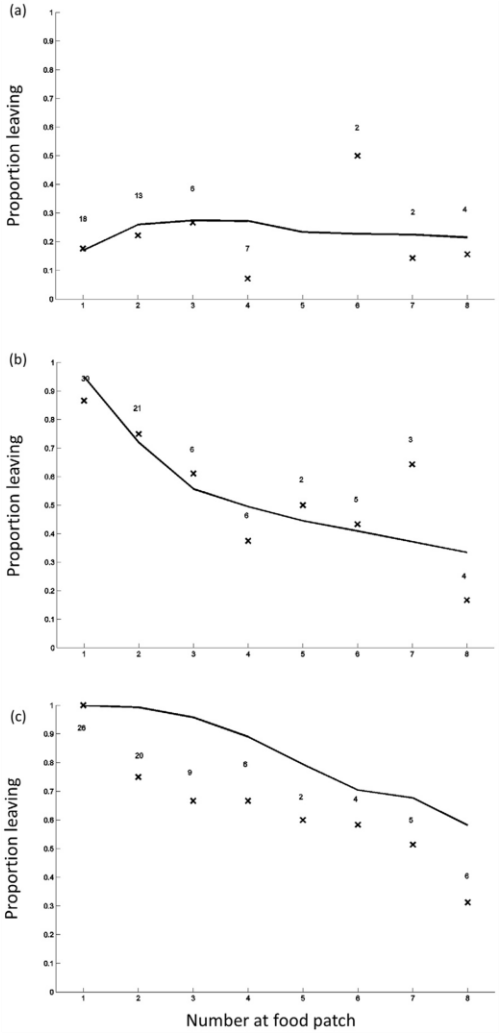

Figure 2.1: Distribution of the number of fish that went to the food patch for each group size for (a) no replica fish, (b) one replica fish and (c) two replica fish. The solid line represents the quorum response model.

Figure 2.2: The crosses represent the proportion of leaving the food patch following the departure of the replica fish for (a) no replica fish, (b) one replica fish and (c) two replica fish. The numbers represent the number of the observations in which fish was observed at the food patch. The solid lines illustrate the model prediction based on a quorum response.

(Ward et al., 2012)

4. Conclusion

In this experiment the movement decisions of three-spine sticklebacks toward and then away from a food patch can be explained by a quorum rule. Fish approach and then leave the food patch when a number of conspecifics were raised above a threshold number of initiators. This threshold number is constrained by the group size.

The greater tendency to follow replica fish in smaller groups could be explained by the fact that group living animals in smaller groups are at a greater risk of predation than those in larger groups (Godin et al., 1985). In contrast fish in larger group are less responsive to the departure of a single replica fish, whereupon the departure of at least two replica fish triggers a greater following response. This could be explained by the need of a threshold number of leader fish to release a following response. Additionally the departure of a single fish could be an error and therefore a disadvantage for the following fish (Ward et al., 2012).

Further experiments showed that the quorum rule is also consistent with group-living behavior in other contexts, e.g. behavior under predation risk (Ward et al., 2008) and in distinguishing phenotypic difference (Sumpter et al., 2008). Therefore the quorum rule provides a general standard to explain decision-making in group-living animals and could even predict the behavior of group-living animals.

References

Godin JGJ, Morgan MJ (1985) Predator avoidance and school size in a cyprinodontid fish, the banded killifish (Fundulus diaphanus Lesueur). Behavioral Ecology and Sociobiology 16: 105–110

Lee D (2008) Game theory and neural basis of social decision making. Nature Neuroscience 11: 404-409

Sumpter DJT, Krause J, James R, Couzin ID, Ward AJW (2008) Consensus decision making by fish. Current Biology 18: 1773–1777

Ward AJW, Sumpter DJT, Couzin LD, Hart PJB, Krause J (2008) Quorum decision-making facilitates information transfer in fish shoals. Proceedings of the National Academy of Sciences of the United States of America 105: 6948–6953

Ward AJW, Krause J, Sumpter DJT (2012) Quorum Decision-Making in Foraging Fish Shoals. PLoS ONE 7(3): e32411. doi:10.1371/journal.pone0032411

Decision-making and Weber's law: a neurophysiological model

by Gustavo Deco & Edmund T. Rolls
published in 2006

Term Paper by Jörg Meier

Content

---

1. Introduction

The term paper summarizes the investigations and results presented in [Deco et al, 2006] and is structured as follows: at first, related experiments and issues are overviewed. The model itself is described and explained afterwards before the results of theoretical and experimental analyses are presented and finally discussed.

Deco and Rolls describe in [Deco et al, 2006] a leaky integrate-and-fire attractor model which aims to reflect the decision-related activity of neurons in the ventral premotor cortex (VPC) during a vibrotactile frequency comparison task.

1.1. Flutter discrimination task

The model presented in the considered paper ([Deco et al, 2006]) describes neuronal activities which occur during a vibrotactile frequency comparison task, presented in [Romo and Salinas, 2003]. In this task, a monkey (*Macaca mulatta*) must compare two different frequencies, which are presented to the monkey one after another both for 500 ms with a short delay of 3 seconds in between. One hand of the monkey is restrained, such that a mechanical stimulator, which will oscillate vertically during the test, touches one digit of the monkey's hand. The other hand is placed on an immovable key by the monkey, which triggers the test to begin. At first, the stimulator vibrates at a base frequency f_1 and after a short delay at a comparison frequency f_2. Afterwards, the monkey releases the key with the unrestrained hand and presses one of two possible buttons, one representing $f_1 > f_2$ and the other $f_1 < f_2$ respectively. Note, that prior to the tests the monkey was trained to push the one button when f_1 was the higher frequency and the other button otherwise.

Thus, the monkey's task conceptually consists of the following sequence of neural operations: encoding the frequency f_1 of the first stimulus, maintaining it in working

memory, encoding f_2, compare f_2 with memorised f_1 and finally output the result of the comparison via the motor system.

Note that investigations ([Mountcastle et al, 1968]) have found that 'humans and monkeys have similar abilities for detecting and discriminating the frequencies of mechanical sinusoids delivered to the hands' ([Deco et al, 2006])

1.2. Weber's law

In 1834, Ernst Heinrich Weber discovered that the ratio of the *difference-threshold* Δf (or *just noticeable difference*, i.e. the amount of change needed for a sensory organ to recognize that a change occurred) to the background intensity f is a constant $k = \Delta f / f$.

1.3. Background of the model: neuronal data underlying the vibrotactile discrimination

Since the objective is to model the process of decision-making, it would be nice to detect a confined area in the brain about which there exists good evidence that this process is located there. Thus, important areas of the brain and their relevance to the neural operations, mentioned in subsection 1.1., and vice versa are described in [Deco et al, 2006] and will be briefly, and hence without references, summarized here.

In [Deco et al, 2006], it is said that spiking neurons in the primary somatosensory area (S1) only reflect the stimuli frequencies themselves during the stimulation periods. This also accounts for neurons in the secondary somatosensory area (S2), but furthermore there are activities during the later part of the second stimuli (with f_2), which are said to reflect the comparison and thus the result of the decision. However, the authors of [Deco et al, 2006] describe the ventral premotor cortex (VPC), the medial premotor cortex (MPC) and the primary motor cortex (M1) as areas which represent the decision-process. Especially neurons in the VPC area 'seem to reflect the core of the processing that links sensory information with action, and therefore they may represent the decision-making process itself, rather than the representation of the stimulus' ([Deco et al, 2006]).

2. The leaky integrate-and-fire attractor model

An *attractor model* can be described as an often recurrently connected network of nodes with weighted transitions. Such a network, depending on its input and the interconnectivity of the nodes, gradually converges to some stable patterns, called

attractors. An attractor might be one-dimensional (*point attractor*), two-dimensional (*line*, *ring* and *plane attractor*) or even of higher dimension.

Simplified, a *leaky integrate-and-fire* (LIF) neuron with some input (inhibitory or excitatory) and output connections works in a way that it integrates all incoming currents from afferent spikes and fires when the depolarization of the cell membrane crosses a specific threshold. Note, that this model is detailed enough to represent the functioning of the underlying biophysical system including time constants, latencies and conductance.

In [Deco et al, 2006], the probabilistic decision-making is modelled by an attractor network of LIF neurons (depicted in Figure 1), which has two pools of neurons representing the two decision states ($f_1 > f_2$) and ($f_1 < f_2$). Furthermore, there is a state of nonspecific excitatory neurons, which contains all other excitatory neurons not included in the task, and a state of inhibitory neurons. Conductance values for the synapses are modelled by the connection weights, which represent interneuron connections established by Hebbian learning ('*what fires together, wires together*'), and are assumed to be formed preliminary (e.g. by self-organization mechanisms). Hence, the weights are set as follows (as a result of a mean-field analysis of the network; details are omitted here): $W_+ = 2.2 > 1$, $W_- = 0.86 < 1$, $W_I = 1.015$ and all other weights set to 1.

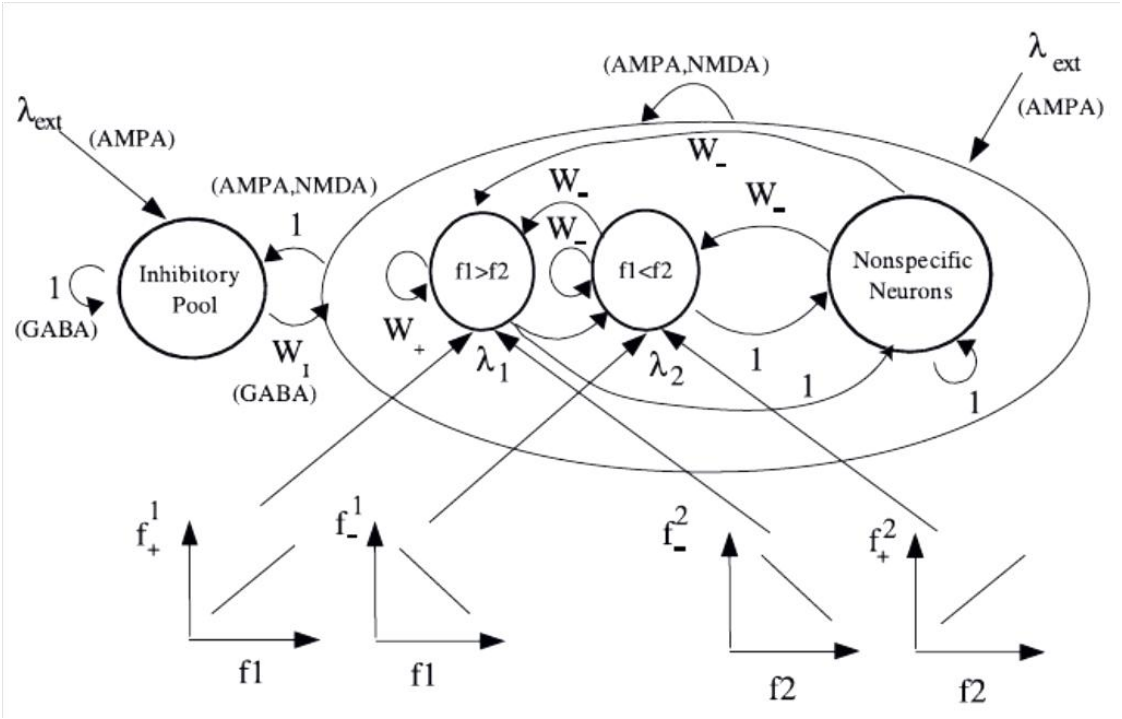

Figure 1: The architecture of the neurodynamical model for a probabilistic decision-making network. (taken from [Deco et al, 2006])

In this model, all four pools of neurons receive as input a spontaneous background activity from external excitatory connections typically found in neurons in the cerebral cortex, denoted by λ_{ext} = 2.4 kHz. In addition, both pools ($f_1 > f_2$) and ($f_1 < f_2$) receive inputs encoding the stimulus-specific information at the time when the second stimuli f_2 is presented, which is λ_1 for ($f_1 > f_2$) and λ_2 for ($f_1 < f_2$). In [Deco et al, 2006], it is assumed that these information originate from S2, as well as from the prefrontal cortex (PFC) and it is found that there are two types of S2 and PFC neurons: 'neurons with positive (f_+) and others with negative (f_-) monotonic relationships between the firing rate and the stimulus vibrotactile frequency' ([Deco et al, 2006]). Thus, $\lambda_1 = f_+^1 + f_-^2$ and $\lambda_2 = f_-^1 + f_+^2$.

3. Results

During their investigations, the authors of [Deco et al, 2006] found that the LIF network is subject to finite size noise and hence always converges to either one of the two attractors with neuron pools ($f_1 > f_2$) or ($f_1 < f_2$) active, which represent the decision states. Thus, the network presented is a biased competition model of decision-making.

To fully characterize the dynamics and the probabilistic behaviour of the system described above, a computer simulation of the spiking network model is run.

Figure 2 illustrates the probability of correct discrimination as a function of the difference between the two presented vibrotactile frequencies to be compared. In all tests, $f_1 = f_2 + \Delta f$ holds and thus $f_1 > f_2$. Hence, Δf (called 'Delta frequency (f1 – f2)' in Fig. 2) describes the difference between both frequencies. The lines in Fig. 2 were calculated by fitting the diamond points (the actual measured results) with a logarithmic function. If, during the 500 ms of comparison in one test, the network converges towards a point-attractor with a spiking activity > 10 Hz for the pool ($f_1 > f_2$) and at the same time the spiking activity for the pool ($f_1 < f_2$) is low, the classification is defined to be correct.

In the second panel of Figure 2 the stars (*) indicate the actual neuronal data measured in the real experiment with the monkey for f_2 = 20 Hz, as reported in [Romo and Salinas, 2003].

The main result, illustrated in Figure 2, is that the difference Δf between f_1 and f_2 in order to reach a threshold of 85% of correct classifications (dashed lines in Fig. 2) must increase when the base frequency f_2 increases. Furthermore, the authors of [Deco et al, 2006] found that the difference-threshold Δf increases linearly as a function of the base-frequency f_2. This surely corresponds to Weber's law regarding the vibrotactile discrimination task.

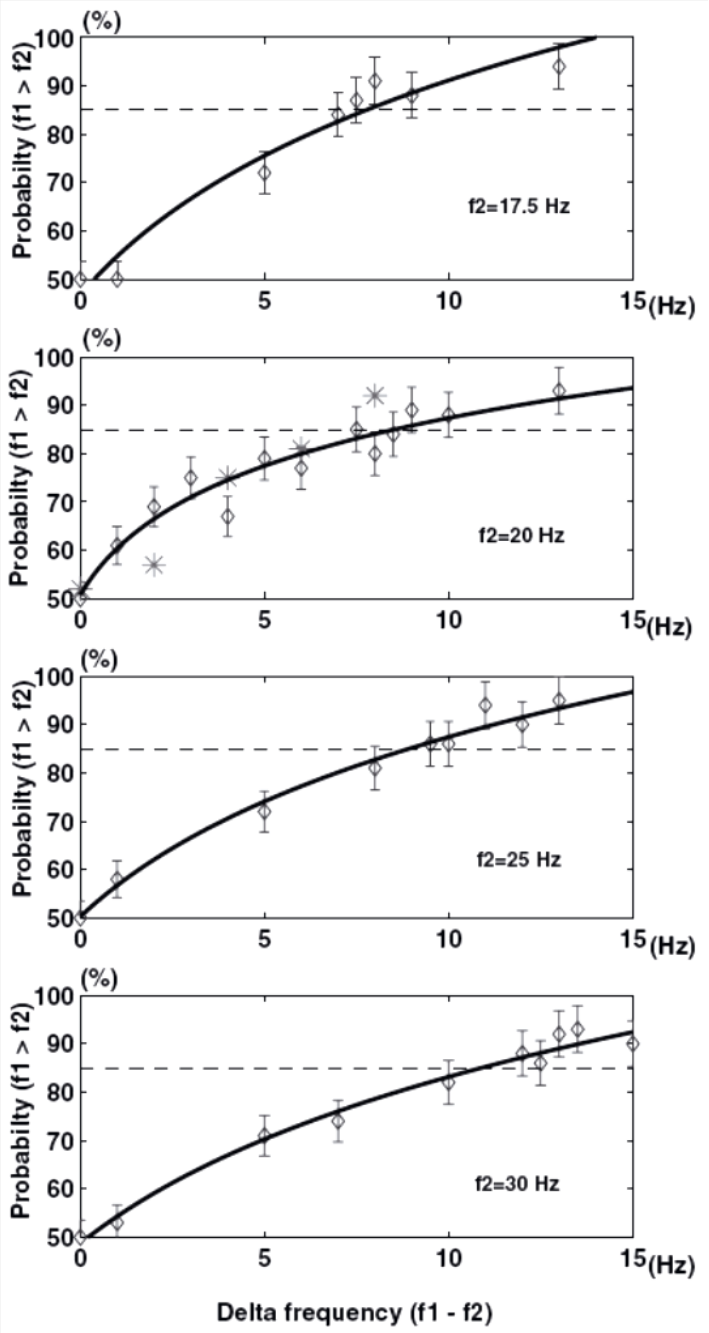

Figure 2: Probability of correct discrimination as a function of the difference between the two presented frequencies to be compared. The dashed line represents the threshold of correct classification for a performance of 85% correct discrimination. (from [Deco et al, 2006])

4. Discussion

The authors of [Deco et al, 2006] presented an attractor network which models probabilistic decision-making. As a main result they found that the just-noticeable-difference, at which two stimuli can be discriminated, increases linearly as a function of the base frequency. This corresponds to Weber's law. Furthermore, they note that 'this is the first time we know when the implementation of a psychophysical law is not the firing rate of the neurons, nor the spike timing, nor is single neuron based, but instead is based on the synaptic connectivity of the network and on statistical fluctuations due to the spiking activity in the network' ([Deco et al, 2006]).

5. Literature

[Deco et al, 2006] **Deco G., Rolls E.T.** (2006): *Decision-making and Weber's law: a neurophysiological model.* Eur J Neurosci. 24(3): 901-16.

[Romo and Salinas, 2003] **Romo R., Salinas E.** (2003): *Flutter discrimination: neural codes, perception, memory and decision making.* Nature Rev. Neurosci., 4, 203-218.

[Mountcastle et al, 1968] **Talbot, W. H., Darian-Smith, I., Kornhuber, H. H. & Mountcastle, V. B.** (1968): *The sense of flutter-vibration: comparison of the human capacity with response patterns of mechanoreceptive afferents from the monkey hand. J. Neurophysiol*. **31**, 301–334.

A Neuronal Model for Sequential Decision Making based on Synaptic Facilitation

A summary of „Synaptic dynamics and decision making“

by Gustavo Deco, Edmund T. Rolls and Ranulfo Romo,

Proc Natl Acad Sci U.S.A. 107, 7545–7549 (2010)

Philipp Norton

19.08.2012

Introduction

Decision making is a cognitive process that is performed when evaluating information and, based on this information, choosing one of two or more alternative actions (Wang, 2008). To experimentally analyze the execution of decision making on a neuronal level, the presented information and possible outcomes should be as straightforward and repeatable as possible. An example of an experiment that fulfills these requirements is the comparison of two subsequent vibrational stimuli (in the range of 10-50 Hz) applied to the skin of trained rhesus monkeys (*Macaca mulatta*) (Hernández et al., 1997; Romo et al., 2004). In these experiments the monkeys were presented with a vibrotactile stimulus of a certain fequency f_1, followed by a delay period and then the presentation of a second stimulus of a different frequency f_2. If they correctly discriminated which stimulus was higher in frequency, they were rewarded with a drop of liquid (Hernández et al., 1997). In order for this discrimination to take place, the intensity of f_1 must be stored in working memory during the delay period as well as the presentation period of f_2.

Recording from single neurons in the ventral premotor cortex (VPC) during the experiment, Romo et al. (2004) found out that some neurons diplay a high firing rate if the first stimulus was stronger than the second ($f_1 > f_2$) while others respond to the decision $f_2 > f_1$. A third group of neurons – named “partial differential neurons” – reflects the memory of f_1. Their behaviour during the experiment is illustrated in Figure 2A. The firing rate of these partial differential neurons is high during the presentation period of f_1 (with the maximum being proportional to the intensity of f_1) and low at the beginning of the delay period. During the delay the rate gradually increases to a level that again reflects f_1. The further increase while f_2 is presented depends on the intensity of f_2. Since the firing rate is higher when $f_1 > f_2$ than when $f_2 > f_1$ for a given f_2, the response of the partial differential neurons might play a role in the decision making process (Romo et al. 2004).

The summarized publication (Deco et al., 2010) proposes a synaptic mechanism that contributes to the response properties of these partial differential neurons. The authors present a model in which they play a major role in sequential decision making, improving upon a previously proposed attractor model.

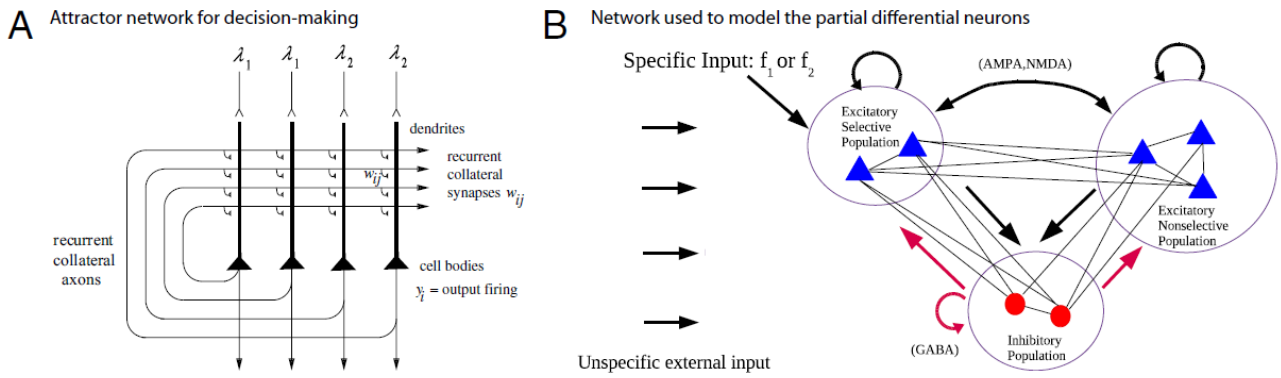

Figure 1. (A) Attractor network architecture for decision making. The evidence for decision 1 is applied via the λ1 inputs and that for decision 2 is applied via the λ2 inputs. **(B)** Neural network with synaptic facilitation between excitatory neurons to model the "partially differential" neurons recorded in the VPC. The recurrent arrows indicate recurrent connections between the different neurons in a pool. The gray lines show the connections in the fully connected network. Modified after Deco et al. (2010)

Attractor Model

Deco and Rolls (2006) described a model in which an attractor network consisting of two populations of neurons, each with it's own input (λ_1 and λ_2) encoding f_1 and f_2, respectively, compares the stimuli (Figure 1A). Recurrent collateral excitatory connections between the neurons in each of the populations enhance the response to their input through positive feedback. At the same time the two populations compete with each other through another population of inhibitory neurons. Through the mechanisms of inhibition and recurrent feedback the network has a tendency towards one of two steady states depending, amongst other factors, on the inputs (Deco et al., 2012). Once reached, these "attractive" states (hence the name attractor network) are hard to leave, thus forming a persistent neural activity and consolidating the decision.
In the VPC, though, vibrotactile stimuli are encoded by the same neurons (Deco et al., 2010), which constitutes a problem for the described network, as it relies on two distinctive inputs.

Partial Differential Model

The model of the partial differential neurons (Figure 1B; Deco et al. 2010) consists of an excitatory selective population of interconnected neurons receiving input from the vibrotactile stimuli (f_1 as well as f_2). Connected to the selective population is an excitatory nonselective population of neurons (without an input) and both populations connect to an inhibitory pool of neurons. Every neuron in the model also receives a nonspecific external stimulation. This signal – described by the authors as „a learned attention signal" (Deco et al., 2010, p. 7546) – is linearly increased from 2.4 kHz (sum of spikes received over all synapses by each neuron) to 2.544 kHz over the duration of the delay period.

Unlike in the attractor network model, here the the memory of the first stimulus is not upheld by recurrent connections, as this would result in a constant high firing rate during the delay period, which is not the case in partial differential neurons (Fig. 2A; Romo et al., 2004). Instead, a process called short-term synaptic facilitation is used the explain the slow ramping of the firing rate during the delay. This process arises after an action potential opens Ca^{2+} channels in the presynaptic terminal. The temporarily increased Ca^{2+} concentraiton now increases the amount of neurotransmitter released during following spikes (Zucker & Regehr, 2002).

Therefore the synapses in the excitatory selective population are strengthened during the presentation of f_1, when these neurons fire at a high rate. Then, during the following delay period the activity gradually ramps up due to the increase of the nonspecific external stimulation. The slope of this ramp depends on the amount of synaptic facilitation received earlier, which in turn depends on the intensity of the first stimulus (f_1). Thus the firing rate of the differnetial selective neurons at the end of the delay period again encodes f_1. During the comparison period (the presentation of the second stimulus) the excitatory selective neurons receive f_2 as input, while still being synaptically facilitated by the presentation of f_1. Therefore the firing rate at this point reflects the sum of the memory of f_1 and the current input of f_2, which is lower for $f_1 < f_2$ than for $f_1 > f_2$ (for a given f_2).

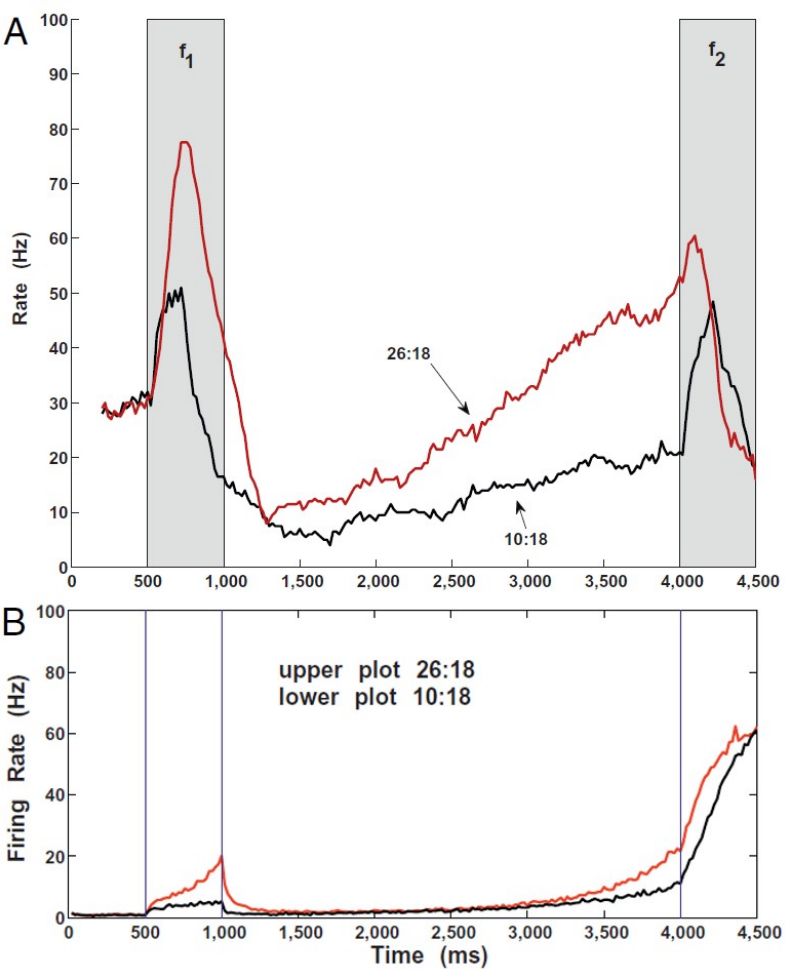

Figure 2. Modified after Deco et al. (2010) **(A)** Activity of a single partial differential neuron recorded in the VPC during the vibrotactile discrimination task, after Romo et al. (2004). The f_1 period was from 500 to 1000 ms, f_2 from 4,000 to 4,500 ms. f_2 was 18 Hz in both cases. When f_1 was 26 Hz (red plot), the firing rate during f_1, at the end of the delay period, and during the comparison period when f_2 was being applied was higher than when f1 was 10 Hz (black plot). Approximately 30 trials were used to generate these peristimulus time histograms for each pair for this single neuron. **(B)** Activity of the modeled partial differential neurons. Temporal evolution of average firing rates across trials and neurons for the comparison of f_1 = 10 Hz < f_2 = 18 Hz (black) and f_1 = 26 Hz > f_1 = 18 Hz (red).

Results

Figure 2B illustrates the firing rate of the modeled partial differential neurons over time. Similarly to the the neurons recorded in the VPC (Fig. 2A) the responses are high during the presentation of f_1 and low at the beginning of the delay. Towards the end of the delay they slowly ramp upwards to represent the memory of f_1. During the comparison period again the firing rate is lower for $f_1 < f_2$ than for $f_1 > f_2$ (Fig. 2B).

Discussion

The presented model describing the response of the partial differential neurons by using a single input neural network as well as simulating the synaptic facilitation process offers a possible explanation for the previous recordings of single neurons in the VPC during a vibrotactile discrimination task. While the activity of the modeled neurons (Fig. 2B) does not exactly mirror the response of the neurons recorded in the VPC (Fig. 2A), it exhibits the basic characteristics of the partial differential neuron behaviour. Specifically, the firing during the comparison period is higher if $f_2 > f_1$.
If the partial differential neurons – encoding the sum of the two stimuli – are fed into one input of the previously described attractor network (Deco & Rolls, 2006) and neurons that only encode the second stimulus (Romo et al., 2004) into the other input, the attractor network could subtract the second stimulus from the sum of both stimuli to effectively compare f_1 against f_2 (Deco et al., 2010). In conclusion the combination of the two models suffice to propose a neuronal mechanism for sequential decision making using a single input for subsequent stimuli.

References

Deco G, Rolls ET (2006) Decision-making and Weber's law: A neurophysiological model. *Eur J Neurosci* 24, 901–916.

Deco G, Rolls ET, Romo R (2010) Synaptic dynamics and decision-making. *Proc Natl Acad Sci U.S.A.* 107, 7545–7549.

Deco G, Rolls ET, Albantakis L, Romo R (2012) Brain mechanisms for perceptual and reward-related decision-making. *Prog Neurobiol* [in print].

Hernández A, Salinas E, García R, Romo R (1997) Discrimination in the sense of flutter: New psychophysical measurements in monkeys. *J Neurosci* 17, 6391–6400.

Romo R, Hernández A, Zainos A (2004) Neuronal correlates of a perceptual decision in ventral premotor cortex. *Neuron* 41, 165–173.

Wang XJ (2008) Decision making in recurrent neuronal circuits. *Neuron* 60, 215–234.

Zucker RS, Regehr WG (2002) Short-term synaptic plasticity. *Annu Rev Physiol* 64, 355–405.

Cortico-basal ganglia circuit mechanism for a decision threshold in reaction time tasks

Course: Role of Decision Making
A summary by
Michael Rauer

1 Introduction

In 2002 Roitman and Shadlen performed trials on rhesus monkeys which had to solve reaction time tasks [Roitman and Shadlen, 2002]. They exposed monkeys to screen, with randomly moving dots. Also known as random-dot motion discrimination task. Depending on the chosen coherence level, a certain amount of dots take a similar direction und the monkey reacts with a saccade to follow the majority of dots. This saccade is defined as a decision in this setup. Choosing a low level of coherence makes it harder to decide in which direction the dots are moving since less information is provided.
During these experiments the correlation of saccades and lateral intraparietal (LIP) area were investigated. Here they found a correlation between decision speed and accuracy, depending on the amount of noise (randomly moving dots) in the stimulus intensity (coherently moving dots). To find out what the circuit mechanisms may look like, it is important to figure out the important areas which are involved. This summary is based on the publication of Lo and Wang, which introduce and describe a cortico-basal ganglia circuit mechanism for a decision threshold in reaction time tasks [Lo and Wang, 2006].

2 The cortico-basal circuit mechanism model

The cortico-basal ganglia circuit mechanism is an approach to describe the uptake of a visual stimulus where the system may respond by a saccade. The model implements a competition mechanism such that the system response is either a left- or right-wise saccade. For illustration and abbreviations of the description below, see figure 1. The network distinguishes between left and right pathway (superscripts L and R, respectively). Connections consist of inhibitory (suffix 'i') and excitatory (suffix 'e') synapses. The model builds on a stochastic multi-compartment scheme.
Here, three layers are used to build the model. An input layer, a regulatory layer and an output layer which triggers the reaction.
The Cortex (Cx) is known to process visual stimuli [Roitman and Shadlen, 2002], so this forms the input layer of the presented model.
For the output layer, Superior Colliculus (SC) is associated with optico-motorical properties, which triggers the saccades [Saito and Isa, 1999].
Basal Ganglia represent the regulatory layer in the model. Here the Basal Ganglia are split into the Caudate Nucleus (CD) and Substantia Nigra pars Retina (SNr).
The network further includes inhibitory and excitatory connections. Since the network distinguishes between right and left, it shows a pathway for each side, and both pathways are connected to each other. They are symmetric, so everything which is true for the left population, is true for the right one.
To keep the order of signal propagation first the Cortex is described, which is the input layer. The Cxe^L takes up the stimulus and shows self-excitatory behavior. It also excites Cxe^R. But the more one or both excitatory populations are stimulated the more likely it is for Cxi to inhibit Cxe^L and Cxe^R. Further Cxe stimulates SCe and CD of Basal Ganglia.

Second, Superior Colliculus, taking excitatory stimulus from the Cortex, SCe is directly excited by Cxe. SCe also shows self-excitatory behavior, but also takes part in a negative feedback loop. While the self-excitation only works as self-transition on SCe^L or SCe^R itself, the negative feedback, once stimulated by one, inhibits both of the SCe population. SCe is also inhibited from Basal Ganglia. SCe exhibits a 'winner-takes-it-all' situation, meaning either SCe^L or SCe^R sends out a burst and triggers the saccade. Additionally, Cx builds a positive feedback loop with SC, which causes the inhibitory Cxi to inhibits both Cxe populations.
Third, the regulatory layer, the Basal Ganglia is responsible for regulating the propagation of signals. SNr shows tonic behavior and inhibits SCe. But when CD becomes stimulated and a certain threshold is crossed it inhibits SNr and the inhibition on SCe vanishes. This layer takes great responsibility for triggering saccades. As the inhibition vanishes, it takes less to excite SCe and cross its threshold and consequently trigger a saccade. [Lo and Wang, 2006]

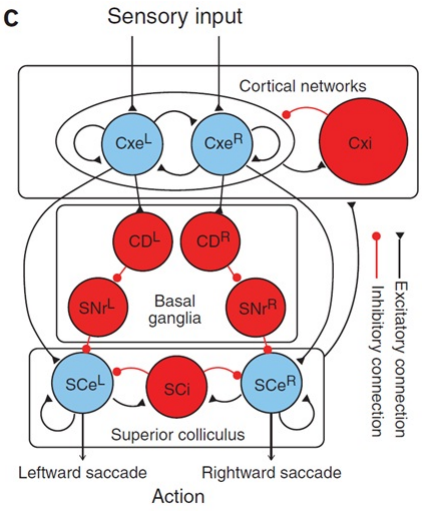

Figure 1: Network model

3 Model behavior

As illustrated in section 2 the system consists of several excitatory and inhibitory connections. So how does the system's response depend on the strength of stimuli? First we assume the threshold for SCe (see figure 1) is lower than the threshold of CD. In case where stimuli are not strong enough to cross either thresholds, no saccade will be triggered at all. If the stimulus exceeds the threshold of SCe, SCe remains inhibited by SNr and does not trigger a saccade. So this requires a stimulus to be strong enough, such that the Cxe cross the threshold of CD, which inhibits SNr and consequently, SNr releases SCe from inhibition. Since we assume that the threshold of Cxe-CD is higher than the threshold of Cxe-SCe, a saccade is only triggered if the CD threshold is crossed.
Figure 2 shows an example of what happens as coherence of the random dot motion raises to 12.8 %. At this coherence level enough information is provided to determine a direction. The dots are directed to the right. So in a) the frequency for the Cxe^R raises higher than in Cxe^L. It reaches a peak at about 480 ms with 20 Hz.
In b) the same time axis is shown describing CD^R and SNr^R. Where SNr is at a constant frequency of 80 Hz, CD remains silent at 0 Hz. As the stimulus of the Cxe-CD connection (see a)) crosses the threshold at about 480 ms, CD sends out a brief burst of 60 Hz at

maximum, which reduces the frequency of SNr to almost 0 Hz.
In c) both, SCe and SCi remain silent until the threshold of Cxe-CD is crossed. Then at around 480 ms SCe performs a strong burst raising up to at least 250 Hz stimulating SCi, which immediately inhibits SCe to 0 Hz frequency. The short burst of SCe triggers is a right-wise saccade. To the the system behavior Lo and Wang varied the thresholds of Cx-CD

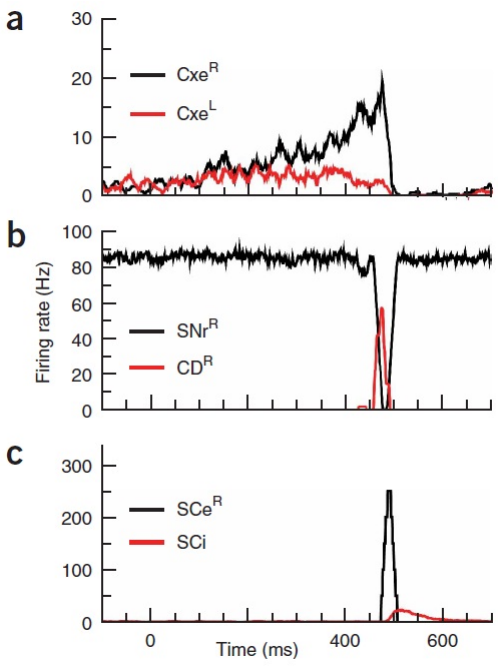

Figure 2: Frequencies of single neuron populations: The stimulus is at 12.8 % coherence. a) The frequency of the right cortical neuron population rises until it reaches a peak at about 20 Hz and becomes silenced (about 0 Hz). Left neuron population frequency rises, but does not exceed a frequency of 5 Hz. b) SNr shows tonic behavior with a frequency of about 80 Hz. CD remains at 0 Hz. At about 480 ms, CD^R is stimulated and inhibits SNr^R. The frequency of SNr^R drops to 0 Hz. c) As only the right 'path' is stimulated, SC^R shows as short, strong burst slightly delayed to the peak of Cxe^R in a). Frequency of SC^L slightly rises but does not exceed the threshold. Output of the system is a right-wise saccade.

and Cx-SC. The reaction of the model showed that the threshold of Cx-CD has a huge impact on whether a saccade is triggered or not. In contrast, changing the threshold of the Cx-SC connection shows only a small effect on the experimental outcome. Both findings are consistent with biological measurements, and leads to the interpretation that the basal ganglia represent a regulatory unit in this context.
The variation in thresholds are a time-accuracy trade-off. So if there is a few information and a lot of noise (only a small amount of dots are moving coherently) and the thresholds are low, there might be a fast decision, which is more likely to be wrong. On the other hand, when the threshold is too high, it may take too long to find a decision. This leads to the idea that the thresholds are highly variable in biological systems.

4 Results and conclusions

Lo and Wang built cortico-basal circuit model for describing a reaction time task. It is based on the reaction of a neuronal network being exposed to an optical stimulus.
The model is built from three functional regions, such that there is an input, a regulatory and an executing part, which in biological systems are a part of the Cortex, the Basal Ganglia, and the Superior Colliculus. By threshold changing it can be shown that the model behaves consistently with measurement data. So Lo and Wang were able to create a simplified and still consistent model using the cortico-basal ganglia regulation mechanism [Lo and Wang, 2006]. Since the model is simplified, it can be extended to model more neural regions and maybe use different task to find out how the system behaves.

References

[Lo and Wang, 2006] Lo, C.-C. and Wang, X.-J. (2006). Corticobasal ganglia circuit mechanism for a decision threshold in reaction time tasks. *Nat. Neurosci.*, 9(7).

[Roitman and Shadlen, 2002] Roitman, J. D. and Shadlen, M. N. (2002). Response of Neurons in the Lateral Intraparietal Area during a Combined Visual Discrimination Reaction Time Task. *J. Neurosci.*, 22(21).

[Saito and Isa, 1999] Saito, Y. and Isa, T. (1999). Electrophysiological and morphological properties of neurons in the rat superior colliculus. I. Neurons in the intermediate layer. *J. Neurophysiol*, 82.

The Role of Memory in Decision Making

Piéron's Law and optimal behavior in perceptual decision-making

Term Paper by Martin Seeger

Original article: van Maanen, L., Grasman, R. P. P. P., Forstmann, B. U., & Wagenmakers, E.-J. (2012). Piéron's Law and Optimal Behavior in Perceptual Decision-Making. Frontiers in neuroscience, 5 (January), 143.

Structure of this paper

1. Introduction to Piéron's Law and the original article

The relationship between stimulus intensities and perceptual observables has been studied early on in psychophysics. E.g., the works on the Weber-Fechner law and later on Stevens' power law [1] were concerned with the connection between the physical strength of a stimulus and its perceived magnitude. Stevens was able to establish power laws for a wide range of stimuli.

In a related context, Piéron's Law [2, 3] is a psychophysical observation which connects another variable, the mean response time (MRT), to stimulus intensity. In close analogy to Stevens' law, it states that MRT decreases as a power function of the stimulus intensity *I*, i.e.

$$\mathrm{MRT} = \alpha I^{-\beta} + \gamma,$$

where $\alpha, \beta > 0$ are parameters,
$\gamma > 0$ denotes the non-detection related time and
$\mathrm{MRT} - \gamma$ denotes the detection-related time.

According to Piéron's Law, human brains respond quicker to more intense stimuli and slower to less intense stimuli. This contrasts with mechanical machines for which the response time to a stimulus is usually fixed. The power law equation is expected to hold with specific parameters for each individual and stimulus modality.

A possible interpretation suggests that smaller stimulus intensities are associated with more uncertainty. Therefore more evidence must accumulate for a response where the uncertainty is larger. The power law implies that the rate at which the MRT improves decreases as the intensity increases.

Since the original publication [2], Piéron's Law has been confirmed for various sensory modalities and decision tasks, including brightness [2], tone [4], taste [5], odor [6], heat [7] and color perception [8]. The authors of the present paper [9] extend Piéron's law to a more general context: the law is hypothesized to hold in general for decision-making under uncertainty. In this formulation, stimulus intensity is replaced by the degree of discriminability between two noisy stimuli. Correspondingly, the notion of signal detection gets replaced by a decison between two or more alternatives.

The first part of [9] describes a two-alternatives forced choice (2AFC) experiment in which this hypothesis is confirmed. In the second part a theoretical foundation of Piéron's law by means of a Bayesian ideal observer model is described.

Generally, two main categories of models to study decision-making have been proposed (see [10] and references therein): one category, biologically motivated models, is built “bottom-up“ using neurophysiological entities such as individual neurons. The other category are phenomenological models. Usually, these models use a threshold concept together with stochastic processes to model the accumulation of evidence before a decision is made.
The simplest phenomenological model is the drift–diffusion model, in which the first passage of one random process through the threshold determines the decision. The model can be modified to reproduce the speed-accuracy tradeoff (i.e. the negative correlation between response time and rate of correct results) which has been, e.g., observed in random dot motion experiments (cf. [11, 12]).
In the race model two or more random processes race towards their thresholds and compete for alternative decisions. This model allows a biological interpretation of the random variables as representing different pools of neurons. Importantly, both the linear ballistic accumulator model [9, 13] and the assumptions underlying the Bayesian Ideal Observer [9] are conceptually close to the race model. Both will be introduced below.

2. Description of the experimental methods

The main experiment in [9] is concerned with stimulus discriminability in a random dot-motion task. Participants were six students. The authors used a MATLAB program to create a moving-dot kinematogram as described below and displayed in Figure 1.

In each stage of the experiment, 25 % of the dots in a circle were moved in a certain direction (the “target” direction) while the rest moved randomly. The target direction and another, “false” direction at an angular distance d were presented along a surrounding circle. The alternatives were chosen randomly from the top half of the circle, the angular distance was sampled from an exponential distribution.

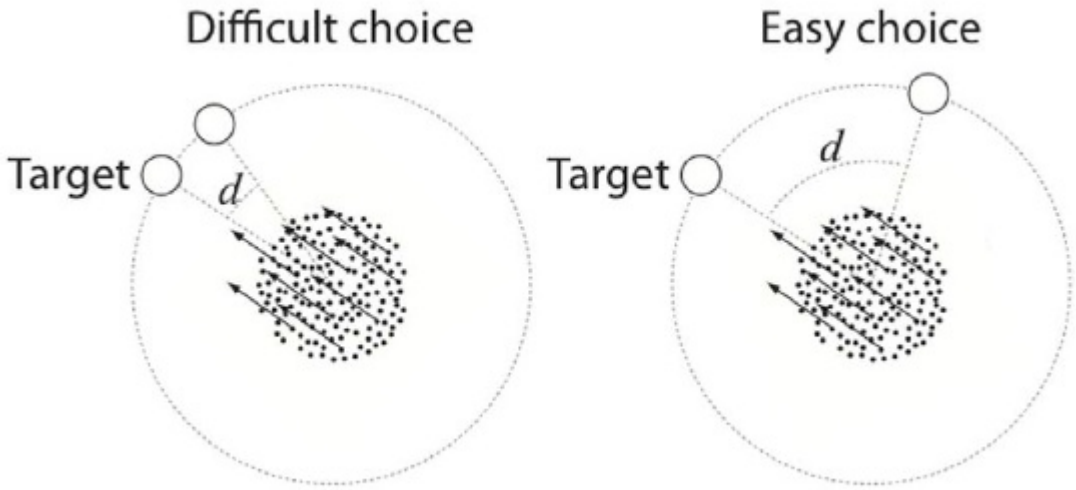

Figure 1 [9, p. 2]: The moving-dot kinematogram. A certain percentage of the dots moves in a target direction, the rest moves randomly. The difficulty of the task is varied by changing the angular distance d between the true and false alternatives.

The task consisted in deciding between the two alternatives by pressing certain keys on a keyboard. Times were accepted between 200 ms and 2000 ms post stimulus presentation, other times were discarded. Each participant repeated 210 x 7 (number of directions) iterations of the task after an initial training period.

3. Description of the statistical methods and results

3.1 Direct approach, results and discussion

In a first attempt, the authors of [9] fit two models directly to the experimental data. As no further statistical modelling was performed, this approach was termed “direct“. The two model equations used are:

Power model (Piéron's Law):

$$\mathrm{MRT} = \alpha d^{-\beta} + \gamma,$$

Exponential model (alternative):

$$\mathrm{MRT} = \alpha \exp(-\beta d) + \gamma.$$

For each combination of model and participant, the model's quality was assessed by calculating the correlation between actual and predicted values, and the model's Bayesian information criterion (BIC), defined as

$$\mathrm{BIC} = -2 \ln L + k \ln n,$$

where L = maximised likelihood of the parameters, given the data,
k = 2 = number of parameters,
n = number of data points.

The BIC penalizes the number of parameters in a model and trades it off against its log-likelihood. High values of BIC indicate overfitting and/or low likelihood of the model.
Power and exponential models are then compared by means of their evidence ratio,

$$\exp[-(\mathrm{BIC}_{\mathrm{pow}} - \mathrm{BIC}_{\mathrm{exp}})/2],$$

indicating how many times more likely the data had occured under the power model than under the exponential model.

The direct statistical approach was discarded because the non-decision time γ took unrealistic values under this approach. (658 ms on average for the exponential, between 0 ms and 810 ms for the power function, where plausible values would range from 200 ms to 500 ms.)

3.2 Linear ballistic accumulator (LBA) model, results and discussion

Instead of the one-stage, three-parameter optimisation, a two-stage parameter estimation procedure was applied:

Stage 1: estimation of γ using the LBA model,
Stage 2: estimation of α, β, keeping γ fixed.

LBA model

The LBA model [13] assumes that a decision is made after accumulation of evidence for a particular option when a decision threshold has been reached. For each competing alternative, one accumulator random variable is maintained. The starting amount of evidence is drawn from a uniform distribution. Evidence for each alternative accumulates by adding random variables which are sampled successively from a normal distribution $N(v_d, \sigma)$. v_d is called the drift rate. That decision is made for which cumulative evidence reaches a threshold first. Because of the randomness, both correct and false decisions are made by the model.

To determine the LBA model parameters, decision times and choices are fitted to the experimental values for each participant. It was found that introducing angular dependencies besides that of v_d did not improve BIC. The fitted models allowed to two conclusions. Firstly, for each participant, the drift rates were monotonically increasing with the angular distance, and secondly, the non-decision time γ was for all participants between 270 ms and 504 ms with an average of 381 ms, i.e. it fell into the expected range.

With the obtained γ parameter, the α and β parameters were again fitted numerically. Typically, β ranged from 0.2 – 0.3 for the power law. As expected, the correlation between actual and observed values dropped slightly. On the other hand, now for four participants the evidence ratio was 15 to 415 times in favor of the power model, and for the remaining individuals still greater than one. Overall results are displayed in Figure 2, comparing the exponential and power function fits.

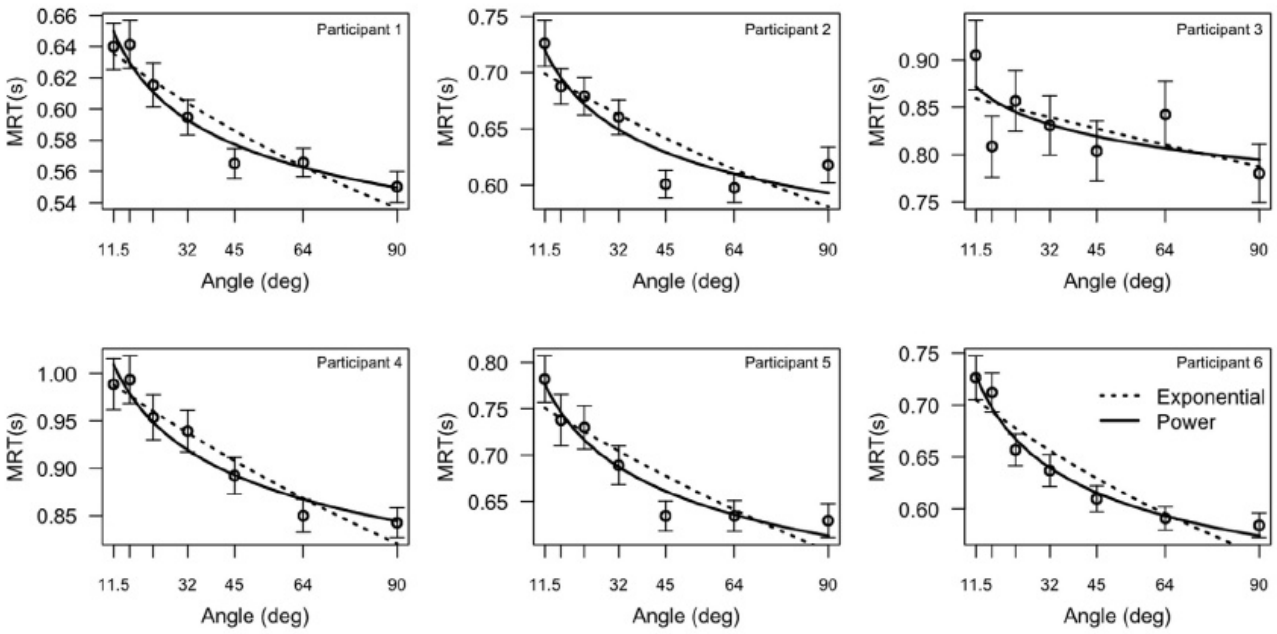

Figure 2 [9, p. 4]: Power vs. exponential functions. Each panel represents one individual. The abscissa shows MRT, the ordinate shows stimulus discriminability (angular distance). One can see that the power law tends to fit the data better than the exponential function.

4. A theoretical framework for Piéron's Law: the Bayesian ideal observer model

A Bayesian ideal observer model was designed in [9] to model an observer making optimal choices given a task under uncertainty (for example, a noisy stimulus). It is assumed that the observer is able to process information optimally by conditioning on all prior data. Such an ideal observer model is able to reproduce Piéron's Law as demonstrated in the following.

The analysis starts from the fact that given observed motion directions *D*, under a uniform prior distribution, a decision favoring direction *i* occurs as soon as

$$P(H_i|D) = \frac{P(D|H_i)P(H_i)}{\sum_{j=1}^{2} P(D|H_j)P(H_j)} = \frac{P(D|H_i)}{\sum_{j=1}^{2} P(D|H_j)} \geq \theta,$$

where H_i corresponds to the hypothesis that the correct direction is *i*, and θ is an unknown threshold parameter. Hence, assuming a normal distribution for the individual pieces of evidence x_t, without loss of generality

$$\theta^* := \frac{\theta}{1-\theta} \leq \frac{P(D|H_1)}{P(D|H_2)} = \prod_{t=1}^{DT} \exp[-\frac{1}{2\sigma^2}((x_t-\mu_1)^2 - (x_t-\mu_2)^2)],$$

where DT denotes the decision time and the μ_1, μ_2 can be interpreted as the target and false directional alternatives, respectively.
Taking the logarithm and the expectation value, one obtains a proof for (the decision time related part of) Piéron's Law with β = 2,

$$\mathrm{MDT} = 2\sigma^2 \ln \theta^* (\mu_1 - \mu_2)^{-2}.$$

In summary this shows that in this framework Piéron's Law emerges if optimal information processing is assumed in the Bayesian ideal observer model.

5. General discussion and conclusion

Piéron's Law had previously only been studied in experiments in which stimulus intensity was the degree of freedom. The new findings derived in the present article [9] are twofold.

First, a more general regularity was postulated extending from intensities to the more comprehensive notion of choice difficulty (discriminability), even in situations in which stimulus intensities are kept constant. MRT relates to choice difficulty in the same way as to stimulus intensity under the classical formulation.
This hypothesis was confirmed in a random dot motion 2AFC experiment. While a direct statistical approach did not yield the expected results, evidence for the hypothesis was overwhelming when a two-stage statistical procedure involving a LBA model was employed.

Finally, a Bayesian observer model was constructed which is able to explain the power law behaviour, thus linking human decision-making to ideal information processing. The numerical discrepancy between the power law exponent β in the theoretical model and the one seen in the experiment remained unexplained.

In a broader context, the results of [9] generalize previous findings and establish a theoretical connection between phenomenological models of decision-making and Piéron's Law. It would be interesting to see whether this generalization also works for other classes of stimuli for which the classical notion of Piéron's Law has previously been confirmed.

References:

[1] Stevens, S.S. (1957). On the psychophysical law. Psychological Review 64 (3), 153–181.

[2] Piéron, H. (1914). Recherches sur les lois devariation des temps de latence sensorielle en fonction des intensités excitatrices. Année Psychol. 22, 17–96.

[3] Pieron, H. (1952). The Sensations: Their Functions, Processes and Mechanisms. London: Frederick Muller Ltd.

[4] Chocholle, R. (1940). Variation des temps de réaction auditifs en fonction de l'intensité à diverses fréquences. Année Psychol. 41, 65–124.

[5] Bonnet, C., Zamora, M. C., Buratti, F., and Guirao, M. (1999). Group and individual gustatory reaction times and Piéron's law. Physiol. Behav. 66, 549–558.

[6] Overbosch, P., de Wijk, R., de Jonge, T.J., and Köster, E. P. (1989). Temporal integration and reaction times in human smell. Physiol. Behav. 45, 615–626.

[7] Banks, W.(1973). Reaction time as a measure of summation of warmth. Percept. Psychophys. 13, 321–327.

[8] Stafford, T., Ingram, L., and Gurney, K. N. (2011). Piéron's law holds during Stroop conflict: insights into the architecture of decision making. Cogn. Sci. 35, 1553–1566.

[9] van Maanen, L., Grasman, R. P. P. P., Forstmann, B. U., & Wagenmakers, E.-J. (2012). Piéron's Law and Optimal Behavior in Perceptual Decision-Making. Frontiers in neuroscience, 5 (January), 143.

[10] Deco, G., Rolls, E.T., Albantakis, L. and Romo, R. (2012). Brain mechanisms for perceptual and reward-related decision-making. Prog. Neurobiol. 1–20. Elsevier Ltd.

[11] Bogacz, R., Wagenmakers, E.-J., Forstmann, B. U., & Nieuwenhuis, S. (2010). The neural basis of the speed-accuracy tradeoff. Trends in Neurosciences, 33, 10–16.

[12] Palmer, J., Huk, A.C., Shadlen, M.N. (2005). The effect of stimulus strength on the speed and accuracy of a perceptual decision. J. Vis. 5, 376–404.

[13] Brown,S., and Heathcote, A.(2008). The simplest complete model of choice response time: linear ballistic accumulation. Cogn. Psychol. 57, 153–178.

Comments on drafts

- Abo-Rady sends comments on Gross's draft
- Bilz sends comments on Camarillo's draft
- Camarillo sends comments on Rauer's draft

- Duwal sends comments on Meier's draft
- Gross sends comments on Seeger's draft
- Kolbe sends comments on Norton's draft

- Mangold sends comments on Wegner's draft
- Meier sends comments on Schmoldt's draft
- Meyer sends comments on Seeger's draft

- Nowak sends comments on Abo-Rady's draft
- Norton sends comments on Bilz's draft
- Joachim Haenicke sends comments on Meyer's draft

- Rauer sends comments on Seek's draft
- Seeger sends comments on Nowak's draft
- Seek sends comments on Kolbe's draft

- Schmoldt sends comments on Schneider's draft
- Schneider sends comments on Mangold's draft
- Wegner sends comments on Duwal's draft